CASE STUDIES ON FREE DRYING SHRINKAGE TEST SENSITIVITY AND ON CARBONATION RATE OF MORTAR WITH PHOTOCATALYTICS

by

Lingkun Li

A thesis submitted to the faculty of
The University of Utah
in partial fulfillment of the requirements for the degree of

Master of Science

Department of Civil and Environmental Engineering

The University of Utah

May 2017

The University of Utah Graduate School

STATEMENT OF THESIS APPROVAL

The thesis of **Lingkun Li**

has been approved by the following supervisory committee members:

Amanda Bordelon	, Chair	**10/07/2016** Date Approved
Pedro Romero	, Member	**01/19/2017** Date Approved
Geoffrey Silcox	, Member	**01/18/2017** Date Approved

and by **Michael E. Barber** , Chair/Dean of

the Department/College/School of **Civil and Environmental Engineering**

and by David B. Kieda, Dean of The Graduate School.

ABSTRACT

A number of recent studies have examined different methods for preventing concrete distresses and limiting structural failures in order to reduce construction repair costs. Common distresses are cracking, scaling, delamination, and spalling. The causes of these concrete distresses can be from a wide variety of mechanisms, two of which are shrinkage and carbonation, which will be investigated in separate case studies. A common influence on both shrinkage and carbonation is the environmental exposure effect.

In one case study, shrinkage was investigated to find out the effects of different environmental conditions (specific relative humidity RH and temperatures) and specimen size (or surface area exposed to the environment). The free drying shrinkage based on ASTM C157 was measured for two mortar mixtures but with different storage conditions (ranging from 4.5% RH to 99.9% RH and 11.2 °C to 25.4 °C on average) from 12 hours to 56 days. Three to four replicates of these mortar samples in each storing environment were also tested at each sample size of 1” prisms (1”×1” ×11.25”), 2” prisms (2”×2” ×11.25”), and 3” prisms (3”×3” ×11.25”). The results verified that high humidity reduces shrinkage. It was also found that 3” prisms (surface area to volume ratio of 1.51) reduce shrinkage sensitivity among any storage environment. In another case study, carbonation was investigated to find out if the rate and depth were influenced by the presence of a photocatalytic material TiO_2. A plain mortar mixture was compared to the same mortar

with the TiO_2 sprayed on the sample surface, and compared to the same mortar with 1% cement replacement of TiO_2 particles. All samples were exposed to the same outdoor environment for up to 100 days. A scanning electron microscope and energy dispersive spectroscopy was used to verify the interior TiO_2 content in the mortar. Thermo-gravimetric analysis and mass spectrometry were used to determine the amount of carbonation from samples taken at different ages and different depths. Result indicated mortar containing photocatalytic materials either embedded or sprayed on the surface have more carbonation at later ages and at the surface.

TABLE OF CONTENTS

ACKNOWLEDGEMENTS

The research funding came from the Mountain Plains Consortium and Dr. Bordelon's startup funds. I want to express my thanks for the SEM training, the equipment, and the chance they gave to me to chase my dream.

I could not have finished my master's thesis without all those who helped me. Firstly, I want to show my sincere thanks to my advisor, Dr. Amanda Bordelon. Her knowledge, friendship, and guidance have always shown me the right way to conduct my research. Thanks also to my committee members, Dr. Pedro Romero and Dr. Geoff Silcox; without their help, I could not have finished my research. Mark Bryant always helped me set up all the equipment in the laboratory. Dr. Brian Van Devener and Paulo Perez from University of Utah Nanofab helped me with the SEM/EDS analysis. Dr. Joel S. Miller and Eric Campbell from the Chemistry Department provided me help with the TGA analysis in my research. The UATAQ lab provided me the CO_2 data.

Most importantly, I want to say thank you to all my family and my girlfriend, Yurou Gan; without them, I could be lost. They gave me strength and always encouraged me.

Besides, I express my thanks to my colleagues, Dillon Li, Jafar Allahham, Siddharth Rayaprolu, James Holt, Martin Dinsmore, and Catalina Arboleda. They gave me the inspiration in my research. My friend, Chenyu Cui, from Ireland, helped me mix concrete.

CHAPTER 1

INTRODUCTION

1.1 Concrete Properties and Distresses

As a common construction material, concrete has been widely used in residential and commercial structures, freeways, and bridges as concrete can have high durability, a good workability, and a desired strength. The popularity of concrete, however, does not mean this material is without limitations. In fact, concrete distresses happen all of the time, which could lead to higher cost to repair or even structures' failure. The common distresses according to ACI 201.1R-08 from the American Concrete Institute (ACI) are cracking and deterioration such as chalking, pitting, scaling, deformation, etc. (ACI Committee 201 2008).

According to the Portland Cement Association (PCA), there are some factors that could influence concrete distress: chemical attack, alkali-aggregate reactivity, heat, overloads, volume changes, etc. (PCA 2002). PCA has also noted that shrinkage due to water loss and carbonation are two major factors, which could be classified under volume change and corrosion of embedded metals distresses.

1.2 Shrinkage

Drying shrinkage is a common phenomenon that happens over time in concrete after hardening, and is caused by water loss. Drying shrinkage leads to concrete cracking, when base friction or restraint resists volume change. Restraint to concrete shrinkage is considered the most common cause of concrete cracking (PCA 2002).

Studies on concrete drying shrinkage date back to the 1920s, when an article focused on the drying behaviors of clays and shales (McClenahan and Rigling 1929). Nowadays, investigations focus more on the shrinkage of concrete due to the addition of admixtures (Domingo-Cabo et al. 2009; Duan et al. 2016; Güneyisi et al. 2014; Yoo et al. 2015). For concrete and mortar, shrinkage behaviors influenced by curing, ambient environmental conditions, exposed surface area, mixture components, and proportions are all expected to contribute to the crack formation and crack widths.

1.3 Carbonation

Carbonation is the chemical reaction resulting when CO_2 in the air and $Ca(OH)_2$ in hydrated concrete gradually react to form $CaCO_3$. The carbonation reaction rate mainly depends on the concentration of CO_2, the permeability of concrete, reaction temperature, ambient humidity, chemistry of the cement, age of the concrete, and existence of previous cracks (Ashraf 2016). This rate is nonlinear and increases with the increase of exposure time. Additionally, there are several other factors that could increase carbonation rate, including increased CO_2 concentration, an environmental RH range of 50% to 75%, moisture content in concrete, high water/cement ratio, low cement content, etc. (PCA 2002).

By adding chemicals or chemical admixtures, concrete properties could be adjusted, or an additive like titanium dioxide may influence the environment. For example, water reducers are used to reduce the water amount that is needed for a given workability, shrinkage-reducing chemicals are used to reduce concrete shrinkage, etc. An example of chemicals that impact the environment is titanium dioxide. Titanium dioxide is a photocatalytic material that could be applied in concrete to clean NO_x gas, a major component of air pollutions, in the air. Since concrete is widely used in constructions and pavements, TiO_2 particles have been increasingly applied to concrete or the concrete surface to clean the air (Ballari and Brouwers 2013; Chen and Poon 2009; Diamanti et al. 2013; Shen et al. 2012). Recent studies have found concrete embedded with TiO_2 does not clean the air beyond a 4-month to 1-year period of exposure (Bogutyn et al. 2015). Analysis of these inefficient TiO_2 applications revealed that carbonation on the surface blocked the reaction with NO_x (Bogutyn et al. 2015; Hanson 2014).

1.4 Objectives

Two specific cases were investigated in this study regarding concrete drying shrinkage and carbonation. In Chapter 2, the sensitivity of the free shrinkage test method is evaluated based on different average and daily fluctuation magnitudes of relative humidity during air drying, and different surface-to-volume ratios, to give recommendations to future laboratory testing conditions. In Chapter 3, it is hypothesized that mortars containing TiO_2 particles will have more carbonation at later ages and greater depths than plain mortar.

1.5 Scopes

In Chapter 2 on free shrinkage sensitivity, a modified ASTM C157 free shrinkage test method was performed to evaluate the air-storage shrinkage without any moist curing. The range of humidity will be varied from 4.5% to 100%, with the lowest humidity also being at a lower temperature. The daily fluctuation in humidity was monitored at each storage location and compared to average humidity for overall sensitivity of the shrinkage measurement. Specimen prism sizes of 1", 2", and 3" provide the range of surface area-to-volume ratios of 4.178, 2.178, and 1.511. Only two mixtures were studied both with mortar and varying aggregate-to-cement proportions of 1.23:1 and 1.17:1. Additionally, a shrinkage prediction was calculated from ACI Committee 209 equations and was compared to measured values.

Chapter 3 covers using energy dispersive spectroscopy for the verification of TiO_2, thermo-gravimetric analysis (TGA), and mass spectrometry (MS) for the estimation of carbonation rate between plain mortar to two mortars embedded with 1% photocatalytic TiO_2 particles and sprayed on TiO_2 particles. All samples will be exposed to an outdoor environment with a CO_2 concentration of around 410 ppm in Utah for up to 100 days.

1.6 Techniques

1.6.1 Standard Test Procedures Used or Modified in Studies

The American Society of the International Association for Testing and Materials (ASTM) is an international standards organization for testing methods and materials. In this study, the materials and concrete mix procedures were followed based on the standards listed below.

- ASTM C150 / C150M – 11 Standard Specification for Portland Cement
- ASTM C157 / C157M - 08 Standard Test Method for Length Change of Hardened Hydraulic-Cement Mortar and Concrete
- ASTM C192 / C192M - 16a Standard Practice for Making and Curing Concrete Test Specimens in the Laboratory
- ASTM C33 / C33M – 16 Standard Specification for Concrete Aggregates
- ASTM C305 – 11 Standard Practice for Mechanical Mixing of Hydraulic Cement Pastes and Mortars of Plastic Consistency
- Petrographic Methods of Examining Hardened Concrete: A Petrographic Manual (2004), Federal Highway Administration.

1.6.2 Statistics Used in Shrinkage Study

The sensitivity will be ranked by comparing the difference of slopes for each two sets of data for the same variable (humidity) in this study. It will be considered “less sensitive” when the percent difference in slopes is small.

A T-test will be used to statistically compare the mean values between different shrinkage measurements. A T-test is used instead of a normal distribution when there are small sample sizes (O'Mahony 1986). When performing a T-test, a null hypothesis is created and a level of significance is selected (in this study 5% was chosen). The result shows a probability P-value. For this study, when the P-value is smaller than 0.05, the null hypothesis is rejected, indicating that the means are statistically different.

Coefficient of variance (CV) will also be used in this study to statistically analyze the

variability of replicas. Statistically, CV values smaller than 15% are considered to be low variability and to be eligible for performing a T-test.

CHAPTER 2

FREE SHRINKAGE ON CEMENT MORTARS

Cement mortar is widely used in masonry, and it can bind concrete, bricks, and stones. Cement mortar is also a good finishing and repairing material that could be used to fix cracking on concrete or asphalt pavements. Drying shrinkage happens in concrete or cement mortars due to water loss. The larger coarse aggregates in concrete resist the volumetric change. Thus, cement mortar is considered to have more paste volume fraction compared to concrete mixtures. To avoid the influence of aggregate size on the measured shrinkage, only cement mortar was investigated based on ASTM C157 in this chapter.

2.1 Shrinkage Types and Mechanism

Shrinkage happens when concrete starts hardening, exhibits logarithmic growth with time, and is mostly irreversible. There are four different types of shrinkage, thermal shrinkage, plastic shrinkage, drying shrinkage, and autogenous shrinkage (Li 2011) as described herein.

Thermal shrinkage is the concrete contraction caused by the temperature difference between concrete and the surrounding environment. When the ambient temperature is lower than that of concrete, the concrete will shrink.

Plastic shrinkage happens at a very early age, only a few hours after adding water, before the concrete has hardened. When the rate of water evaporation from the concrete surface exceeds that of the migration of internal water to the surface, the surface layer volume decreases causing shrinkage, often leading to spalling and surface micro-cracking.

Drying shrinkage occurs after the concrete has set and hardened and is the loss of the water that has not reacted with cement. The excessive water in the interior of concrete that migrates to the surface and evaporates to the environment produces a net volume reduction and causes cracking if the concrete is restrained from this volumetric change.

Autogenous shrinkage is the volume contraction of concrete that happens at an early age, less than 24 hours after adding water. Autogenous shrinkage occurs without moisture transfer from concrete to environment, which is a result of chemical shrinkage due to the hydration of cement.

This shrinkage study will primarily investigate drying shrinkage and has some concurrent influence from thermal shrinkage that will be accounted for with back-calculation, as detailed in section 2.3.4.

2.2 Shrinkage Magnitude Prediction

There are many factors that could have an influence on drying shrinkage. Since it is the water loss that leads to drying shrinkage, the Portland Cement Association states that a low water content would decrease the magnitude of shrinkage, as well as by maximizing coarse aggregate content (PCA 2002).

In 1929, an article originally proposed the length change test to measure the drying shrinkage behavior for clay and shales. At the time, the authors investigated the influence

of different temperature and humidity conditions, such as 26 °C versus 105 °C temperature and 85% versus 94% RH. From this early study, they found that the shrinkage was greater with increased drying time and at 26°C and 94%RH (McClenahan and Rigling 1929).

Studies have shown that ambient relative humidity has an influence on concrete shrinkage. Pihlajavaara investigated cement mortar specimen shrinkage in storing environments from 0% RH to 100% RH and found that shrinkage is greater in the low humidity environments (Pihlajavaara 1974). Cebeci et al. studied the shrinkage for concrete mortars moist cured at 33%, 75% and 92%RH; the investigation found that drying shrinkage was increased with curing in lower humidity environments (Cebeci et al. 1989). Alsayed and Amjad studied concrete slabs for shrinkage under different humdity conditions. The results again verified that low humidity environment resulted in more shrinkage than high humidity conditions (Alsayed and Amjad 1994).

2.3 Shrinkage Prediction and Moisture Diffusion

American Concrete Institute's Committee 209 has derived a set of equations to predict drying shrinkage as shown below, estimating after 7 days moist curing that at an ambient 40% RH would produce an ultimate shrinkage of 780 x 10^{-6} in/in, and at 70% RH would produce 546 x 10^{-6} in/in. (ACI Committee 209 1992). The definitions and calculations for each coefficient are shown in Table 1.

In 1995, Bažant and Baweja developed a shrinkage prediction equation based on the different humidity in the pores and environment as shown in Equation (1) (Bažant and Baweja 1995).

$$\frac{\varepsilon_{sh}(t)}{\varepsilon_{sh\,\infty}(h_e)} = \frac{h_0 - \overline{h}(t)}{h_0 - h_e} - \tanh\varphi \quad (1)$$

where,

$\varphi = \sqrt{\frac{t-t_0}{\tau_{sh}}}$;

h_0: initial relative humidity in the pores;

h_e: environmental relative humidity;

ε_{sh}: average shrinkage strain in the cross section;

$\varepsilon_{sh\,\infty}$: final value of shrinkage strain corresponding to h_e;

τ_{sh}: time at half drying shrinkage;

$t - t_0$: duration of drying.

Based on a composite model (cement and aggregate), Eguchi and Teranishi predicted drying shrinkage of concrete using Equation (2) (Eguchi and Teranishi 2005).

$$\frac{\varepsilon_{sc}}{\varepsilon_{sm}} = \frac{[1-(1-m*n)V_a][n+1-(n-1)V_a]}{n+1+(n-1)V_a} \quad (2)$$

where,

the suffixes *c*, *a*, *m* stand for the entire concrete composite, the aggregate, or the matrix, respectively;

ε_s: drying shrinkage strain;

$n = E_a/E_m$;

$m = \varepsilon_{sa}/\varepsilon_{sm}$;

E: Young's modulus;

V: volume ratio;

Another shrinkage prediction equation was introduced by Moon and Weiss in 2006, based on the change of humidity as shown with Equation (3) and (4) (Moon and Weiss 2006).

$$\varepsilon(t) = \varepsilon_{SH-const} * \Delta RH(t) \tag{3}$$

$$\Delta RH(x,t) = RH_i - (RH_i - RH_s) * \left[erfc\left(\frac{x}{2\sqrt{D \cdot t}}\right)\right] \tag{4}$$

where,

$\varepsilon_{SH-const}$: constant shrinkage coefficient;

$\Delta RH(t)$: the difference between 100% RH and the internal relative humidity RH of a concrete specimen at a given time and depth;

RH_i: internal relative humidity;

RH_s: relative humidity at the surface of the specimen;

x: depth from the drying surface;

D: aging moisture diffusion coefficient;

t: drying time.

Drying shrinkage is closely related to diffusion rate, which is related to the surface area-to-volume of the concrete. In 1946, Pickett studied the relationship between diffusion of vapor and moisture content in concrete, and a linear diffusion equation was solved by applying the heat transfer equation (Pickett 1946). However, later studies found that the moisture diffusion in concrete follows a nonlinear equation (Bažant and Najjar

1972). In 1982, Sakata also predicted the moisture distribution in concrete with a nonlinear diffusion equation and compared the experimental values with computed values. Sakata found that moisture diffusion is rapid near the surface but slow in the interior based on Bažant's moisture diffusion equation (Sakata 1983). The ACI 209 prediction equation also included volume-to-surface ratio, an inverse of the surface-to-volume used in the diffusion models (ACI Committee 209 1992).

Despite these previously mentioned studies, most experiments were performed following ASTM C157 standard. However, the suggested curing environment, surface-to-volume ratios, and air storing conditions cannot be followed exactly. Thus, this study investigates the influence of surface-to-volume ratios using different specimen sizes, the specimen storage environment ranging from about 10 to 90% RH and 10 to 25°C, and for two different fine aggregates to cement mass proportions partially followed by ASTM C157 standard.

2.4 Methodology

2.4.1 ASTM C157 Modification

The shrinkage test in this study was based on ASTM C157 standard, but three modifications were made to meet the research objective. These modifications were on specimen size, curing procedure, and air storage environment as described herein.

2.4.1.1 Specimen Sizes

ASTM C157 defines the test specimens. For mortar, the test specimens shall be 1" prisms. For concrete, the test specimens shall be 4" prisms if all the coarse aggregate

passes through a 2-in sieve, or shall be 3” prisms if all the aggregate passes through a 1-in sieve. In this study, there were no coarse aggregates used at all, but three different test specimens were investigated (1”, 2”, and 3” prisms) to determine the sensitivity of the shrinkage magnitude relative to different surface area to volume ratios of 4.178, 2.178, and 1.511, respectively.

2.4.1.2 Curing Procedures

To minimize the variation in length due to temperature, ASTM C157 suggests specimens be moist cured for 28 days before storing. In this study, all specimens were not moist cured at all to investigate temperature influence.

2.4.1.3 Air Storage

ASTM C157 also suggests that to measure shrinkage in an air storage environment, a relative humidity of 50 ± 4% and a temperature of 23 ± 2ºC must be maintained. Not all testing labs can maintain such narrow climate controls. Thus, seven different storing conditions with different average humidity and temperature levels, as well as different magnitudes of fluctuation, were studied to determine the test method sensitivity relative to average humidity levels and daily fluctuation levels on shrinkage values.

2.4.2 Storing Conditions

2.4.2.1 RH and Temperature

Table 2 summarizes the RH and temperature monitoring information gathered for different locations. The resolution of the digital USB logger at the Utah Department of

Transportation (UDOT) was 1°F (0.55°C) and 0.5% RH, while all other digital USB loggers had a resolution of 0.5°C and 0.5% RH. The gauge on the humidity chamber displays to the nearest 0.5°C and 0.5% RH, while the dial gage in the refrigerator showed increments of 2°C and 1% RH (from 10 to 100%). When obtaining RH% data from the refrigerator, and when the dial showed a value below 10%, a rough estimation was used in the analysis of environment condition.

The maximum, minimum, average temperature, and RH data for each location through all the monitoring days are shown in Figure 1 and listed in Table 3. The specific daily measured temperature, humidity, and fluctuation readings for each location can be found in Appendix A. The readings verified that the refrigerator is colder and lower in humidity than any other locations. The highest humidity was found in the fog room. The daily fluctuations of temperature and humidity for each location were calculated and are shown in Table 4. The humidity chamber was verified to maintain a constant temperature and humidity expected for the ASTM C157 specification, and was selected as the control condition. The fog room 130D also had a stable humidity and temperature environment.

A t-test was made between each two of those seven locations. For each combination of data sets, the same recording frequency was used to determine if there is a correlation/trend between locations. By comparing the P-values shown in Table 5 and Table 6, it was confirmed that there were no similarities (p-value < 0.05) in temperature and humidity between these locations. Since the recording dates and time were different for each location, the humidity and temperature data cannot be correlated; thus, p-values were calculated without matching the starting and recording time.

2.4.2.2 Significance of Locations

All seven locations selected in this study were used to simulate six laboratory environments with an additional control location (humidity chamber) that followed ASTM C157 storage requirements. After comparing the shrinkage values in those seven different locations, recommendations on modifying the test standard based on alternative RH and temperature average values and fluctuation will be composed. The goal of these new recommended storage requirements will be based on the location that provides more consistency in shrinkage measurements regardless of the reported shrinkage age and the specimen size selected.

2.4.3 Materials, Mix Design, and Specimens

A local ASTM C150 classified Type I/II/V cement from LaFarge-Holcim's Devil's slide plant was used for this study, as well as an ASTM C33 standard natural sand from Staker Parson's Beck street plant.

Two mix designs were created. A saturated surface dry (SSD) cement:sand:water mass ratio of 1 : 1.23 : 0.53 was used for mix 1 and mass ratio of 1 : 1.17 : 0.53 was used for mix 2. The mix design in pounds per cubic yard was summarized in Table 7. Batch weight can be found in Appendix B showing the oven-dry batched amounts.

Before mixing, all natural sands were oven dried for approximately 24 hours at a temperature of 80 degrees Celsius. Specimens were mixed per ASTM C305. All specimens were air-cured for the entire duration, rather than performing the 28-day lime-saturated bath curing recommended in the ASTM C157 standard. Shrinkage from mix 1 was only measured using the humidity chamber and fume hood locations, while

shrinkage from mix 2 was measured for all locations. For each batch, at least four 1x1x11.25” prisms (surface area to volume ratio of 4.18), three 2x2x11.25” prisms (surface area to volume ratio of 2.18), and four 3x3x11.25” prisms (surface area to volume ratio of 1.51) were made.

2.4.4 Measurements

To determine the shrinkage under different curing conditions, length change tests were performed. Per ASTM C157, a length change test is divided into comparator reading and calculation. In this study, with each test specimen in the comparator, the dial readings were observed and recorded. The length change of any specimen at any age was calculated following Equation (5). The weight change was also measured to verify whether consistent shrinkage was occurring in test specimens.

$$\Delta L_x = \frac{CRD - initial\ CRD}{G} \times 10^{-6} \quad (5)$$

where,

$\Delta L_x =$ length change of specimen at any age, 10^{-6}in/in,

$CRD =$ difference between the comparator reading of the specimen and the reference bar at any age, in,

$G =$ the gage length, 10 in.

For each of those seven locations, at least three replicates of each prism size were measured. All the specimens were demolded at an early age and measured at about 12

hours from the time of mixing. Extra samples were made because sometimes the specimens were fragile and broke during demolding at this early age.

The measurement ages for length change and weight change were taken at 12 hours (0.5 days), 24 hours (1 day), 3 days, 7 days, 14 days, 21 days, 28 days, and 56 days after water was added. The specific dates and times for mixing and measurements are shown in Appendix C.

Even though shrinkage samples were stored in different locations, all samples were measured at a room temperature of approximately 25 ºC and relative humidity of about 40%. Thermal contraction or expansion could happen during measurement. However, since each measurement lasted only for approximately 1 minute, a relatively short period compared with storing time, thermal expansion during the measurement time alone was not considered in this study. Only the shrinkage specimens stored in the refrigerator environment, which had a significantly different temperature of 4.5 ºC on average, were later separated into the predicted thermal contraction versus the remaining net shrinkage assumed to be due to drying in the low RH, as calculated in Equation (6). Additionally, it was assumed that the internal temperatures within the refrigerator samples were uniformly at the external refrigerator temperature.

$$\Delta L = CTE * \Delta t * L_0 \tag{6}$$

where,

ΔL: length change due to temperature change, in;

CTE: thermal coefficient of concrete, range from 7.4 to13E-6/ ºC, here use 10E-6/ ºC;

Δt: temperature change, ºC;

L_0: initial length, in.

2.5 Results

2.5.1 Overall Analysis

2.5.1.1 Repeatability

An example of four 1" prism sample replicates stored in the humidity chamber and fog room is shown in Figure 2. The coefficient of variance (CV) was calculated and is shown in Table 8. The variation in shrinkage for the fog room was significantly high, indicating it is not a suitable environment in which to measure shrinkage.

2.5.1.2 Thermal Contraction Adjustment for Refrigerator

All samples located in the refrigerator were first stored at room temperature (around 25 ºC) for about 12 hours, and after the first readings, they were moved to refrigerator at 10 ºC for storing. Thus, thermal contraction adjustment was applied for specimens stored in the refrigerator in this study. All future graphs and data showing refrigerator results are based on the adjusted values. Adjusted shrinkage values for thermal contraction stored in the refrigerator are compared in Figure 3.

2.5.1.3 Shrinkage for Each Environment

As the humidity chamber was set to be the control environment, a plot that shows the difference between each location and the humidity chamber was generated. A comparison of extreme storage environments (refrigerator to fog room) is to plot the individual

shrinkage in comparison to the same average control (humidity chamber) environment as shown in Figure 4. Comparison plots for other locations are shown in Appendix D.

The average drying shrinkage measurement plots versus age of each environment and each prism size of mix 2 are shown in Figure 5. As expected, the least shrinkage was found in the fog room, which has the highest humidity. Among the 1" prisms, the drying shrinkage is the greatest in the refrigerator after 21 days. For 2" prisms, the shrinkage is the greatest in UDOT after 21 days. While among 3" prisms, the shrinkage appeared to be greatest in the humidity chamber at a constant 50% RH and 23°C. Further analysis on the specific humidity and surface area-to-volume ratio are made hereafter.

A T-test was performed for those shrinkage values at each location. When the P-value is smaller than 0.05, this indicates that the shrinkage magnitudes are different. Tables 9 and 10 show the P-values comparing whether the shrinkage magnitudes are the same between two locations. Since storage room 130C, room 110A, and UDOT lab are all indoor lab rooms, in Table 9, these three rooms were averaged together and classified as "Lab Rooms" when compared to other four locations. A comparison of P-values between just these three lab rooms was created and listed in Table 10. The P-value between the humidity chamber and fume hood is higher than 0.05 at the 56 days and thus these environments cannot be statistically differentiated now. All other storage environments are considered significantly different.

2.5.1.4 Weight Change During Shrinkage

It is expected that weight loss happens for concrete samples when there is a low external humidity compared to the inside of the concrete. Based on the theory proposed

by Pickett, moisture transfer only happens when there is a humidity difference between concrete and environment. It is expected that when the interior moisture reaches the same as the ambient environment, moisture absorption stops. It is also expected that a higher moisture transfer rate exists in samples that have higher surface-to-volume ratio.

First off, all samples exhibited an initial weight loss from the time of mixing to the first 3 days. From the plots shown in Figure 6, the prisms stored in the fog room, regardless of specimen size, started re-gaining some of the weight starting after 7 days, due to the expected absorption of moisture from high humidity environment. It can also be seen in many of the other environments that there is a weight re-gain among the 1" prisms, Figure 6a. The samples stored in the refrigerator at a low humidity all continued to lose weight regardless of specimen size. The samples measured in this study verified that a high surface-to-volume ratio for concrete is more sensitive to humidity, detailed in section 2.4.2.2; and the weight varies more for a sample of high surface-to-volume ratio before humidity equilibrates.

2.5.2 Average and Daily Fluctuation in Humidity Influence on Shrinkage

2.5.2.1 Shrinkage and Average Relative Humidity

The average shrinkage measurement for all the 1", 2", and 3" prisms of mix 2 versus average humidity of each environment are shown in Figure 7. The plot confirms that with the increase of RH, shrinkage decreases and shows that 1" prisms are the most sensitive to RH.

2.5.2.2 Shrinkage and Average Relative Humidity Fluctuation

The comparison of shrinkage values at different relative humidity fluctuations was made. To minimize humidity's influence, five locations were compared without extremely high humidity (Fog Room) and extremely low humidity (Refrigerator). As shown in Figure 8, no trend line was added as low R square values.

2.5.3 Size Effects on Shrinkage

In this study, 1", 2", and 3" prisms were tested and analyzed by their dimensions and surface-to-volume ratios of 4.18, 2.18, and 1.51. Figure 9 shows the average length changes for these three prism sizes for mix 2 stored in the humidity chamber (23 °C, 50% RH), while Figure 10 is the relationship between surface-to-volume ratio and shrinkage. The weight change plot indicates the 1" prisms started absorbing water at 7 days, as explained before. The other shrinkage and weight change figures for other locations can be found in Appendix E. Table 11 lists the p-values to compare specimen sizes at each age; samples stored in the humidity chamber and fume hood were combined due to the similar humidity and temperature environment. Again, p-values less than 0.05 indicate the prisms give statistically different shrinkage values. The table shows that storage room 130C has significant influence on prism sizes; at 56 days, size effects are reduced; and the refrigerator has the least size effects among all locations.

2.5.4 Shrinkage of Mortars with Sand-Cement Proportioning

The mass ratio of cement to aggregate (1:1.17 versus 1:1.23) was also studied on the influence of measured shrinkage. Figure 11 is a comparison of the different mix designs

at the same storage conditions (humidity chamber). No obvious trend can be seen from the plot of average shrinkage values between mixes. Furthermore, Table 12 shows the p-values comparing shrinkage of the different mixtures. Among 1" prisms and the humidity chamber, which are both specified in the current ASTM C157 standard, one cannot distinguish between the mixtures. However, a subtle difference between mixes is shown for 3" prisms after 7-day storing.

2.5.5 Shrinkage Predictions

2.5.5.1 Shrinkage Prediction Based on ACI Committee 209 Equations

The predicted and measured shrinkage values at different locations were compared from ACI Committee 209 equations. The coefficients were determined as follows: all the samples are mortar, thus the fine aggregate coefficient γ_f equals 1.1; the calculation of relative humidity coefficient (γ_h), volume-to-surface ratio coefficient ($\gamma_{V/S}$), thickness coefficient (γ_{th}), and cement content coefficient (γ_c) are listed from Table 13 to 15. A back-calculation of the curing coefficient was made since there was no moist curing while the ACI 209 equation only accounts for shrinkage based on 7 days moist curing. The back-calculated γ_{cp} was found to be 2, so that the measured average shrinkage matched the prediction for a 3" prism (as is used in the ACI 209 equation) after 56 days and for the humidity chamber environment (which meets the ASTM C157 standard RH and temperature requirements); all other coefficients were assumed to be 1.0 since there were no data available on them.

Error and squared error were calculated to compare the difference between the measured and predicted shrinkage values. Table 16 shows the comparison between

predicted and measured shrinkage values for samples stored in the humidity chamber and refrigerator at 56 days while Figure 12 shows the comparison between predicted and measured shrinkage values for samples stored in humidity chamber at all ages. A completed comparison of predicted versus measured values is shown in Appendix F.

The difference between predicted and measured values (measured values minus predicted values) shows where the model underpredicts (positive values) and overpredicts (negative values). The squared error can be used to illustrate that the magnitude of difference is greater in the refrigerator than the humidity chamber or fog room.

Additionally, squared error versus volume-to-surface ratio plots for samples stored in the humidity chamber for 21 days, 28 days, and 56 days were generated, as shown in Figure 13. In general, as the volume-to-surface ratio increased, squared error increased for samples stored for 21 days, while it dramatically decreased for samples stored for 56 days. There was no obvious trend seen from the squared error versus relative humidity plot shown in Figure 14.

2.5.5.2 Moisture Diffusion Prediction (Moon and Weiss)

The prediction was also performed based on the equations induced by Moon and Weiss as shown in Chapter 2. The water diffusion coefficient was selected to be 0.133 cm*cm/day based on 0.53 water/cement ratio and 0-day moist curing (Bažant and Najjar 1972), which was converted to be 0.021 in*in/day.

Two cases were studied and predicted under the Moon and Weiss model, shrinkage for samples stored in the refrigerator and in humidity chamber. The constant shrinkage coefficient (from Equation (3)) was calculated using the initial ACI Committee 209

suggested ultimate shrinkage, and applying the coefficients not associated with drying time, humidity, or specimen size. Thus, the following ACI coefficients were applied to the 780 microstrain: moist curing coefficient, slump coefficient, air entrainment coefficient, fine aggregate coefficient, and cement content coefficient in section 2.4.5.1 as listed in Table 17. The constant shrinkage coefficient was found to be 2094 in/in$\times 10^{-6}$ for the Moon and Weiss prediction.

Since concrete shrinkage was considered due to water diffusion, an internal relative humidity distribution prediction plot at different depths into the specimens was created for these two cases as shown in Figure 15. The figure shows that the shrinkage values decrease with the increasing of depth from sample surface. Additionally, it also confirmed that water diffused out of the sample more for samples at surface at longer storing age in lower relative humidity environment.

The selection of predicted shrinkage values from this model was at the center (1.5" depth of 3" samples, 1" depth of 2" samples, and 0.5" depth of 1" samples, respectively) since the two pins for the measurement were located at the center of samples.

Error and squared error were also used with this prediction model to find out if it is underpredicted (positive error values) or overpredicted (negative error values) from the actual measured shrinkage values. As an example, the comparison between these two cases at 56 days is listed in Table 18. From Figure 16 and Appendix G, the Moon and Weiss model underpredicts shrinkage values at all ages for all storing locations; possible reasons for this could be the selection of diffusion coefficient, the constant shrinkage coefficient, or the parameters from ACI Committee 209 equations. However, from the comparison in Figure 17, this model fits samples stored in the refrigerator better since it

has lower squared error values than those for samples stored in the humidity chamber.

2.6 Summary and Findings

This study focused on the shrinkage of cement mortars, measured from 0.5 to 56 days, and comparing the influence of environmental storage conditions, samples sizes, and aggregate-cement proportioning. The results could be concluded as follow.

- In general, a higher humidity during the storage of the specimens was verified to create the least amount of shrinkage on cement mortars.
- When comparing the sensitivity among sizes of samples at different relative humidity and humidity fluctuations, it was found 1” prisms are most sensitive to RH, while there was no trend to RH fluctuation. Furthermore, a longer storing age increases the shrinkage sensitivities to RH.
- A longer storage age reduces the sensitivity on shrinkage values associated with surface-to-volume ratio. Furthermore, the shrinkage magnitude was higher for greater surface-to-volume ratios.
- For a 1” prism size and humidity controlled environment, a small adjustment in fine aggregates to cement proportioning did not show a significant difference in shrinkage values.
- Using the ACI 209 shrinkage prediction equation, prediction parameters were changed to have no initial curing. In the 50% controlled humidity environment, the model was found to underpredict early shrinkage and overpredict later shrinkage (for ages greater than 28 days). Samples stored in the refrigerator exhibited the greatest difference between the measured lab and the model

predicted shrinkage, with the model highly overpredicting shrinkage at this low humidity environment for 2” and 3” prisms. Samples modelled for the fog room had the least difference but significantly underpredicted compared to the actual lab samples.

- Using the Moon and Weiss shrinkage prediction equations based on moisture diffusion, it was confirmed the internal moisture diffuses out of the sample more for smaller samples and with longer exposure ages. The model prediction significantly underpredicts shrinkage for a 50% controlled humidity environment, but more closely predicts shrinkage for the 5% low humidity environment.

These findings lead to recommended alterations to the existing ASTM C157 standard. If it was wanted to be able to use any specimen size for determining shrinkage, the storage environment in the refrigerator (0% to 10% RH) or with longer storage ages were found to have the least influence of specimen size on shrinkage. Or if it was wanted to have the ability to store samples in any humidity environment, samples should be of 3” size to minimize humidity influences regardless of environment (from 5 to 100% RH).

Table 1 Shrinkage Prediction Coefficients from ACI Committee 209

ε_{sh}	Shrinkage at a given time after curing	$\varepsilon_{sh}(t) = \varepsilon_{sh-ult} * \gamma_t$	t: days after initial curing
ε_{sh-ult}	Ultimate shrinkage	$780^{-6} \times \gamma_{sh}$ where: $\gamma_{sh} = \gamma_h * \gamma_{cp} * \gamma_{th} * \gamma_s * \gamma_f * \gamma_e * \gamma_c * \gamma_{V/S}$	
γ_t	Time coefficient (based on 7 days initial moist curing)	t / (35 + t) for moist curing	
γ_h	Ambient RH coefficient	1.0 for RH<40 $1.4 - 0.0102(RH)$ for 40<RH<80 $3.0 - 0.030(RH)$ for 80<RH<100	RH: Relative Humidity (from 0 to 100)
γ_{cp}	Initial moist curing coefficient	Curing age (days) / γ_{cp} 1 / 1.2 3 / 1.1 7 / 1.0 14 / 0.93 28 / 0.86	
γ_{th}	Thickness coefficient	1.43 for 1-inch thickness 1.3 for 2-inch thickness 1.17 for 3-inch thickness	
γ_s	Slump coefficient	$0.89 + 0.04(S)$	S: Slump (inches)
γ_f	Fines coefficient	$0.33 + F/75$ for F<50 $0.88 + F/430$ for F>50	F: weight % of fine aggregates of total aggregate (from 0 to 100)
γ_e	Entrained air coefficient	$0.95 + A/120$	A: volume % of air entrainment (from 0 to 100)
γ_C	Cement content coefficient	$0.72 + C/2500$	C: cement content (lbs/cy)
$\gamma_{V/S}$	Volume-to-surface coefficient	$1.2\ exp(-0.12\ V/S)$	V/S: volume/surface area ratio (in)

Table 2 RH and Temperature Monitoring Information for Different Locations

Location	Expected Relative Humidity	Expected Temperature	Monitoring Method	Duration between Readings (min)
Refrigerator	10%	10°C	Dial Gauge	Specific dates
Humidity Chamber	50%	23°C	Digital Gauge	Specific dates
Fume Hood	Fluctuating <50%	25°C	USB Logger	10
Room 110A	Fluctuating <50%	25°C	USB Logger	10
Storage Room 130C	Fluctuating ~50%	25°C	USB Logger	10
UDOT	~50%	25°C	USB Logger	30
Fog Room 130D	90%	25°C	USB Logger	10

Table 3 RH and Temperature Data for Different Locations

	RH (%)			Temperature (∘C)		
Location	Minimum	Maximum	Average	Minimum	Maximum	Average
Refrigerator	0.0	12.0	4.5	7.0	15.0	11.2
Humidity Chamber	50.0	50.0	50.0	23.0	23.0	23.0
Fume Hood	18.5	54.5	34.6	21.5	29.0	24.5
Room 110A	14.0	53.0	29.4	16.0	31.5	23.7
Storage Room 130C	26.0	68.5	53.7	15.0	26.5	23.5
UDOT	32.5	55.5	44.3	23.3	27.8	25.4
Fog Room 130D	75.5	104.0	99.9	17.5	25.0	21.9

Table 4 Temperature and Humidity Daily Fluctuation for Different Locations

	RH Fluctuation (%)			Temperature Fluctuation (∘C)		
Location	Minimum	Maximum	Average	Minimum	Maximum	Average
Refrigerator	3.0	5.0	4.5	3.0	6.0	4.0
Humidity Chamber	0.0	0.0	0.0	0.0	0.0	0.0
Fume Hood	7.0	24.0	14.2	1.5	7.0	3.5
Room 110A	6.0	22.0	14.1	1.5	6.5	3.7
Storage Room 130C	3.0	30.0	9.2	0.0	5.5	1.1
UDOT	2.0	14.0	5.7	0.6	2.8	1.1
Fog Room 130D	0.5	21.5	3.7	0.0	2.0	1.0

Table 5 P-values for Temperature

	Humidity Chamber	Fume Hood	Room 110A	Storage Room 130C	UDOT	Fog Room
Refrigerator	5.99E-7	1.27E-8	6.78E-9	2.48E-8	2.12E-7	3.02E-7
Humidity Chamber	-	4.07E-7	0.01	0.02	1.35E-35	3.87E-8
Fume Hood	-	-	0.02	7.30E-4	3.33E-4	1.41E-13
Room 110A	-	-	-	0.50	1.80E-7	1.68E-7
Storage Room 130C	-	-	-	-	4.50E-13	2.97E-8
UDOT Lab	-	-	-	-	-	2.44E-31

Table 6 P-values for Relative Humidity

	Humidity Chamber	Fume Hood	Room 110A	Storage Room 130C	UDOT Lab	Fog Room
Refrigerator	2.61E-8	1.47E-12	8.56E-10	6.37E-14	3.17E-10	1.89E-11
Humidity Chamber	-	1.13E-7	1.59E-35	4.87E-5	1.90E-12	1.26E-95
Fume Hood	-	-	0.02	6.21E-10	4.22E-5	8.76E-19
Room 110A	-	-	-	6.48E-43	1.80E-28	2.05E-78
Storage Room 130C	-	-	-	-	8.81E-15	3.21E-61
UDOT Lab	-	-	-	-	-	8.15E-70

Table 7 Mix Design

Mix		Mix 1		Mix 2	
Materials	Absorption Capacity	SSD Design (pcy)	Mass Ratios	SSD Design (pcy)	Mass Ratios
Type II Cement		1697	1.00	1307	1.00
Natural Sand	2.19%	2083	1.23	1525	1.17
Water		892	0.53	687	0.53

Table 8 Coefficient of Variance at Each Age and Each Environment and Sample Size*

	7 days			14 days		
Locations	1" Prisms	2" Prisms	3" Prisms	1" Prisms	2" Prisms	3" Prisms
Refrigerator	7.67%	**20.2%**	4.55%	5.65%	**25.4%**	4.97%
Humidity Chamber	4.23%	0.72%	5.63%	5.31%	0.55%	8.98%
Fume Hood	5.62%	4.73%	10.24%	6.41%	3.82%	4.03%
Storage Room 130C	1.24%	2.70%	5.84%	1.10%	1.15%	5.62%
Room 110A	1.85%	4.38%	9.02%	1.86%	6.35%	4.42%
UDOT Lab	3.10%	13.01%	12.45%	2.72%	10.94%	8.35%
Fog Room	**31.9%**	**19.2%**	**16.6%**	**51.4%**	8.77%	13.1%
	28 days			56 days		
Locations	1" Prisms	2" Prisms	3" Prisms	1" Prisms	2" Prisms	3" Prisms
Refrigerator	2.61%	**15.1%**	1.92%	2.61%	9.46%	3.44%
Humidity Chamber	5.15%	1.61%	6.59%	6.63%	2.35%	5.55%
Fume Hood	8.91%	3.64%	6.65%	7.77%	3.33%	5.67%
Storage Room 130C	1.15%	1.33%	5.62%	0.80%	1.31%	3.50%
Room 110A	2.44%	3.27%	0.96%	1.27%	2.60%	0.68%
UDOT Lab	2.48%	7.40%	6.84%	2.59%	7.40%	5.09%
Fog Room	**58.2%**	8.44%	**19.6%**	**53.2%**	7.26%	**22.7%**

* Bold value means high variance (CV > 15%)

Table 9 P-values Between Different Environments for 1” Prisms at 56 Days

Locations	Refrigerator	Humidity Chamber	Fume Hood	Lab Rooms	Fog Room*
Refrigerator	-	0.0017	0.0004	4.57E-05	4.13E-05
Humidity Chamber		-	**0.9917**	0.0047	0.0001
Fume Hood			-	0.0024	0.0001
Lab Rooms				-	3.01E-05

* Fog room had a high CV as well.

Table 10 P-values Between Different Lab Rooms for 1” Prisms

	Storage Room 130C	Room 110A	UDOT Lab
Storage Room 130C	-	0.0424	0.0015
Room 110A		-	0.0003

Table 11 P-values Comparing Prism Sizes

	7 days		28 days		56 days	
Locations	1" vs 2"	2" vs 3"	1" vs 2"	2" vs 3"	1" vs 2"	2" vs 3"
Refrigerator	0.0262	**0.2187**	**0.0625**	**0.0956**	**0.1732**	**0.0947**
Humidity Chamber	0.0082	0.0118	**0.5000**	**0.1915**	**0.3416**	0.0194
Fume Hood	0.0027	0.0002	**0.2819**	0.0123	**0.1057**	**0.1046**
Storage Room 130C	2.084E-06	3.225E-05	1.135E-06	0.0006	1.573E-05	0.0008
Room 110A	0.0005	0.0005	**0.1201**	0.0172	**0.6439**	**0.0691**
UDOT Lab	0.0005	0.0028	0.0168	0.0010	**0.2539**	0.0025
Fog Room	**0.0724**	**0.8082**	0.0418	**0.9769**	**0.1484**	**0.7989**

* Fog room had a high CV meaning high p-values could be false due to high variability.

Table 12 P-value Between Different Sand-cement Proportions

	1" Prisms			2" Prisms			3" Prisms		
Days	7	28	56	7	28	56	7	28	56
Humidity Chamber	**1**	**0.5262**	**0.8128**	0.0077	0.0018	0.0161	0.0001	0.0025	0.0023
Fume Hood	0.0011	0.0008	0.0102	0.0079	0.0522	**0.1611**	0.0251	**0.1965**	**0.5997**

Table 13 Relative Humidity Coefficient

	%RH	γ_h
Refrigerator	5%	1
Humidity Chamber	50%	0.89
Fume Hood	35%	1
Storage Room 130C	55%	0.839
Room 110A	29%	1
UDOT	43%	0.9614
Fog Room	100%	0

Table 14 Volume-to-surface Ratio Coefficient

	V/S	γ_{th}	$\gamma_{V/S}$
1" Prism	0.24	1.43	1.17
2" Prism	0.46	1.30	1.14
3" Prism	0.66	1.17	1.11

Table 15 Cement Content Coefficient

	Cement Content	γ_c
Mix 1	1697	1.36
Mix 2	1307	1.22

Table 16 Comparison Between Predicted and Measured Shrinkage Values at 56 Days Stored in Refrigerator and Humidity Chamber Based on ACI Committee 209

		56 Days			
		Prediction	Measured	Error	Square Error
Refrigerator	1” Prisms	2149	1918	-232	53627
	2” Prisms	1903	1703	-200	39804
	3” Prisms	1671	1390	-281	79202
Humidity Chamber	1” Prisms	1913	1393	-519	269718
	2” Prisms	1694	1367	-327	106840
	3” Prisms	1488	1505	17	304

Table 17 Parameters Used for the Calculation of Shrinkage Coefficient for Mix 2

	γ_{cp}	γ_s	γ_f	γ_e	γ_c	Shrinkage Coefficient (MicroStrain)
Refrigerator	2	1	1.1	1	1.22	2094
Humidity Chamber	2	1	1.1	1	1.22	2094

Table 18 Comparison Between Predicted and Measured Shrinkage Values at 56 Days Stored in Refrigerator and Humidity Chamber from Moon and Weiss

		56 Days			
		Prediction	Measured	Error	Squared Error
Refrigerator	1" Prisms	1476	1918	442	194968
	2" Prisms	1015	1703	688	473476
	3" Prisms	644	1390	746	557246
Humidity Chamber	1" Prisms	777	1393	617	380095
	2" Prisms	534	1367	832	692775
	3" Prisms	339	1505	1166	1360279

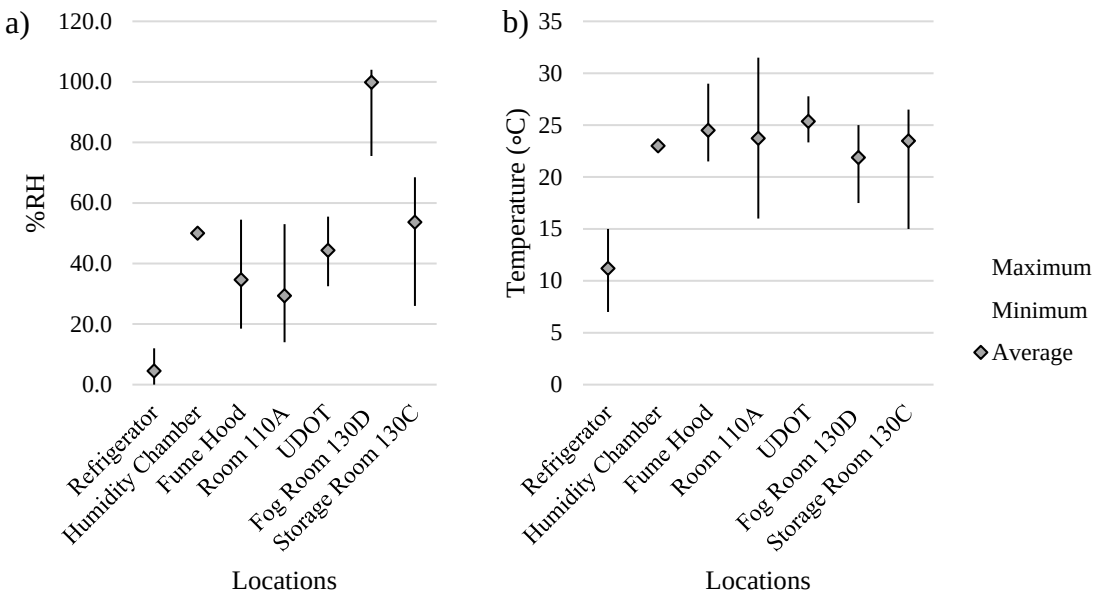

Figure 1. Storing Condition a) %RH Distribution; b) Temperature Distribution

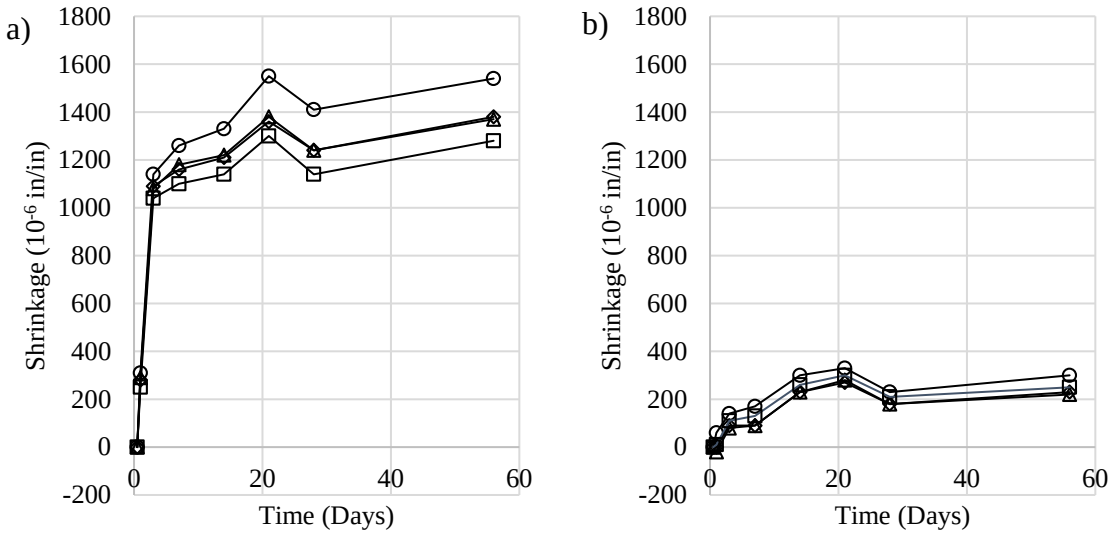

Figure 2. Four 1" Prisms Shrinkage in a) Humidity Chamber; b) Fog Room

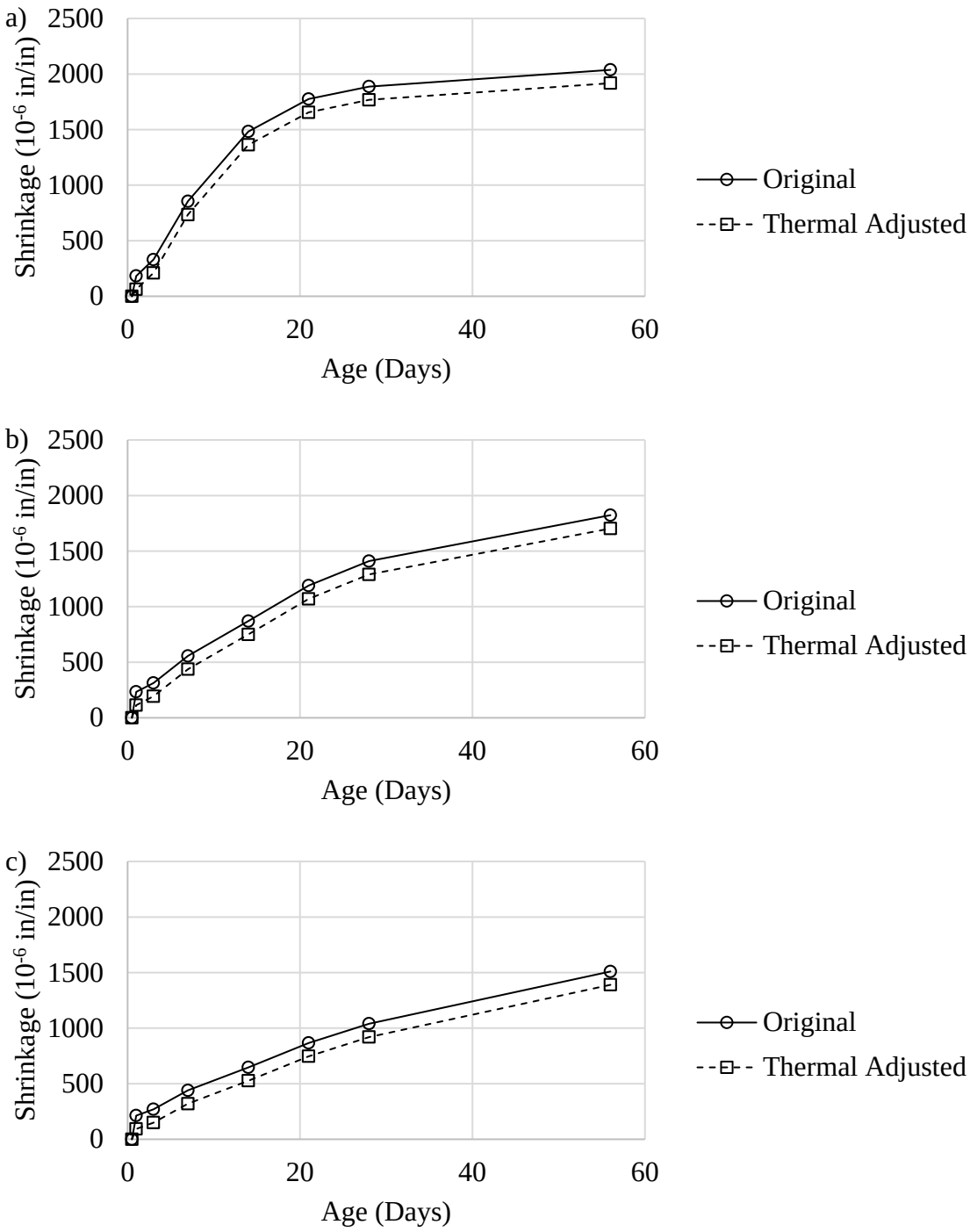

Figure 3. Original and Thermal Adjusted Shrinkage at Refrigerator for a) 1" Prisms; b) 2" Prisms; c) 3" Prisms.

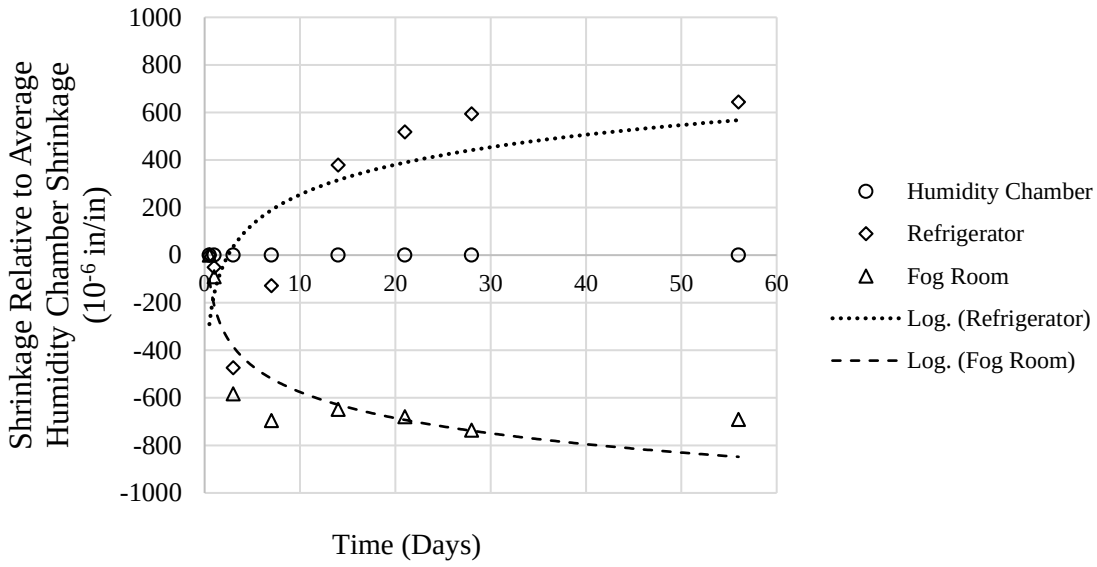

Figure 4. Relative Average Shrinkage for Refrigerator and Fog Room Compared to Humidity Chamber, for 1” Specimens.

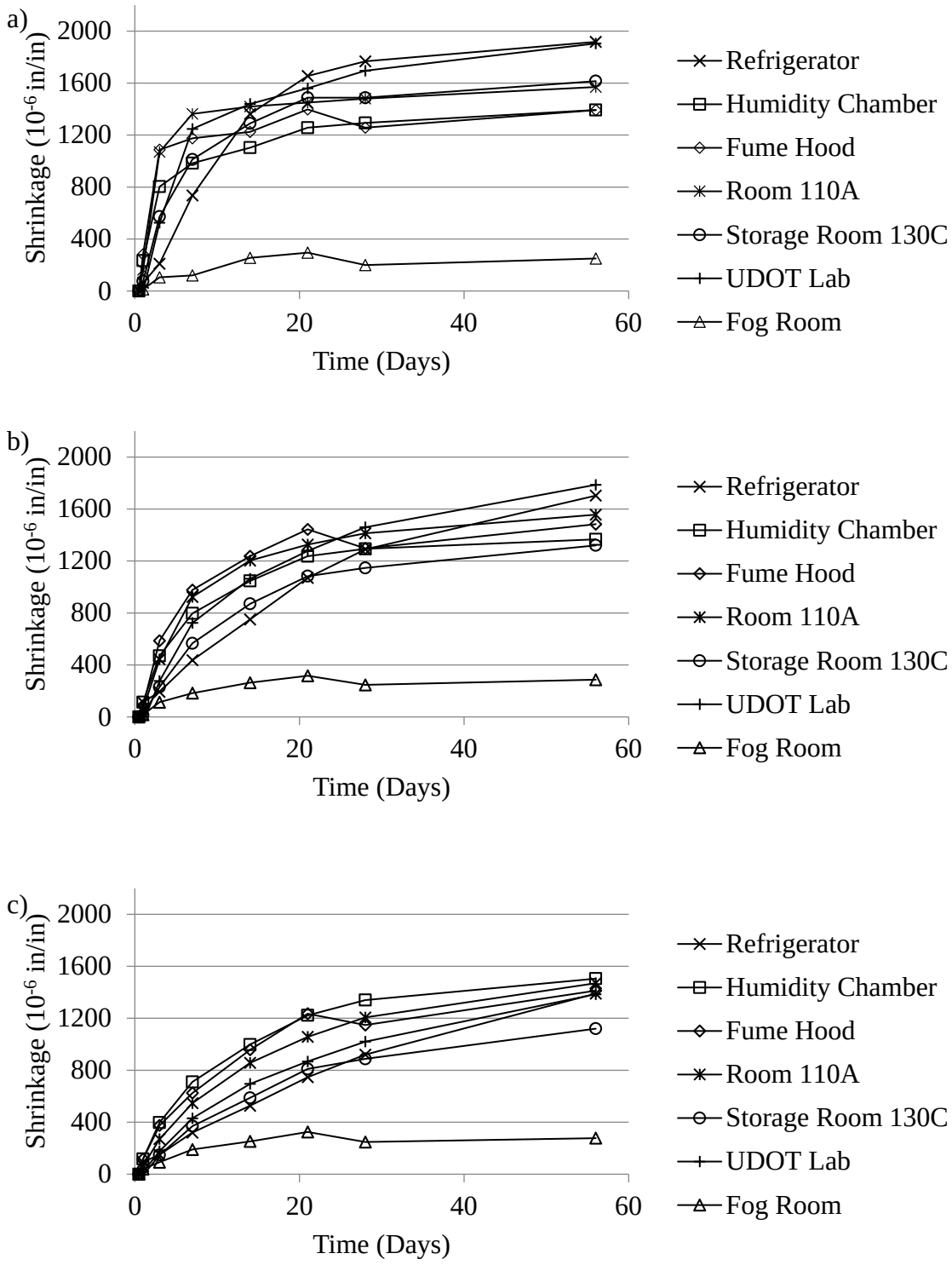

Figure 5. Average Length Change of a) 1”, b) 2”, and c) 3” Prisms at Different Locations for Mix 2.

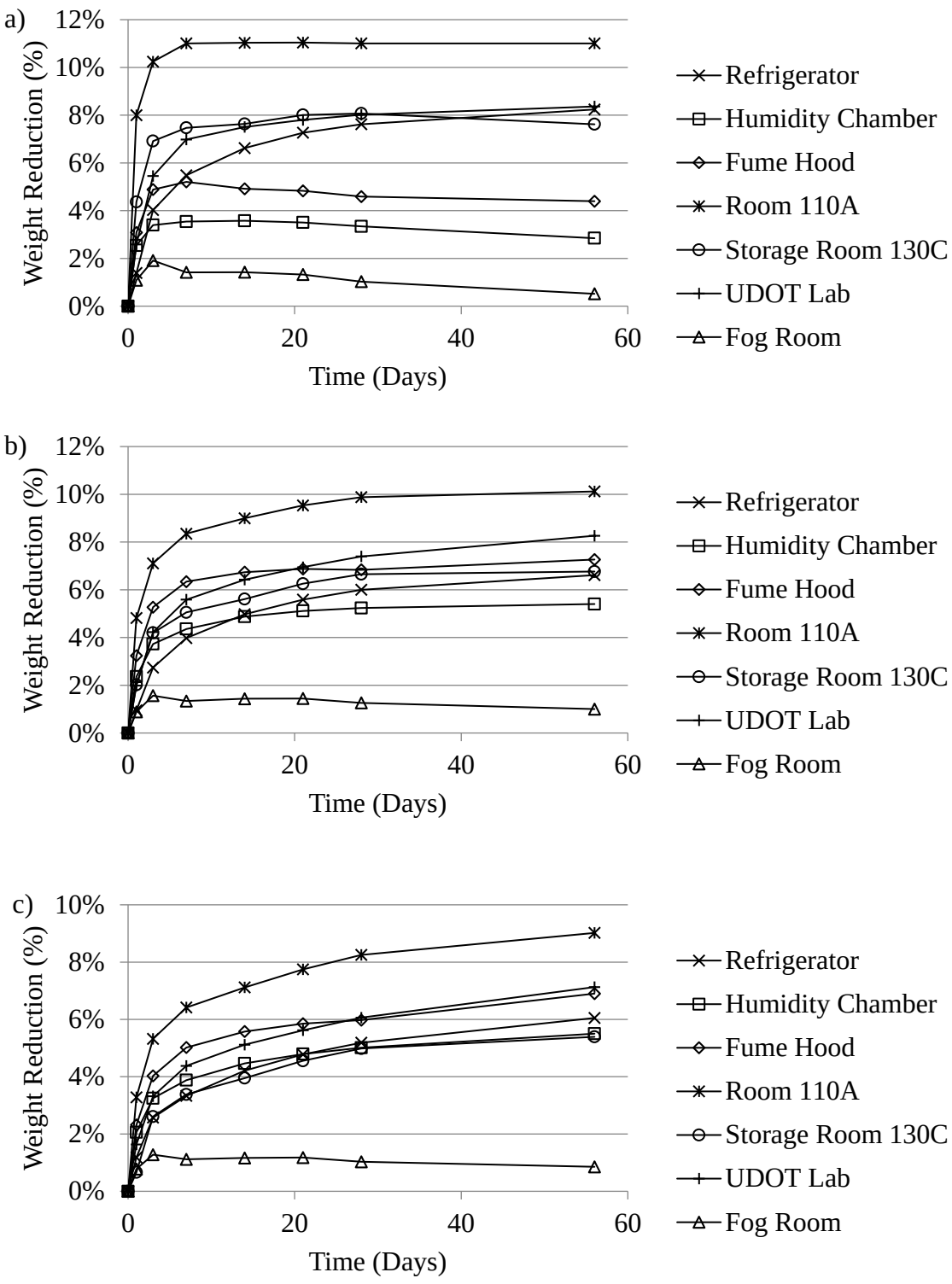

Figure 6. Weight Change of a) 1”, b) 2”, and c) 3” Prisms for Mix 2

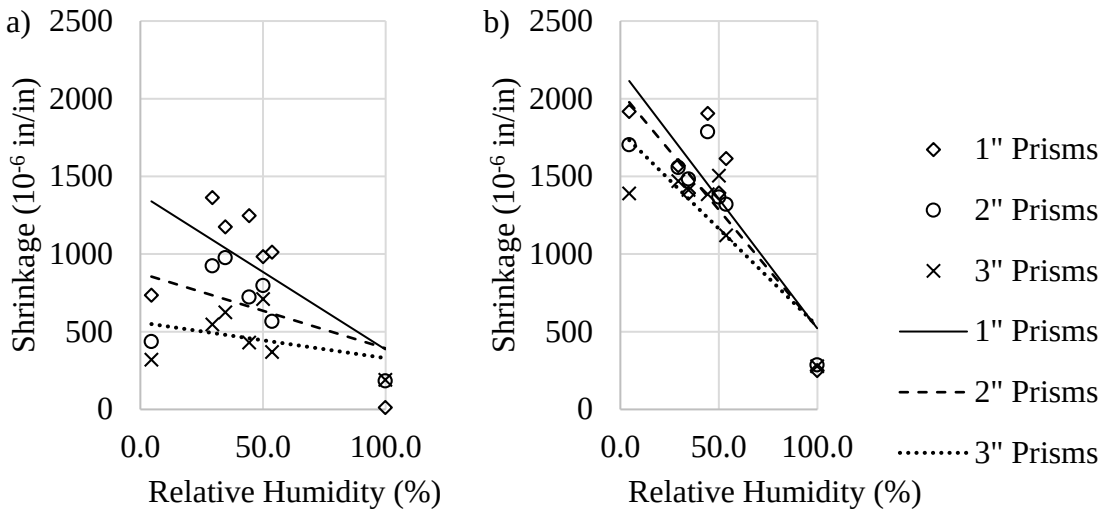

Figure 7. Average Net Shrinkage (After Thermal Adjustment on Refrigerator Storage Samples) versus RH at a) 7 days; b) 56 days

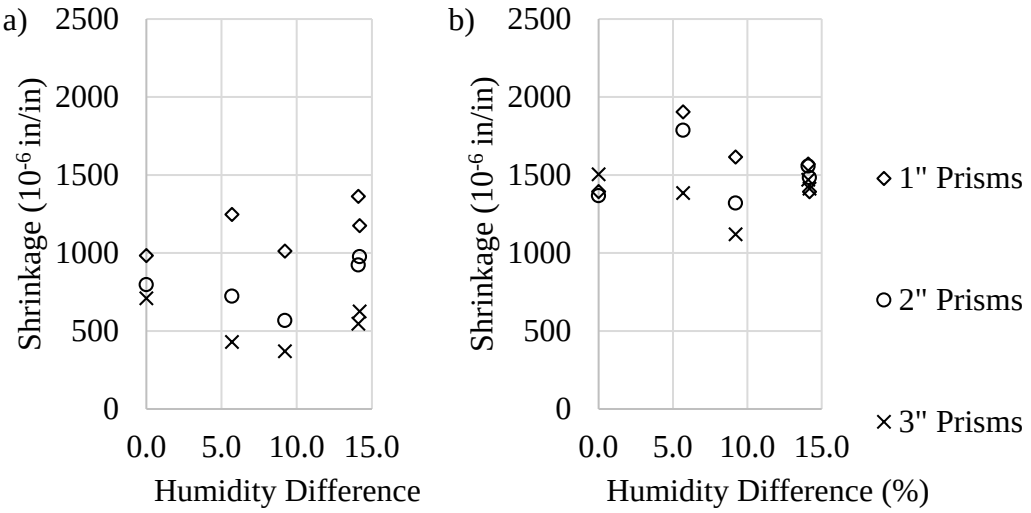

Figure 8. Shrinkage versus RH Fluctuation at a) 7 days; b) 56 days

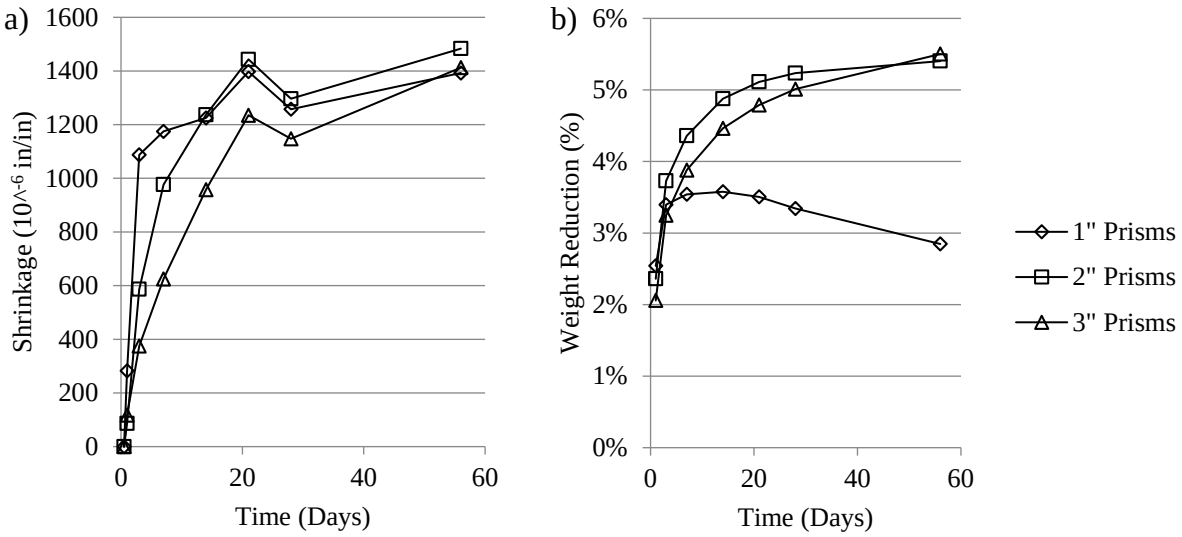

Figure 9. Different Specimen Sizes for Mix 2 Stored in the Humidity Chamber: Average a) Shrinkage and b) Weight Change

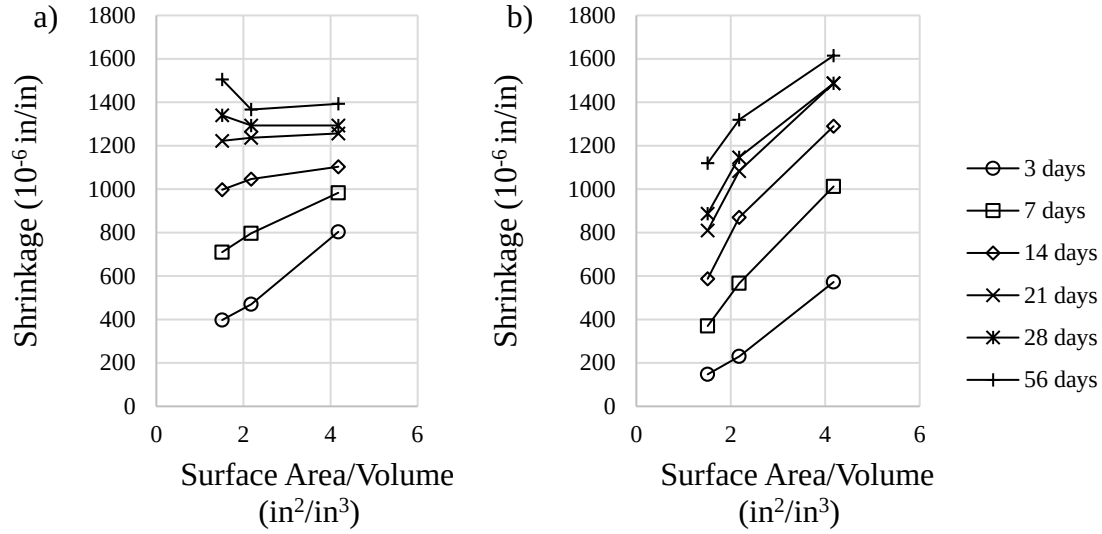

Figure 10. The Influence of Surface-to-volume Ratios for Mix 2 Stored in a) Humidity Chamber; b) Storage Room 130C

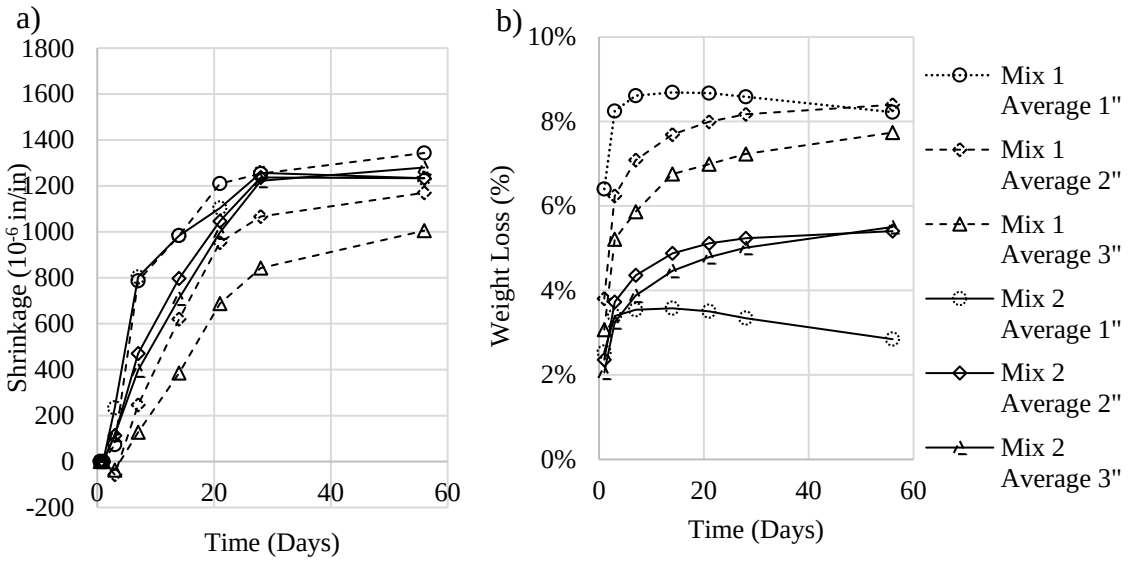

Figure 11. Different Mix Designs in the Humidity Chamber: Average a) Shrinkage and b) Weight Change Comparison

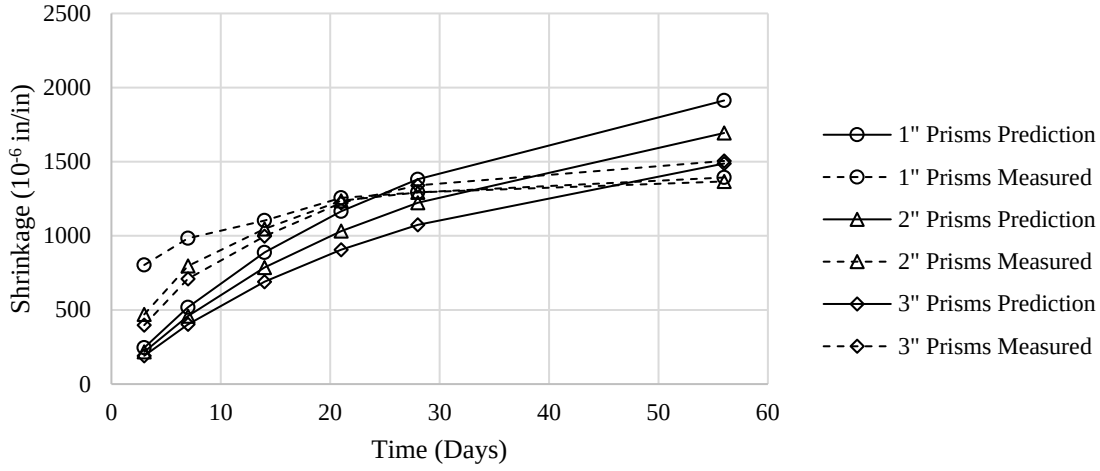

Figure 12. Comparison Between Predicted and Measured Shrinkage Values for Mix 2 Samples Stored in Humidity Chamber at All Ages

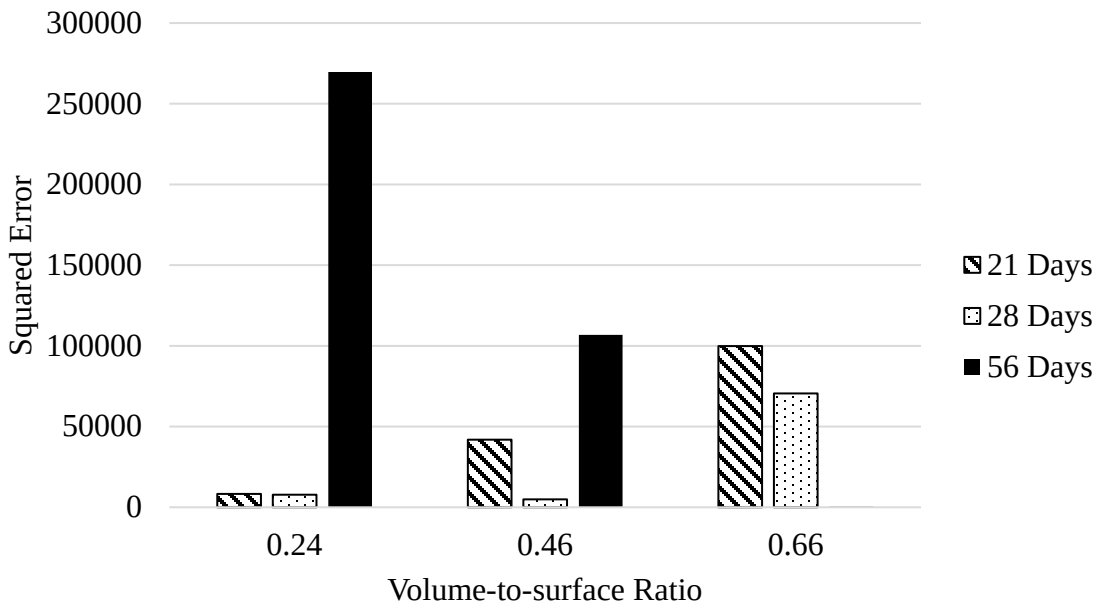

Figure 13. Squared Error versus Volume-to-surface Ratio Plot for Samples Stored in Humidity Chamber at 21, 28, and 56 Days

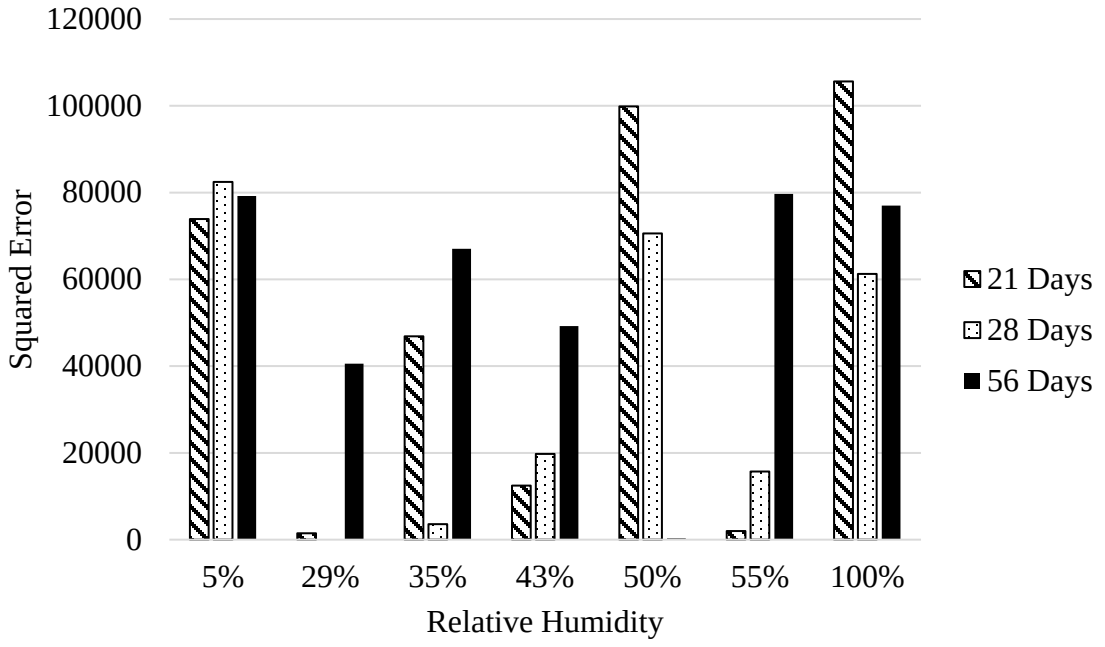

Figure 14. Squared Error versus Relative Humidity Plot for Samples at 21, 28, and 56 Days

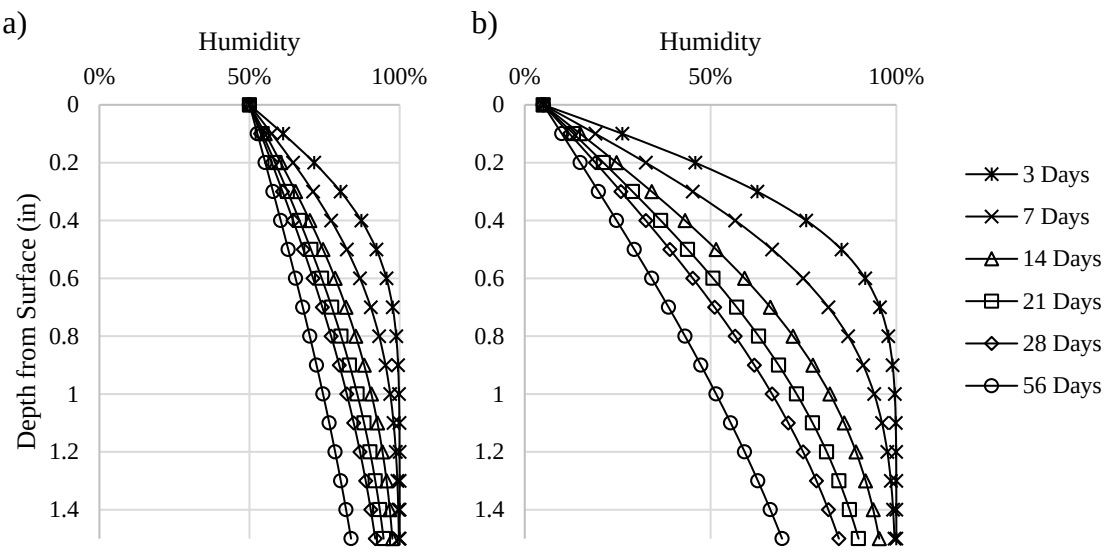

Figure 15. Humidity Change from Surface to Center for 3” Samples Stored in a) Humidity Chamber, b) Refrigerator

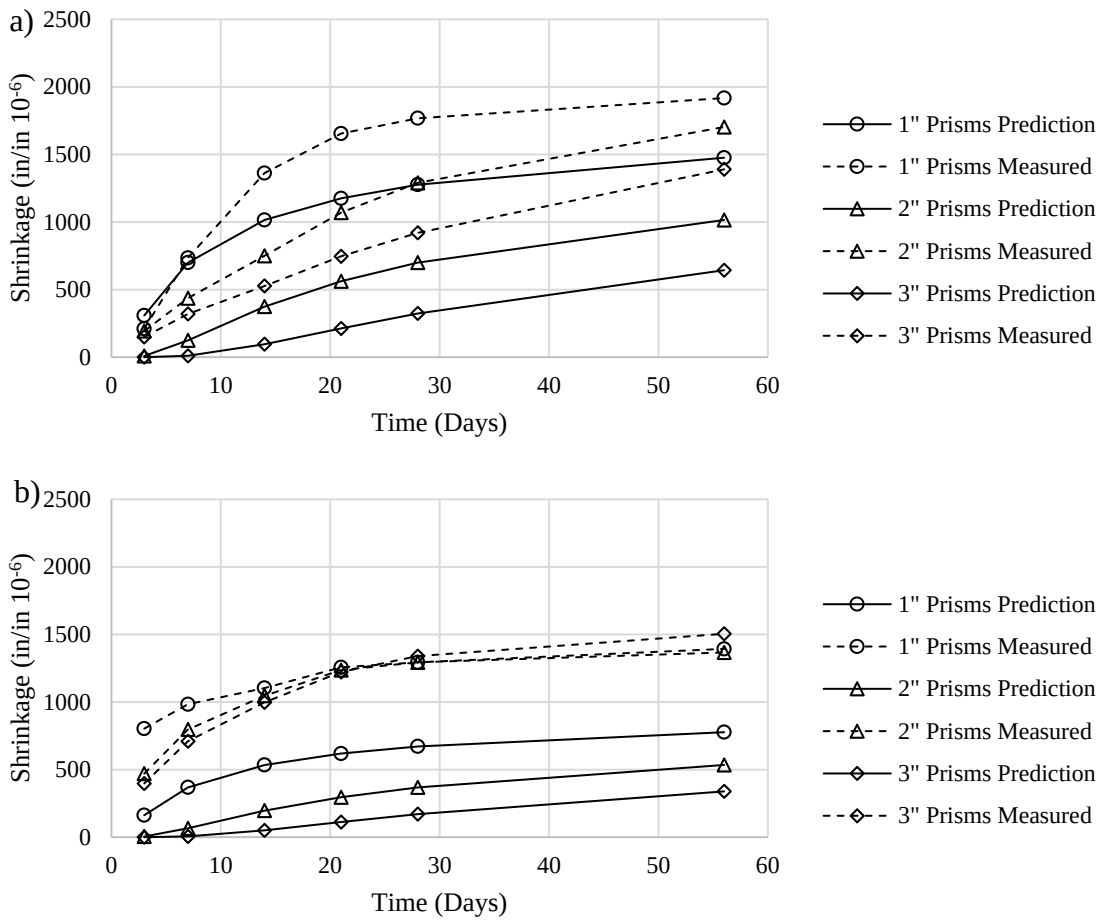

Figure 16. Comparison Between Predicted and Measured Shrinkage Values for Samples Stored in a) Refrigerator and b) Humidity Chamber at All Ages

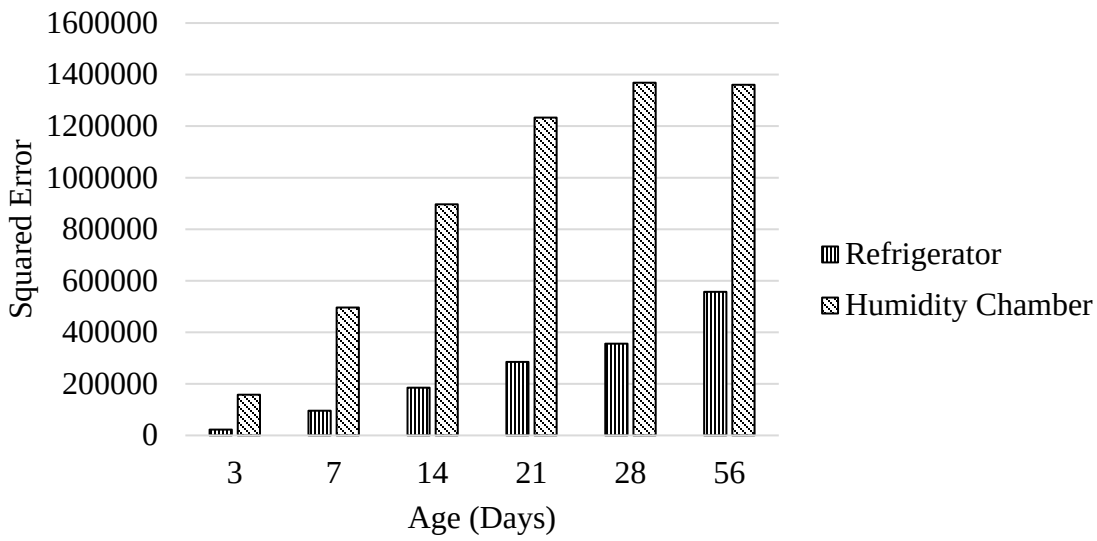

Figure 17. Squared Error versus Storing Ages for 3” Samples Stored in Refrigerator and Humidity Chamber

CHAPTER 3

CARBONATION

Carbonation is a chemical reaction between $Ca(OH)_2$ in concrete and CO_2 in the environment. During this reaction, the product $CaCO_3$ densifies in voids and cracks while also reducing the pH from average values of 12 to 14 down to 8 or 9 in concrete (Li 2011). Carbonation can be harmful if the reaction reaches the depth of steel reinforcement bars and the low pH accelerates corrosion (Klenke 2007). However, Ashraf found that carbonation could increase the compressive and tensile strength of concrete, which is beneficial to structures (Ashraf 2016).

Phenolphthalein is commonly used to determine the depth of concrete carbonation. It is a pH indicator, which will change to pink or purple at the location of the concrete that has a pH value of 9 or more. Carbonation reaction causes a lower pH of 8.2 leading to a colorless section on the surface of the concrete sample where phenolphthalein is applied. In the 1990s, thermo-gravimetric analysis (TGA) was introduced as a more accurate method for the analysis of concrete carbonation (Klimesch and Ray 1997). In this chapter, concrete carbonation depth and rate are described by analyzing samples at different depths and exposure ages using TGA along with other techniques.

3.1 Carbonation Reaction

The carbonation rate for concrete mainly depends on the concentration of CO_2. Cui et al. found that a high concentration of CO_2 in the surrounding environment of concrete would initially increase the carbonation rate; eventually, the $CaCO_3$ fills up surface pores, causing the permeability and the subsequent carbonation rate to significantly decrease (Cui et al. 2015). Salvoldi et al. studied the relationship between oxygen permeability and carbonation and they found that carbonation rate decreases with the decrease of concrete permeability (Salvoldi et al. 2015). It was also found that the most important influence of RH is within the range of 50% to 70% (Ekolu 2016). It was also mentioned that a widely-used carbonation prediction equation is a logarithmic relation with time as shown in Equation (7) (Köliö et al. 2016; Salvoldi et al. 2015).

$$x = k * \sqrt{t} \tag{7}$$

where,

x: carbonation depth, mm;

k: carbonation coefficient, mm/yr;

t: exposure time, yr.

3.2 TiO_2 Properties

TiO_2 has been studied since 1960s as a photocatalytic material to reduce air pollutants (A. Fujishima 1969). TiO_2 reacts with water in the air under UV light, generates H^+ and OH^- (Fujishima et al. 2000), which reacts with NO_2 to purify air.

In recent years, researchers have applied titanium dioxide on construction materials such as concrete since this material covers a large portion of the earth's surface area (Ballari and Brouwers 2013; Chen and Poon 2009; Maggos et al. 2008; Shen et al. 2012). Researchers have noted that the measured TiO_2 reactivity is reduced due to the carbonation reaction occurring in concrete (Chen and Poon 2009). Recently, studies have showed that the carbonation rate accelerates with the addition of Lime-TiO_2 (Karatasios et al. 2010) and there is a decrease of carbonation for geopolymer specimens with the addition of TiO_2 (Duan et al. 2016).

In this study, the rate of and depth of carbonation for mortar mixtures is investigated, in particular to understand if a mortar specimen with a surface TiO_2 coating, not just one containing embedded TiO_2 particles, would have a different carbonation rate than plain concrete. Specimens were exposed in the natural outdoor environment and carbonation is quantified at 23, 59, and 100 days of weathering and at 5 mm increments from the exposed surface. The concentration of titanium dioxide was measured with a scanning electron microscope (SEM) and energy dispersive x-ray spectroscopy (EDS). The carbonation amount was determined with TGA and mass spectrometry (MS). Although phenolphthalein is a traditional method, it does not give an accurate value for the carbonation depth or amount so it was not included in this study.

3.3 Methodology and Materials

This study investigates the influence of a micron-size CristalACTiV^{TM} P105 titanium dioxide powder added at 1% mass fraction of cementitious material, as well as a spray-on sol-gel solution composed of titanium dioxide called PURETi Coat. Both TiO_2 materials

have been previously verified to be highly photocatalytic (Hanson 2014; Shen et al. 2012). A local ASTM C150 classified Type I/II/V cement from LaFarge Holcim's Devil's slide plant was used for this study along with a natural sand from Staker Parson's Beck street plant that meets the ASTM C33 standard. A polycarboxylate W.R. Grace's Advacast 575 high range water reducer was used to adjust the workability so all mixtures exhibited similar flow.

Three batches of specimens were made in the University of Utah Concrete Lab by another graduate student[1]. These samples consisted of a plain mortar, a PureTi coated mortar, and a TiO_2 embedded in mortar. It was assumed the plain and PureTi samples contained the same mortar mixtures. Additionally, the TiO_2 embedded specimens were prepared to have 1% of the total cementitious weight replaced by a TiO_2 powder.

The specimens were 2" x 4" cylinders (diameter of 2", height of 4") mixed and prepared by another graduate student[1] in Fall 2015. The specimens all had a painted epoxy resin on the top and bottom of the cylinder to prevent carbonation from the ends and to have carbonation only in the horizontal radial direction. The specimens were said to be air cured in the lab for 7 days before exposure to the natural outdoor environment. The samples containing the spray-on TiO_2 coating had two coats of the PURETi Coat applied at 4 days into the curing.

The outside environment for storing the specimens was located on the white painted asphalt roof of MCE building as shown in Figure 18a. Specimens with the same TiO_2 batch were placed roughly 2 inches apart on the roof as shown in Figure 18b; each set of the specimens from different TiO_2 batches was kept at least 3 feet apart to avoid interaction between possible local air reactions. Eight specimens are taken for

[1] Catalina Arboleda was in our research group and prepared these samples

measurement of carbonation depth at each testing age. The specimens collected are wrapped in plastic cling wrap to keep from further contact with air until tested. A CO_2 exposure level data during the exposure period was obtained from University of Utah Atmospheric Trace Gas & Air Quality Lab (UATAQ Lab) as shown in Figure 19. A corresponding RH level from the Weather Underground Website (The Weather Company 2015) is shown in Figure 20. The average RH during this time frame was 45%.

3.4 Experiments

3.4.1 Verifying TiO_2 Content

To find the amount of TiO_2 in the specimens, the EDS with a SEM in the University of Utah Nanofab Lab was used to map and quantify chemical elements on the surface of polished specimens.

The sample preparation for SEM/EDS follows four different procedures: sawing, epoxying, polishing, and carbon coating (Goldstein 2003). Specimens were removed from the roof at ages 23, 59, and 100 days. Another graduate student[2] used a tile saw to cut an interior sample; cut samples were then stored in amber glass containers to prevent the exposure to UV lights, with ethanol to prevent additional hydration. For this research, after all the samples were collected, they were further prepared for use in the SEM/EDS analysis. Sample epoxy, polishing, and carbon-coating procedures are listed in Appendix H. An example of the final specimen used in the SEM/EDS can be seen in Figure 21.

The FEI Quanta 600F SEM/EDS testing machine in the Utah Nanofab Surface Analysis Lab was used for mapping and chemical analysis. The general SEM settings

[2] Catalina Arboleda cut those samples.

followed the Federal Highway Administration Research and Technology manual (Walker et al. 2006). The chamber pressure remained in default “HiVac” mode, which was about 1.93E-7 to 1.93E-8 psi. The SEM was used to identify the cement phases and avoid aggregate phases. Three different locations were selected from the cement locations to be analyzed with the EDS, since TiO_2 was expected to only be mixed in cement phase.

An example of the spot location identification is shown in Figure 22. At each of these spot locations, the magnification was increased approximately 1000x from the SEM image to perform the EDS analysis for a chemical composition map and quantification, shown in Figure 23 and Figure 24, respectively. It is possible that some of the sample locations may still have some small portion of fine aggregates included in the analysis. These can be seen in Figure 23 of each composition map, where there is an absence of calcium and a higher concentration of silica.

3.4.2 Carbonation Estimation

Measurement for the carbonation depth was taken at roughly 23 days, 51-59 days, and between 92-100 days of exposure. The TGA was coupled with a mass spectrometry (MS) to analyze specifically the amount of carbon dioxide associated with the specimens.

TGA is a micro-characterization technique that measures the simultaneous mass loss associated with chemical reactions or decomposition as the temperature rises. The differential thermo-gravimetric (DTG) measurement indicates the change in mass loss associated with specific temperatures. This is used to identify when specific decomposition, such as calcium hydroxide $Ca(OH)_2$ or calcium carbonate, may be occurring in the concrete specimen. Synchronizing MS to the TGA/DTG allows us to

correlate the ion current while the sample is heated in the TGA, from which specific gases, such as water or carbon dioxide, can be measured as they leave the sample. The MS and TGA combined will both be used to confirm the quantity of $CaCO_3$ found in the samples at various ages and depths.

For the purposes of this research, it was assumed that the cement powder came from a cut piece from the interior of the cylinder, from which the cut sample was crushed and sieved to eliminate most of the sand particles for TGA analysis. The powder was stored in 2 mL amber glass vials until tested in the STD Q500 Simultaneous TGA/STD equipment in a University of Utah Chemistry Department laboratory. The temperature was set to increase at a rate of 20 °C/min from room temperature to 1000 °C.

Li noted that at roughly 470 °C, $Ca(OH)_2$ would burn off; anywhere from 700 °C to 1000 °C, it is expected that calcium silica hydrate and calcium carbonate would decompose, or possibly at these higher temperatures the CO_2 might recombine with water (Li 2011). Taylor mentioned that the decomposition temperature of $Ca(OH)_2$ is from 425 to 550 °C, while above 550 °C, the loss of CO_2 and dehydration of calcium-silica-hydrate gel exist at the same time (Taylor 1997). From the DTG graph, the starting and ending points of these decompositions were identified from the graph, as shown in Figure 25 for TGA and Figure 26 for MS. The corresponding mass at each temperature or time for these boundary points was used to calculate the amount of material that burned off. Equation (8) and (9) show the calculation of $Ca(OH)_2$ and $CaCO_3$ amounts based on the mass loss and the original sample mass at room temperature. All the raw EDS results and TGA figures are shown in Appendix I and Appendix J, respectively.

$$Ca(OH)_2\ estimate = \frac{74.1 \times Weight\ Loss}{18 \times Sample\ Weight} \quad (8)$$

where,

74.1 is the molar weight of $Ca(OH)_2$, 18 is the molar weight of water.

$$CaCO_3\ estimate = \frac{100.1 \times Weight\ Loss}{44 \times Sample\ Weight} \quad (9)$$

where,

100.1 is the molar weight of $CaCO_3$, 44 is the molar weight of CO_2.

3.5 Results

3.5.1 Chemistry Composition

The analysis from the SEM/EDS verified that there were negligible quantities of titanium dioxide found in the plain concrete samples and PureTi coated samples. The 1% TiO_2 samples were verified to contain around 0.79% on average of TiO_2, as shown in Table 19.

3.5.2 Carbonation Quantity

The carbonation quantity results were obtained and analyzed by the calculation from TGA/MS figures and the two equations mentioned before. To analyze the carbonation, $CaCO_3$ estimation figures along with exposure age and tested depth were created as shown in Figure 27 and Figure 28, respectively.

Figure 27 showed the carbonation amount versus age. Based on TGA and MS results

at 5 mm depth, carbonation amount increased gradually with age; at 15 mm depth, the amount of carbonation remains at low regardless of age. Comparing the carbonation for different specimens, those with photocatalytic materials indicated even more carbonation on the surface at the later age than plain concrete. This affirms the hypothesis indicating that carbonation is greater with TiO_2.

When analyzing the carbonation amount versus depth in Figure 28, the carbonation amount decreases with depth but is still higher at longer exposure ages. By the 90 to 100 days' exposure age, carbonation amount is higher for those specimens containing TiO_2 than plain mortar.

3.6 Summary and Findings

The study was focused on the carbonation depth and rate of mortar in the presence of a photocatalytic material. SEM/EDS were used to confirm the amount of embedded TiO_2, and TGA/DTG and MS were used for carbonation quantity analysis.

From the analyzed results, plain concrete mortar samples had less carbonation even in a long exposure age compared with mortar samples with photocatalytic TiO_2 either embedded or sprayed on. Carbonation was confirmed to be higher near the sample surface and at later ages.

The results may lead to a possible demand for carbonation-resistant mix designs, pre-carbonated mixtures, or alternative backing construction materials for the application of TiO_2 in the future. By negating the influence of new carbonation on TiO_2 surfaces, the reactivity for reducing smog by the TiO_2 is expected to be long-lasting.

Table 19 Percentage Amount of TiO_2 Based on EDS of Three Locations

	Plain Concrete		PureTi		1% TiO_2	
Age (Days)	59	100	59	100	51	92
Minimum	0%	0%	0%	0%	0.65%	0.74%
Maximum	0%	0%	0%	0%	0.79%	0.96%
Overall Average	0%		0%		0.79%	

a) b)

Figure 18. a) Location on Roof Where Samples Were Stored During Exposure to Outside Environment. Image from Google maps. b) Arrangement of Cylindrical Samples of Similar Mix Design at Each Location.

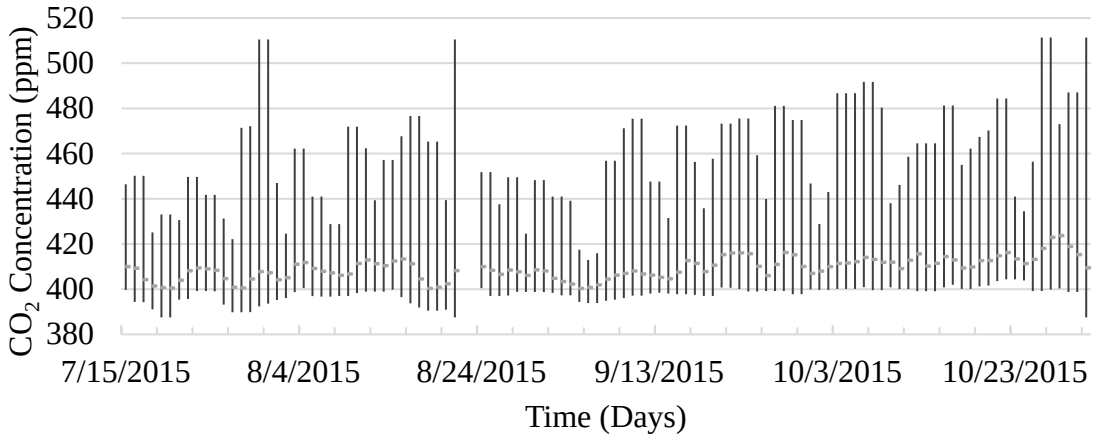

Figure 19. Daily CO_2 Exposure Level in University of Utah from UATAQ Lab

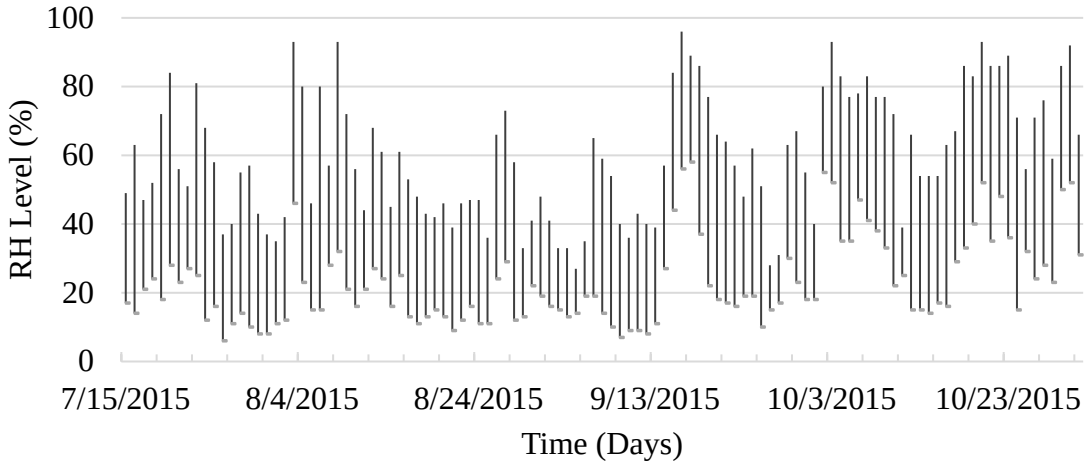

Figure 20. Environmental RH Level During Exposure Days

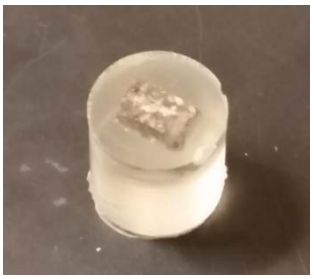

Figure 21. Photograph Sample After Epoxy-impregnation for SEM/EDS Analysis.

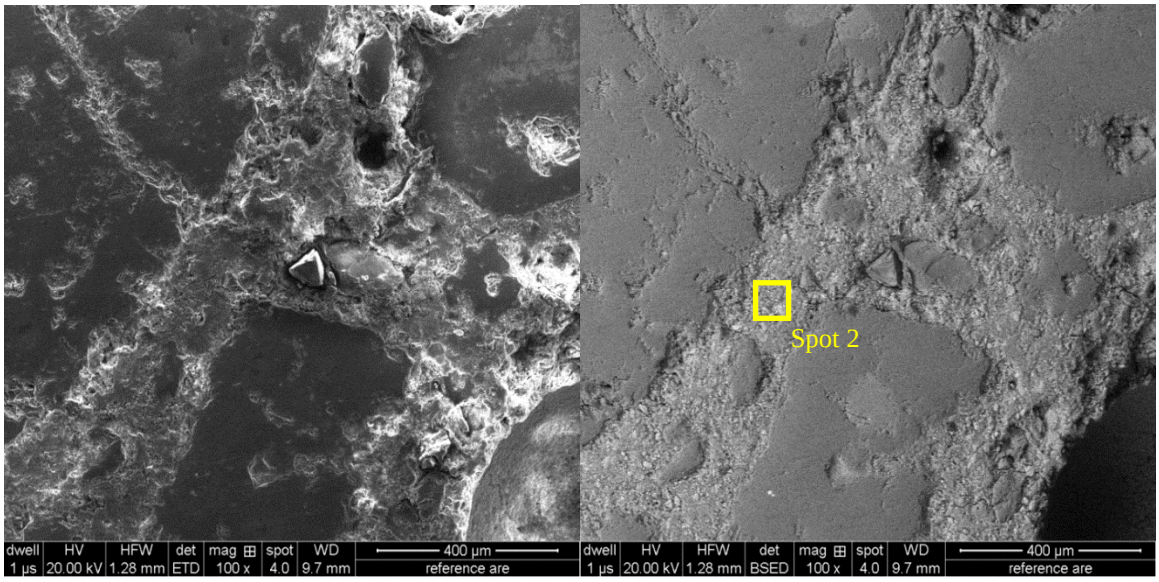

Figure 22. Example of an SEM Secondary Electron and Back-scatter Electron Image for Selecting a Spot in the Cement Phase. The Sample Shown Represents Spot 2 on the 1% TiO_2 Specimen.

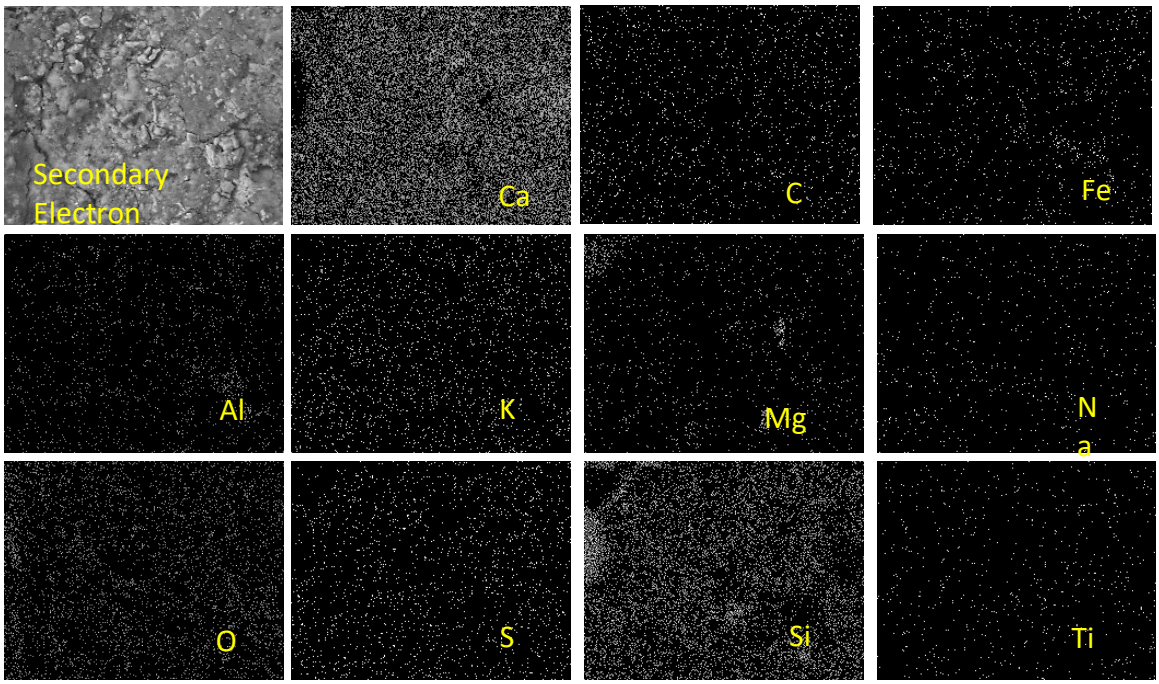

Figure 23. Map of Each Chemical Element Distributed on the Surface of the Spot Image, Superimposed on the Secondary Electron Image. Sample Shown Is from Spot 1 of the 1% TiO_2 Specimen.

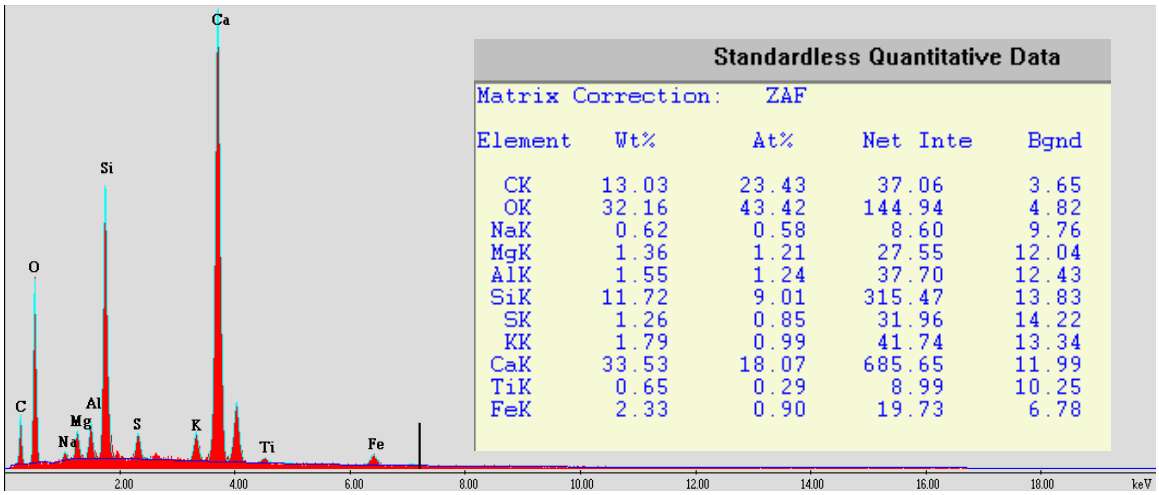

Figure 24. Example of the EDS Analysis Output Showing Quantities of Each Chemical Element Found for Spot 1 of the 1% TiO_2 Specimen

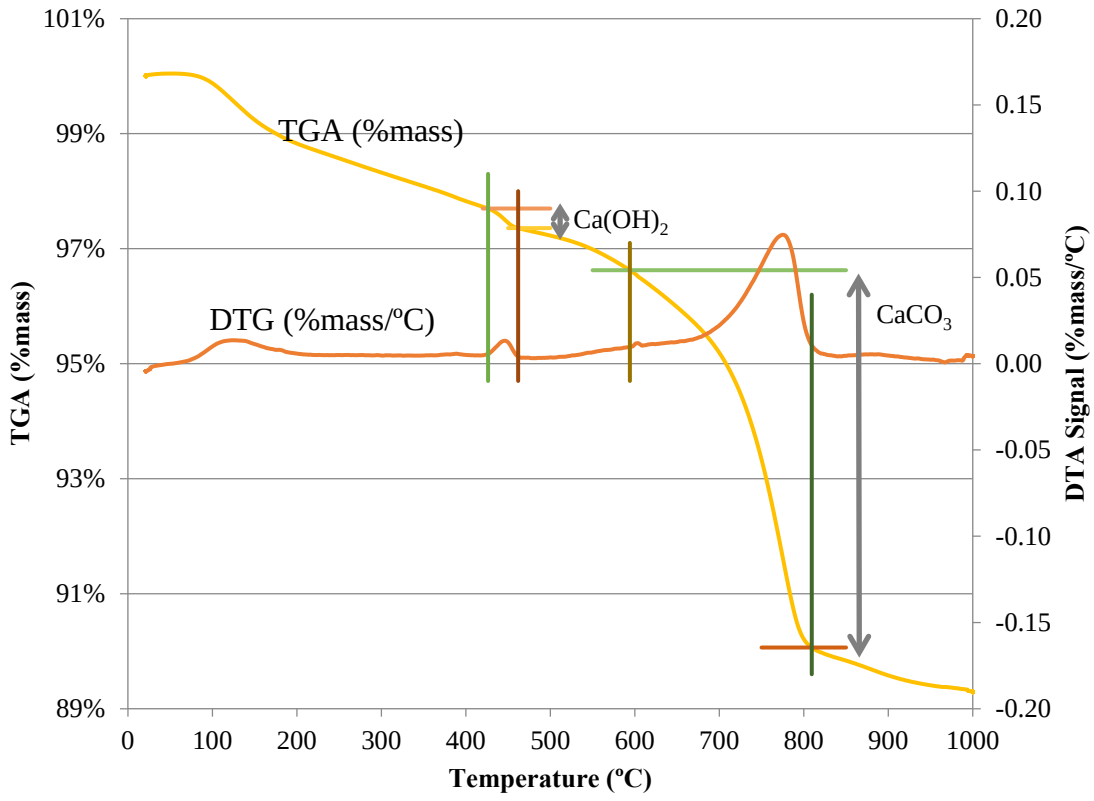

Figure 25. TGA and DTG Plot Along with Indication of Temperatures Selected to Determine Mass Loss. Sample Shown Is from the Top 5 mm of the Plain Concrete After 100-days Exposure.

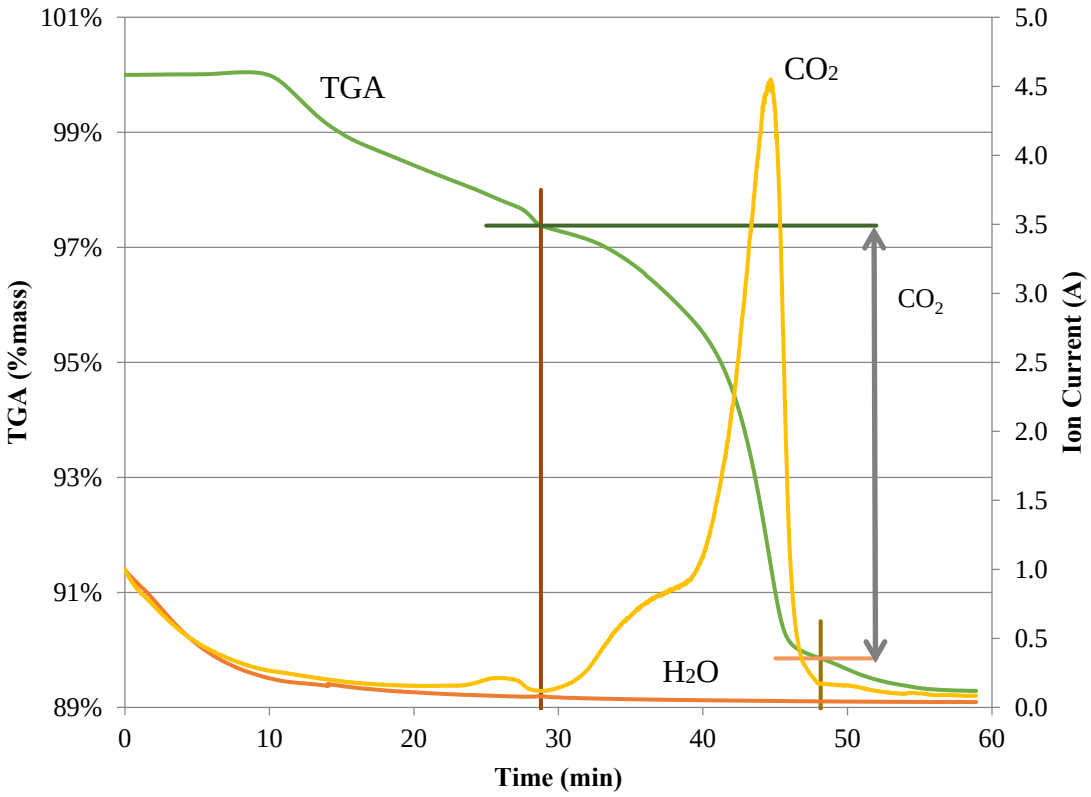

Figure 26. Mass Spectroscopy Plot Along with Indication of Times Selected to Determine Mass Loss. Sample Shown Is from the Top 5 mm of the Plain Concrete After 100-days Exposure.

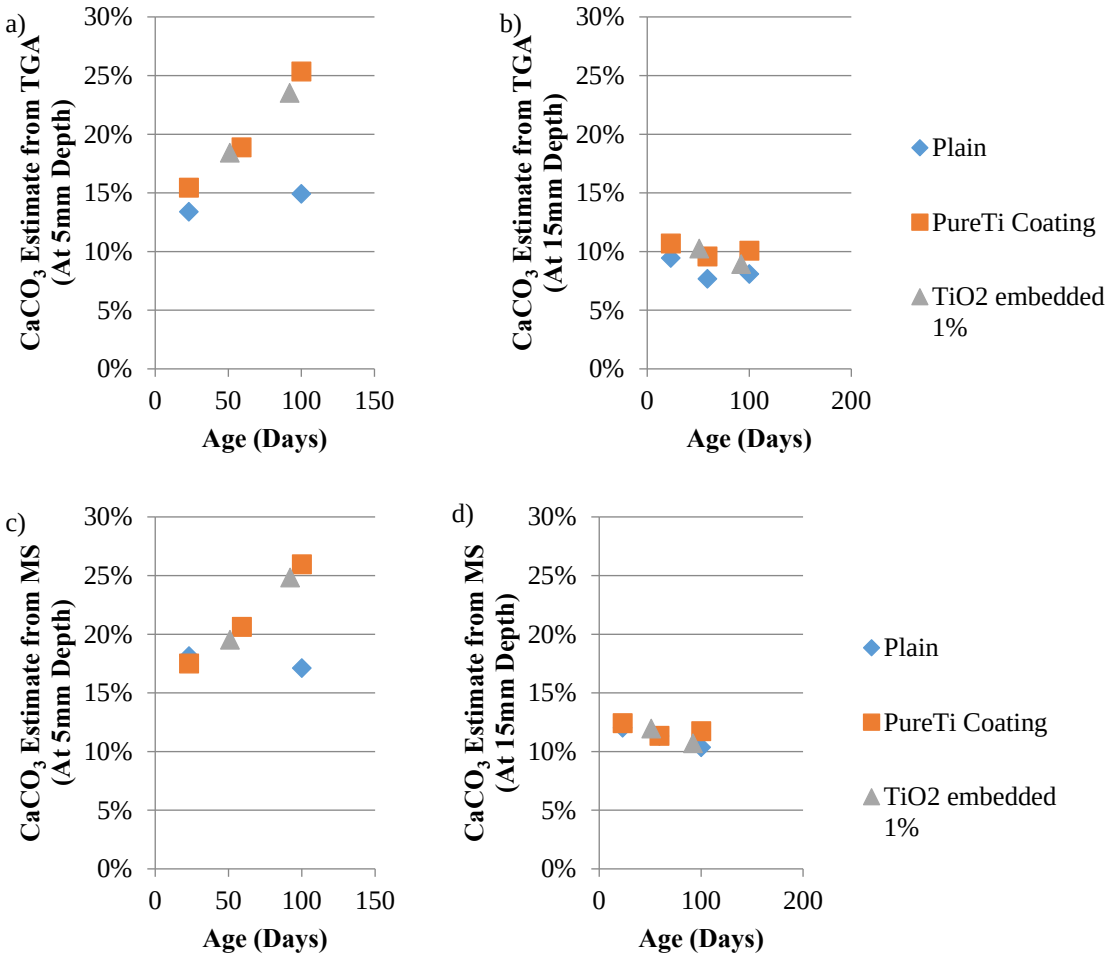

Figure 27. Carbonation Amount versus Age Based on a) and b) TGA; c) and d) MS

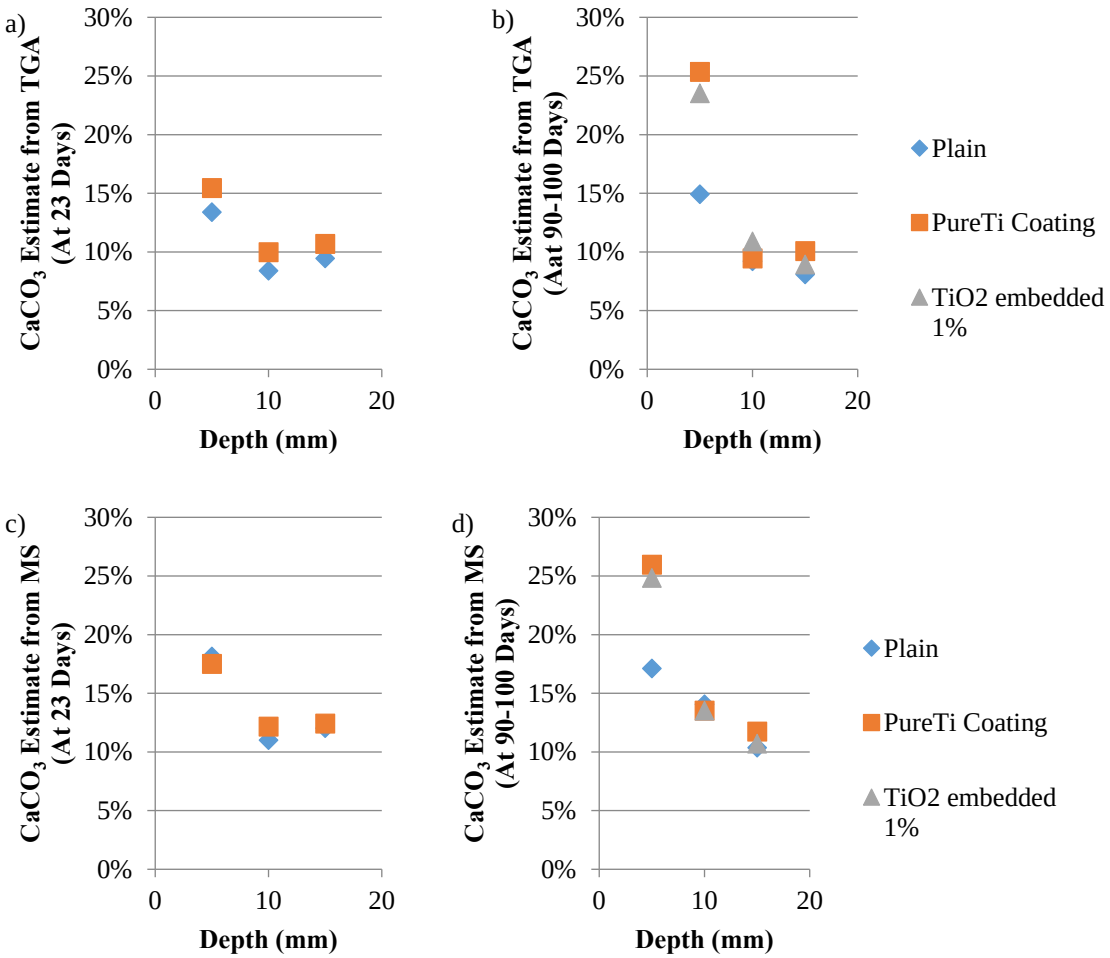

Figure 28. Carbonation Amount versus Depth Based on a) and b) TGA; c) and d) MS

CHAPTER 4

CONCLUSION

4.1 Conclusions and Suggestions

Two specific cases regarding shrinkage and carbonation were investigated to find out the influence from environmental conditions on mortar mixtures. As for the prevention of concrete distresses, the environmental exposure was found to be a dominant influence on shrinkage, and with the combination of other chemical reactions from TiO_2, this environmental effect may be enhanced.

Regarding mortar shrinkage, it is observed that a high humidity environment will be ideal for lowest shrinkage since concrete loses less water in a highly humid environment. This study found the existing standard 1” prism sizes (with a high surface area to volume ratio) had the least amount of shrinkage compared to 2” and 3” prism sizes, while 3” prisms are less sensitive to different humidity environments. Two concrete shrinkage prediction models were also used for the comparison between the predicted and measured shrinkage values; it was found ACI committee 209 prediction model has a lower overall sum of squared error when predicting shrinkage in the 50% humidity chamber storage. The Moon and Weiss model had a lower sum of squared error for predicting shrinkage in a 5% humidity refrigerator storage. Overall, future laboratory testing parameters can be selected and recommended to reduce variation in measured shrinkage values from

different laboratory storage environments.

From the carbonation study, mortars with TiO_2 photocatalytic materials embedded or applied to the surface were both found and confirmed to have more carbonation amount near the surface and at long exposure ages compared to mortar without TiO_2. Although carbonation may be beneficial to protect the interior mortar and increase strength, the faster rate of carbonation with the TiO_2 may lead to sooner reduced efficiency in the photocatalytic capability and can also lead to sooner corrosion of any interior steel.

4.2 Further Studies

These studies were only two specific cases regarding concrete distress. However, this study has limitations regarding the concrete shrinkage: the temperature influences and different water/cement ratios for shrinkage were not studied in this thesis. For the carbonation study, the traditional phenolphthalein method was not analyzed for comparison with the TGA and MS methods used to confirm the carbonation trends. Furthermore, only a small amount of samples was measured for the carbonation study so no statistical analysis can be concluded now.

A recommendation for additional shrinkage tests would be to have more replicates of the specimens for a more precise statistical result. A moist curing age from 0 to 28 days can be varied, as well as different water/cement ratios and other mixture proportions could also be studied. A study regarding concrete with coarse aggregates could also be created to understand the concrete shrinkage effect at different environments.

Additional studies for the carbonation tests include performing a strength test at each age to see if the TiO_2 also effects strength along with carbonation rate. More samples

could be tested at each age and each depth for a better statistical analysis to be calculated. Furthermore, the phenolphthalein method could be used for verification of the carbonation rate trend seen.

APPENDIX A

TEMPERATURE, %RH, AND DAILY FLUCTUATION FIGURES

In Appendix A, the temperature and relative humidity data for all storing locations recorded every 10 minutes through whole storing time was plotted, as well as the daily temperature and humidity fluctuation.

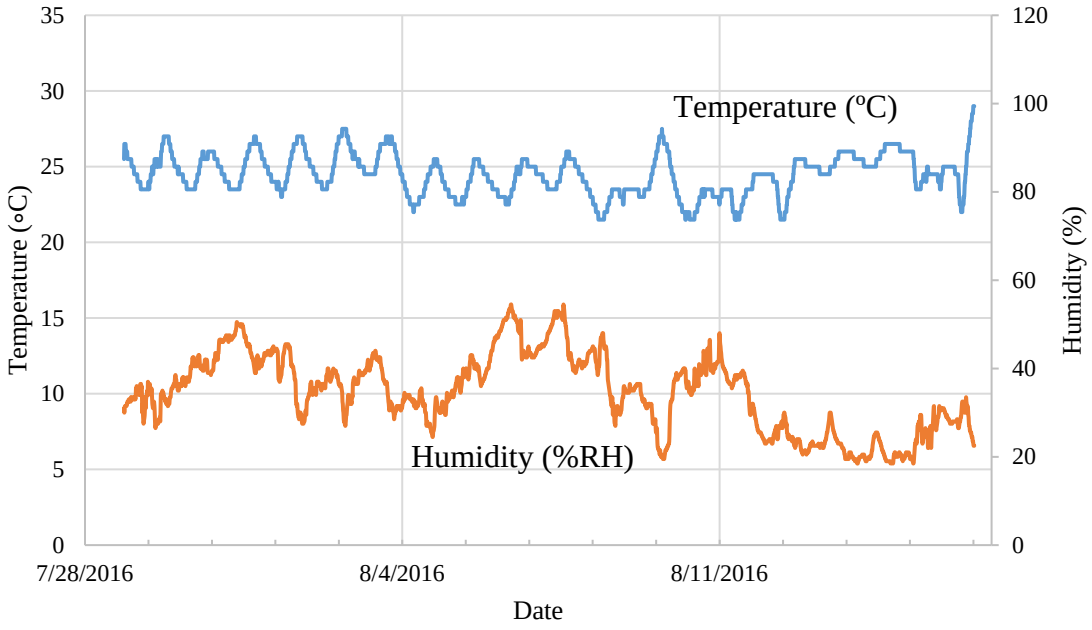

Figure 29. Temperature and Humidity Data in Fume Hood

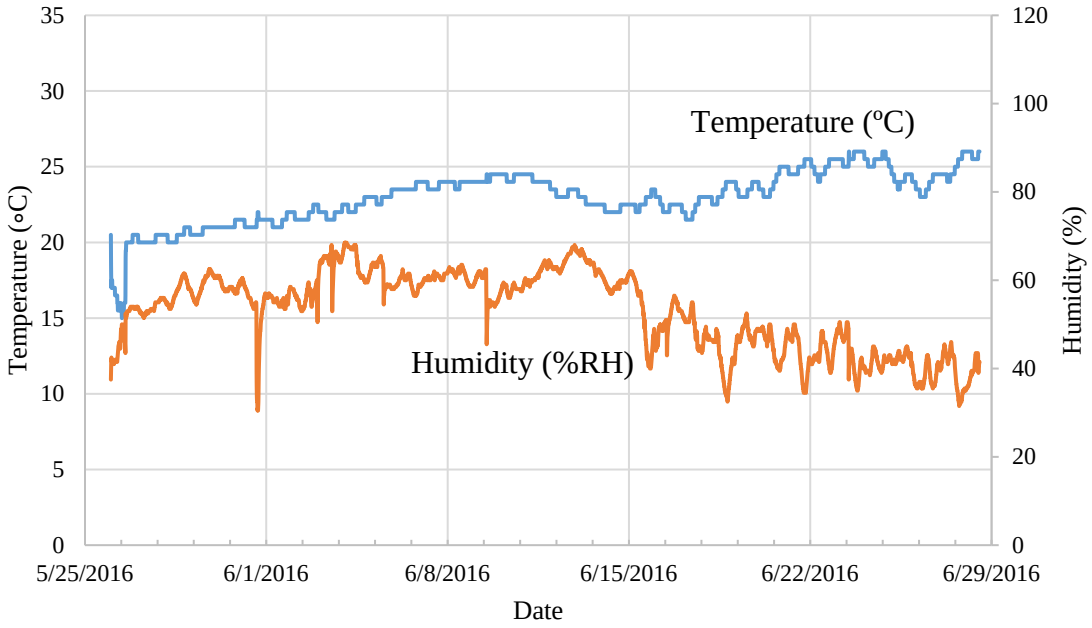

Figure 30. Temperature and Humidity Data in Storage Room 130C

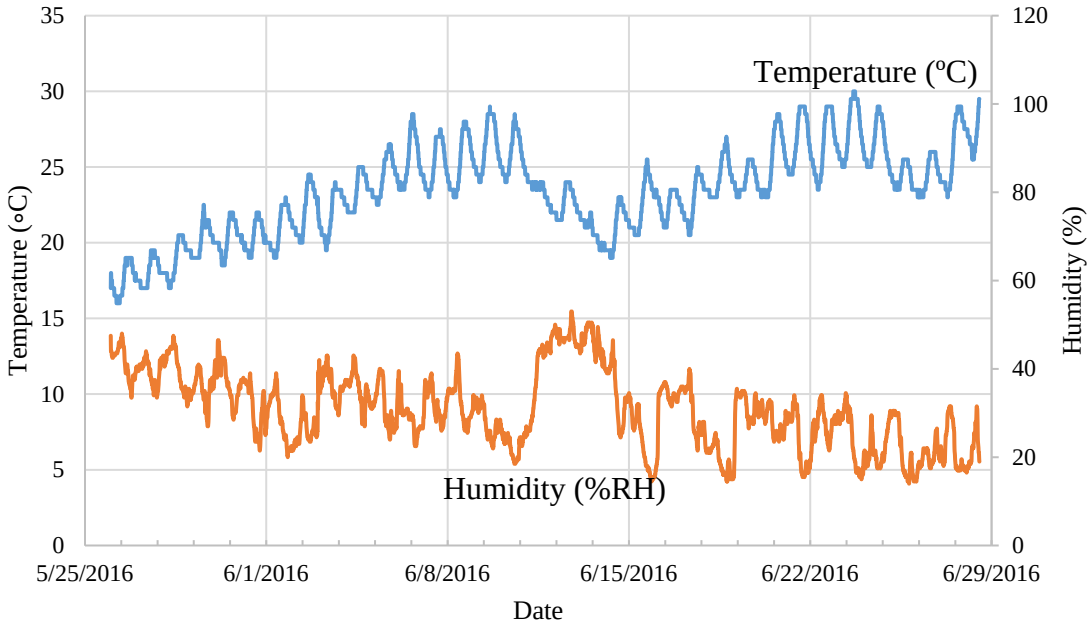

Figure 31. Temperature and Humidity Data in Room 110A

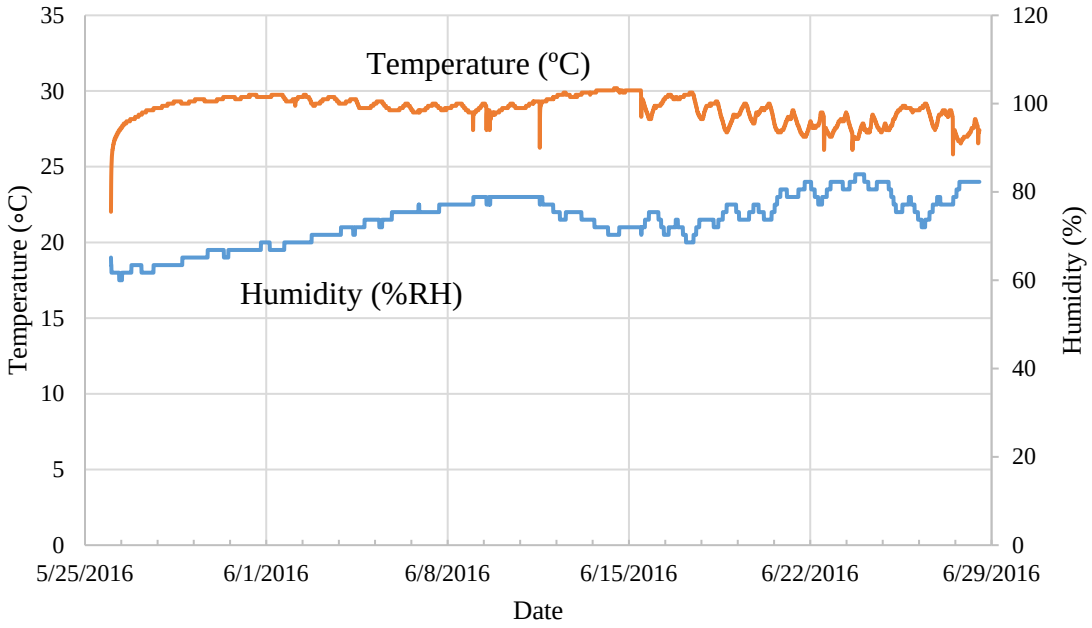

Figure 32. Temperature and Humidity Data in Fog Room

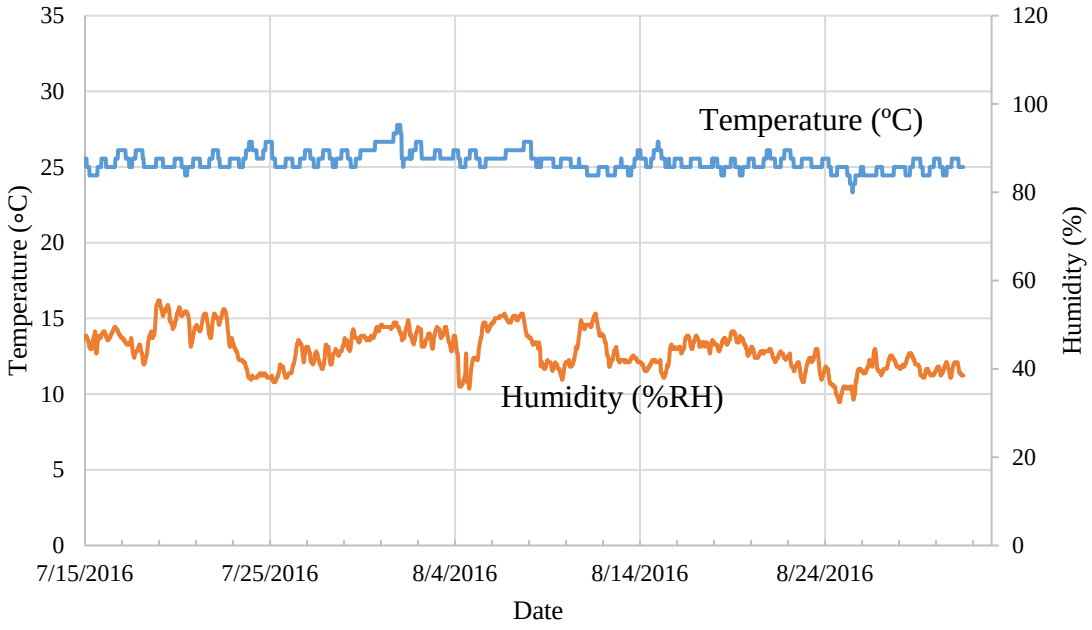

Figure 33. Temperature and Humidity Data in UDOT

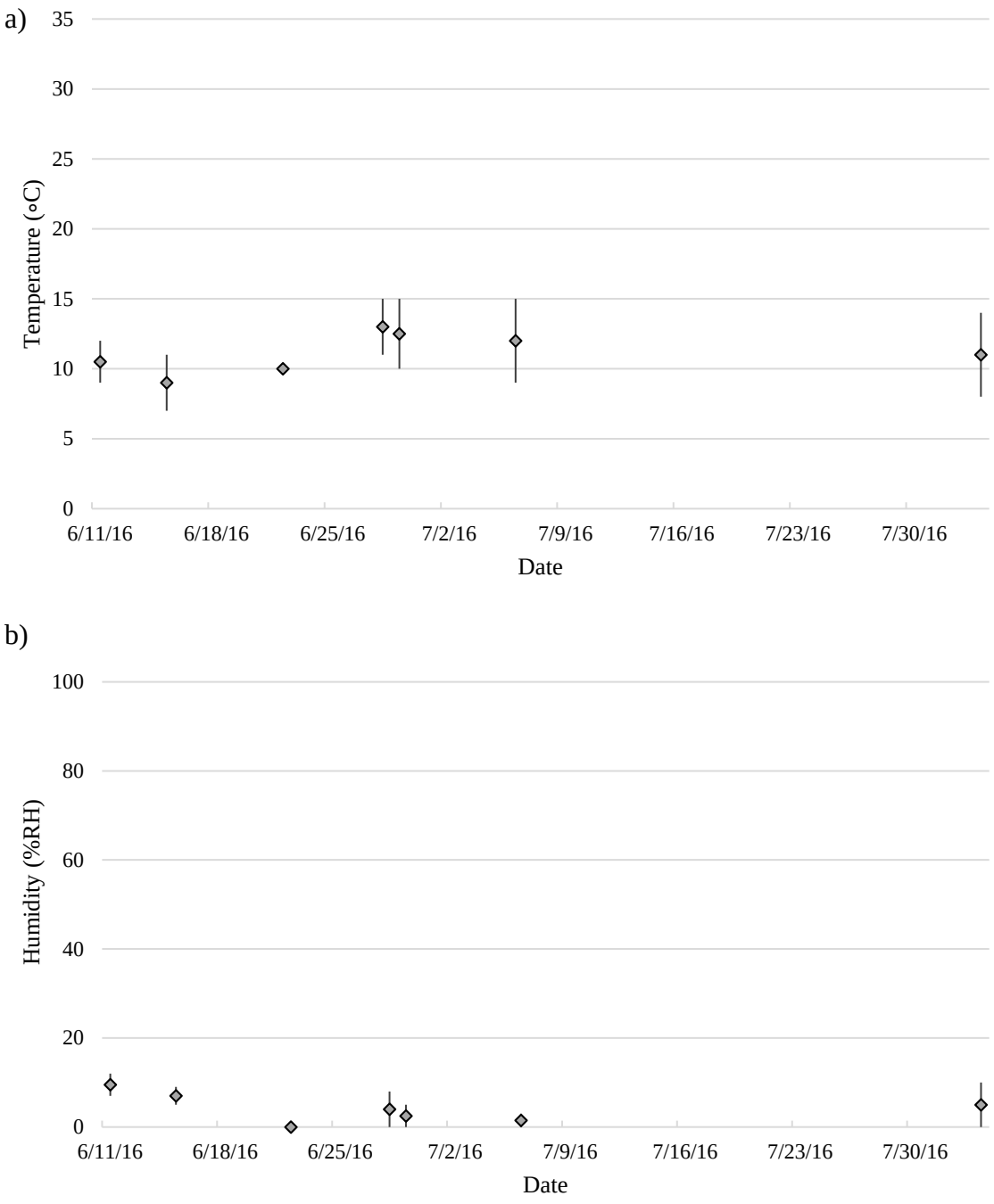

Figure 34. Daily a) Temperature and b) Humidity Fluctuation in Refrigerator

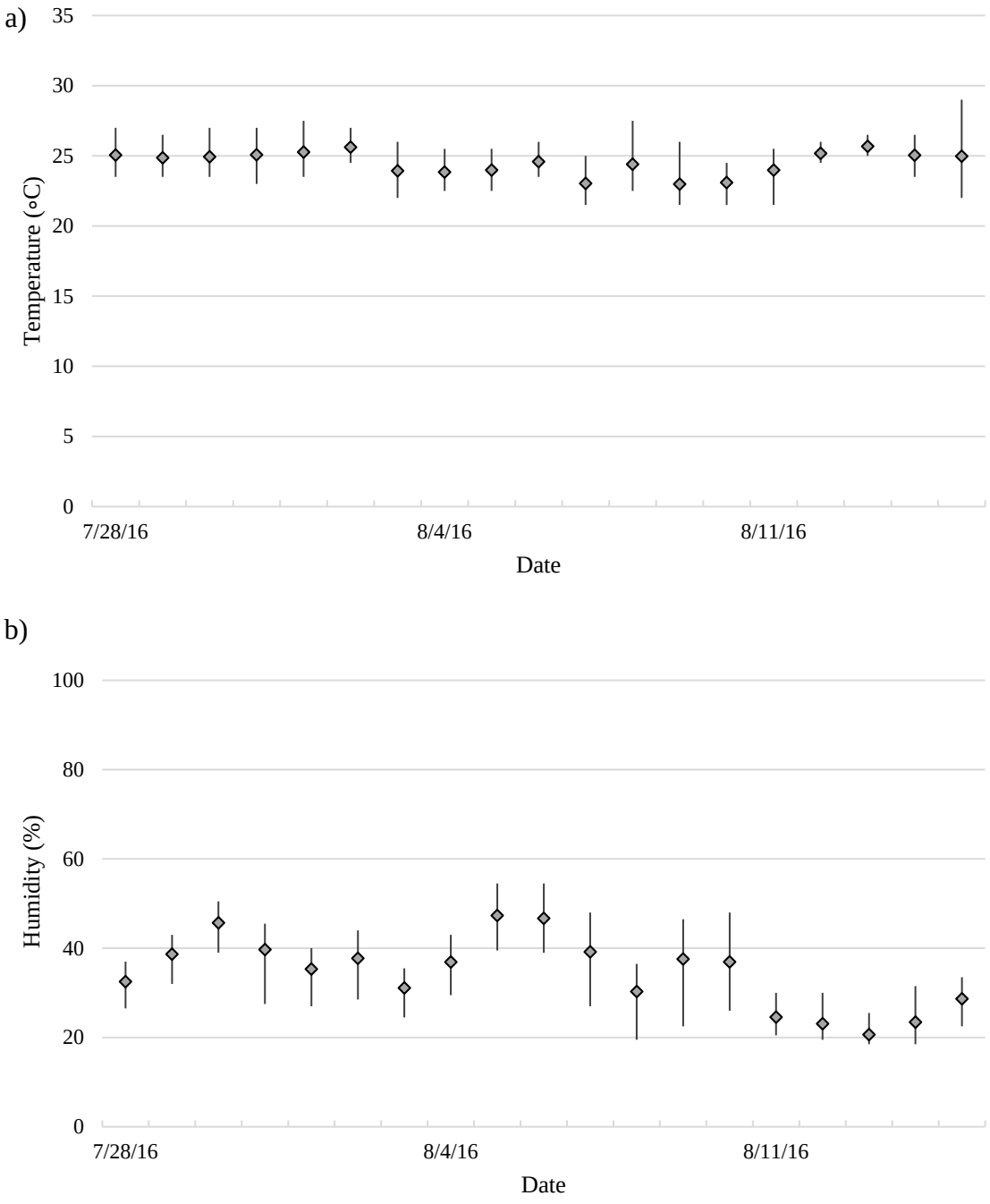

Figure 35. Daily a) Temperature and b) Humidity Fluctuation in Fume Hood

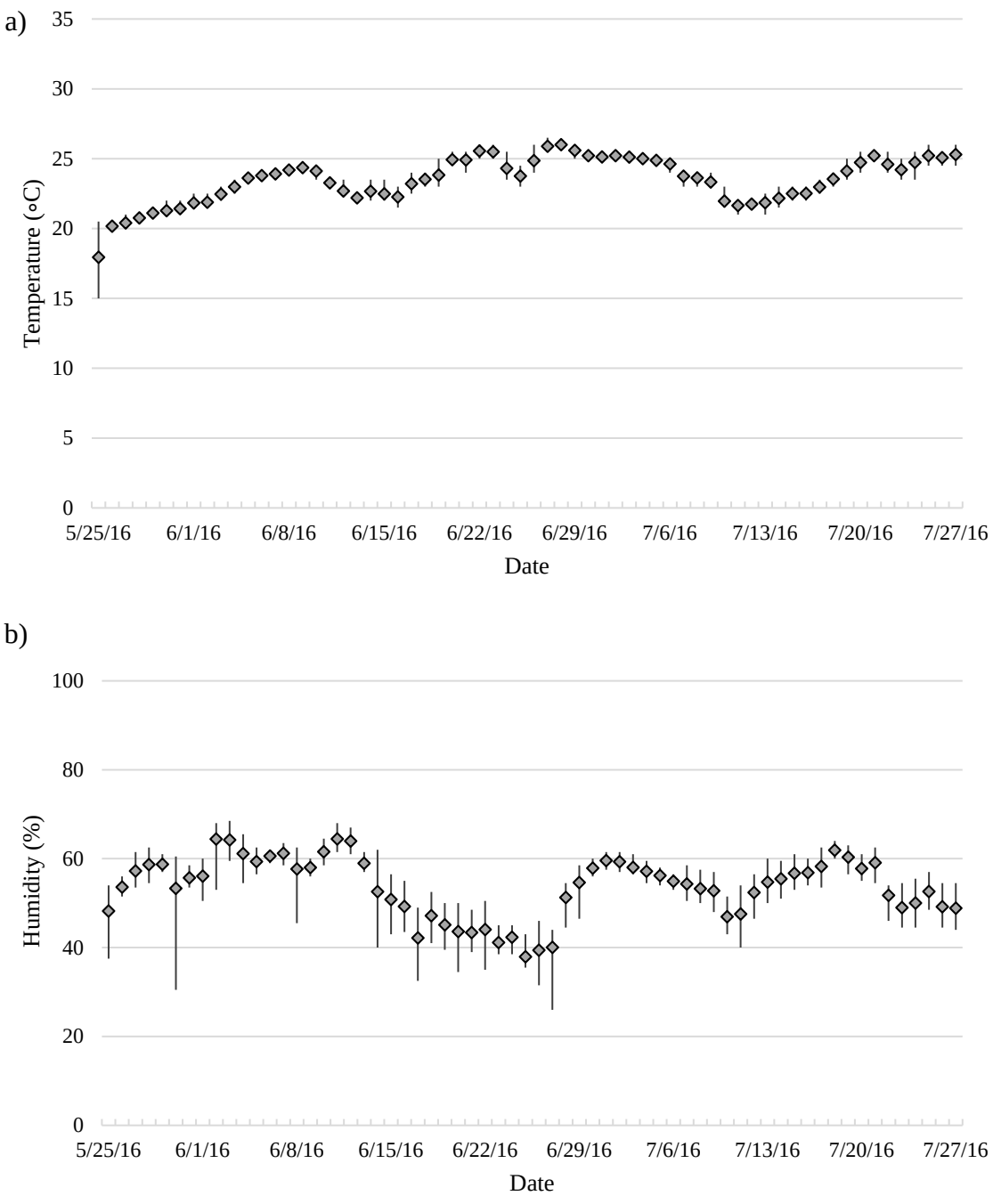

Figure 36. Daily a) Temperature and b) Humidity Fluctuation in Storage Room 130C

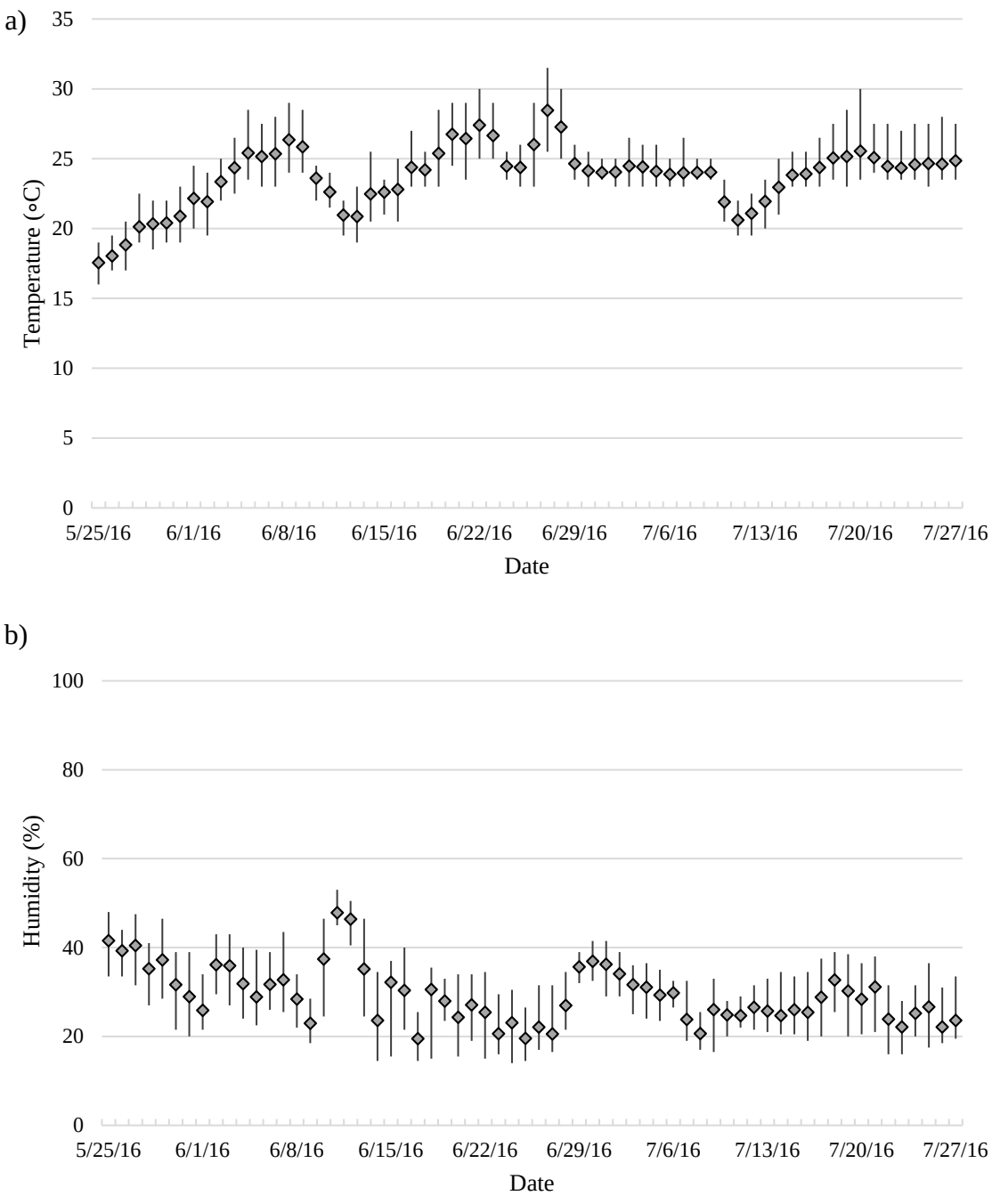

Figure 37. Daily a) Temperature and b) Humidity Fluctuation in Room 110A

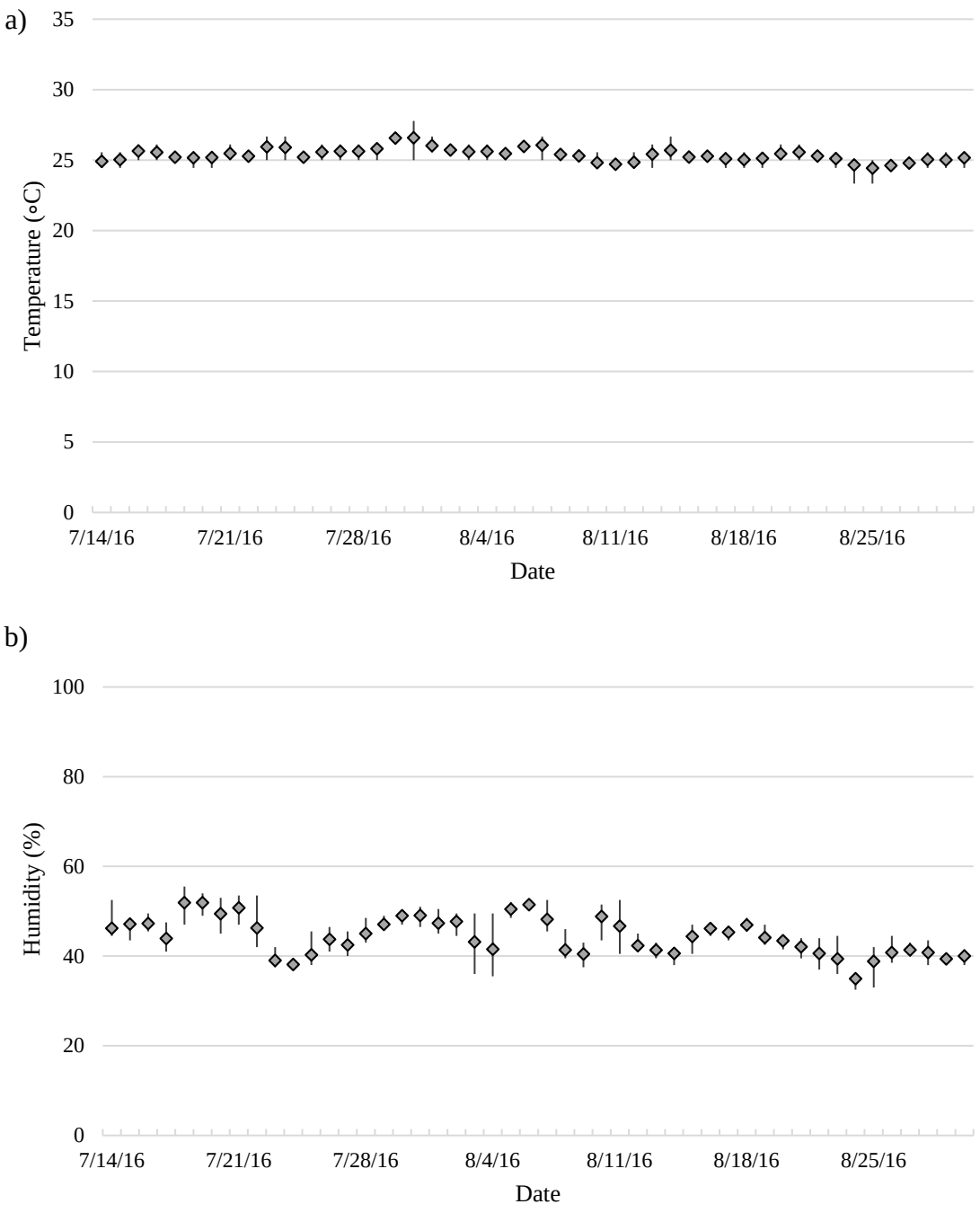

Figure 38. Daily a) Temperature and b) Humidity Fluctuation in UDOT

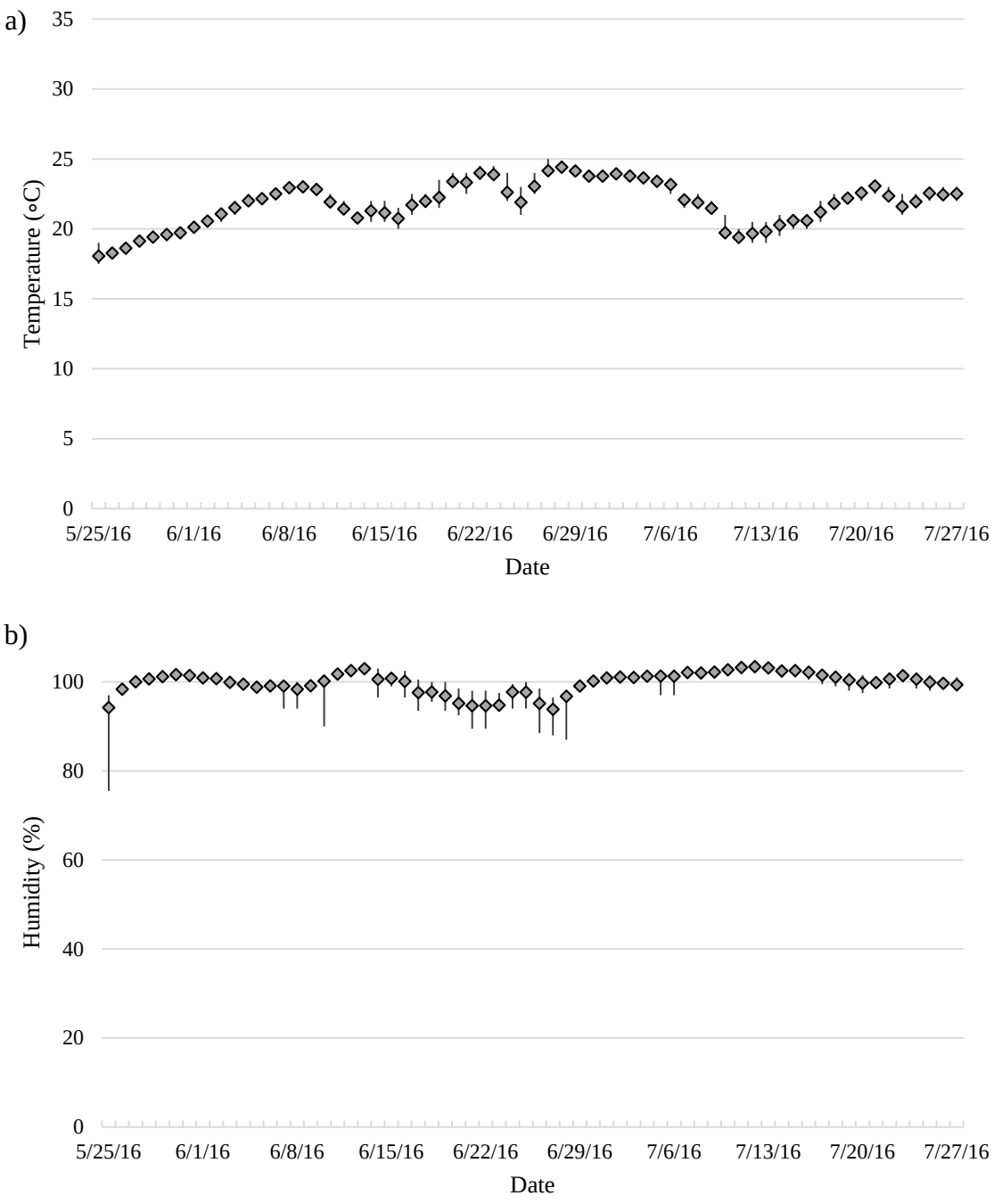

Figure 39. Daily a) Temperature and b) Humidity Fluctuation in Fog Room

APPENDIX B

OVEN DRY (OD) BATCH AMOUNT

Table 20 Oven Dry Mix Design

	Batch 1		Batch 2		Batch 3		Batch 4		Batch 5	
Mix Date	May 24th		Jun 2nd		Jun 8th		Jun 21st		July 18th	
Materials	Batch in OD (lb)	mass ratios	Batch in OD (lb)	mass ratios	Batch in OD (lb)	mass ratios	Batch in OD (lb)	mass ratios	Batch in OD (lb)	mass ratios
Type II Cement	43.50	1.00	42.76	1.00	46.32	1.00	46.32	1.00	114.06	1.00
Natural Sand	52.25	1.20	48.82	1.14	52.89	1.14	52.89	1.14	130.23	1.14
Water	24.00	0.55	23.55	0.55	25.51	0.55	25.51	0.55	62.80	0.55

APPENDIX C

TESTING DATES

Table 21 Testing and Measurements Date

	Measuring Time				
	Mix 1		Mix 2		
	Humidity Chamber, Fume Hood	Storage Room 130C, Room 110A	Refrigerator, Fog Room 130D	Humidity Chamber, Fume Hood	UDOT
Cast	5/24/16 11:00	6/2/16 10:30	6/8/16 11:00	6/21/16 12:30	7/18/16 12:30
.5 days	5/24/16 23:00	6/2/16 23:00	6/8/16 23:00	6/22/16 0:40	7/19/16 0:30
1 day	5/25/16 11:00	6/3/16 12:42	6/9/16 11:49	6/22/16 12:45	7/19/16 12:40
3 days	5/27/16 10:58	6/5/16 12:33	6/11/16 13:00	6/24/16 12:35	7/21/16 12:38
7 days	5/31/16 12:00	6/9/16 12:20	6/15/16 10:58	6/28/16 11:40	7/25/16 12:16
14 days	6/7/16 10:07	6/16/16 11:03	6/22/16 12:20	7/5/16 12:30	8/1/16 12:32
21 days	6/14/16 11:47	6/23/16 11:30	6/29/16 12:15	7/12/16 12:38	8/8/16 12:40
28 days	6/21/16 13:00	6/30/16 13:49	7/6/16 13:07	7/19/16 12:30	8/15/16 14:15
56 days	7/19/16 11:05	7/28/16 12:11	8/3/16 13:20	8/16/16 12:00	9/12/16 12:14

APPENDIX D

SHRINKAGE RELATIVE TO HUMIDITY CHAMBER

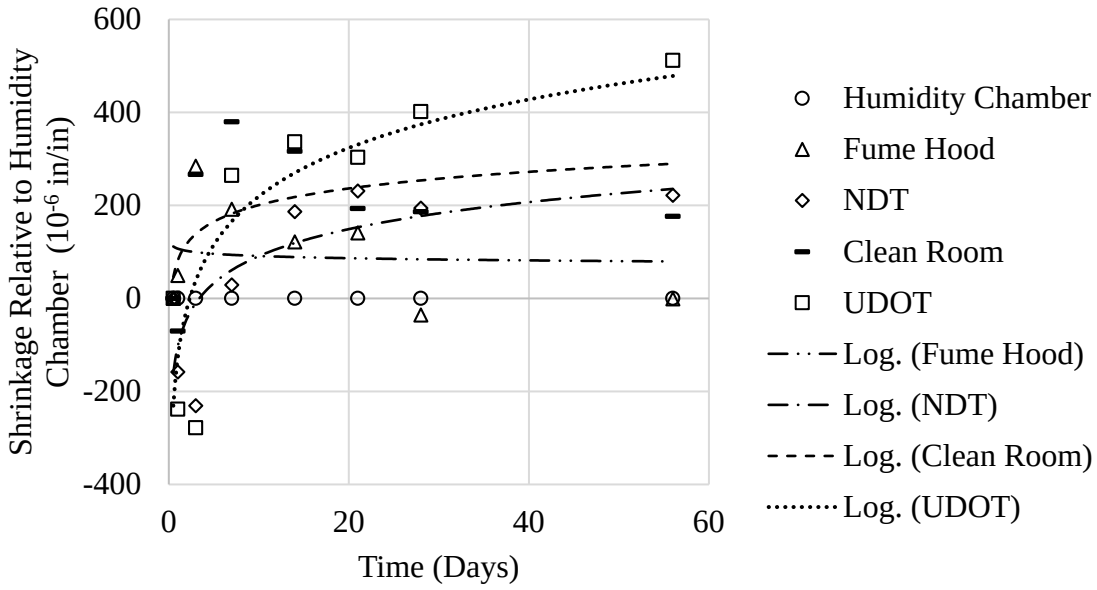

Figure 40. Relative Shrinkage of Samples in Alternative Storage Environments Subtracted from the Average Shrinkage of Samples in the Humidity Chamber

APPENDIX E

SHRINKAGE AND WEIGHT CHANGE FIGURES

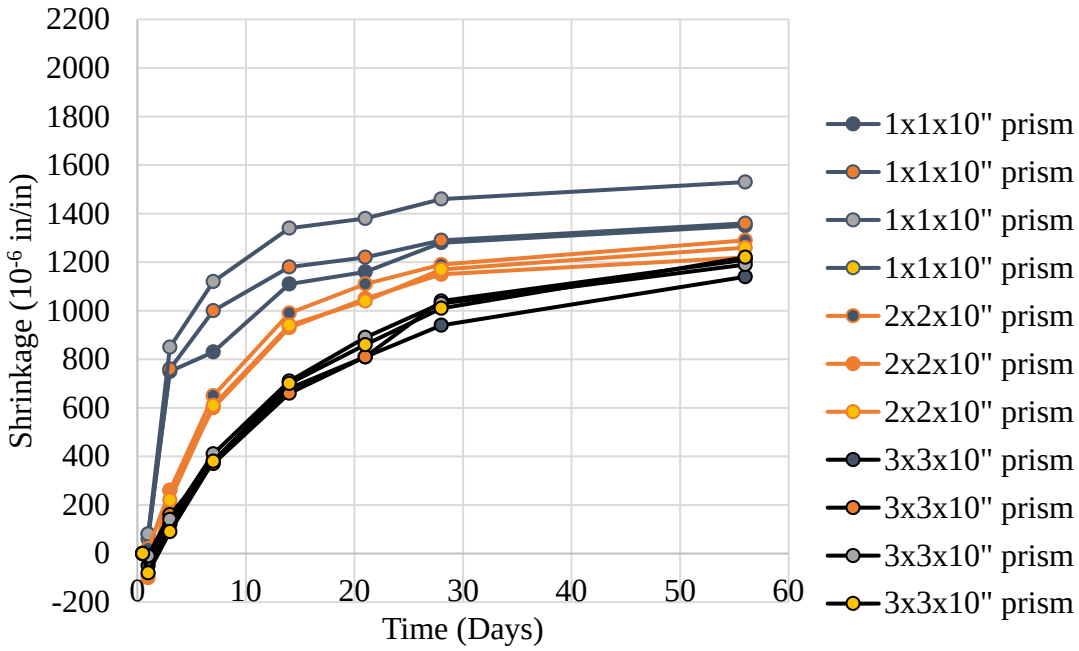

Figure 41. Shrinkage versus Time for Mix 1 Stored in Humidity Chamber

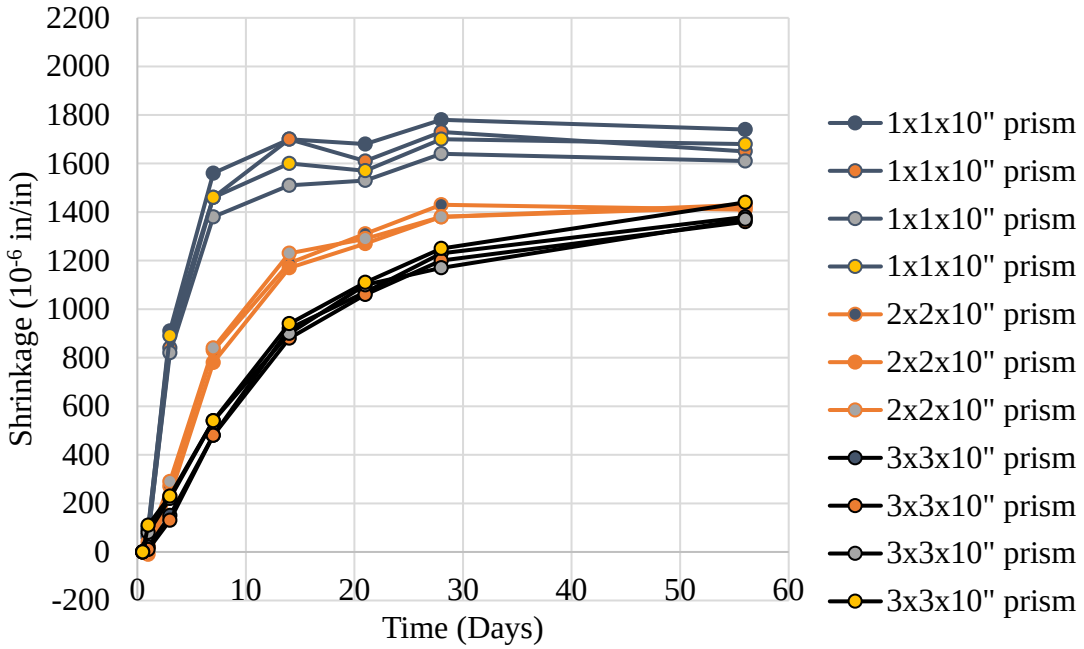

Figure 42. Shrinkage versus Time for Mix 1 Stored in Fume Hood

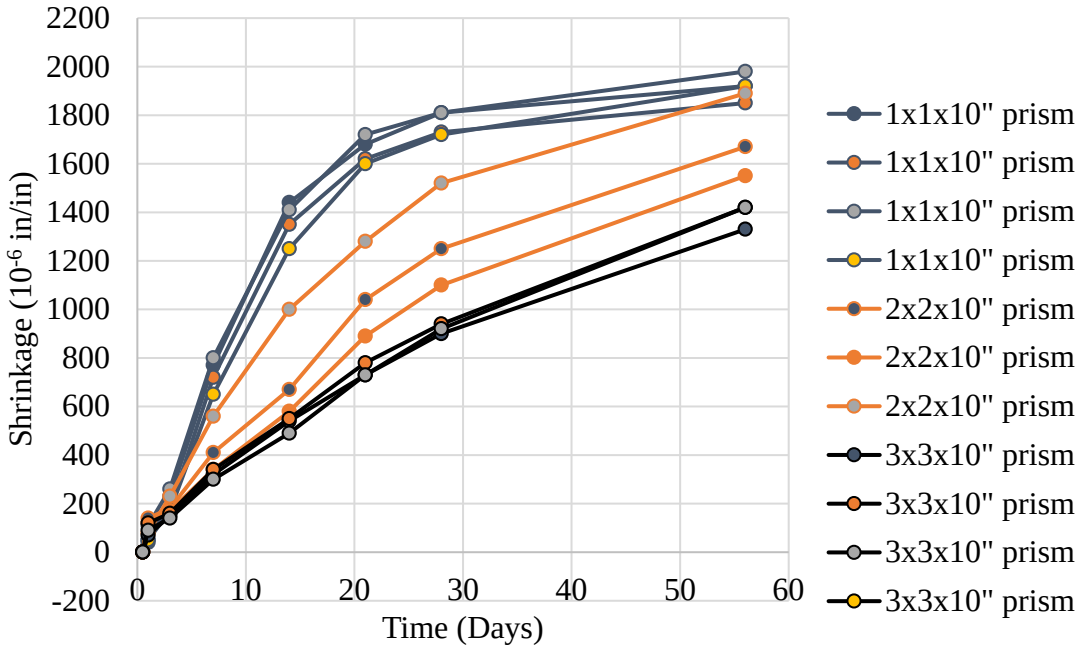

Figure 43. Shrinkage versus Time Stored in Refrigerator (Mix 2)

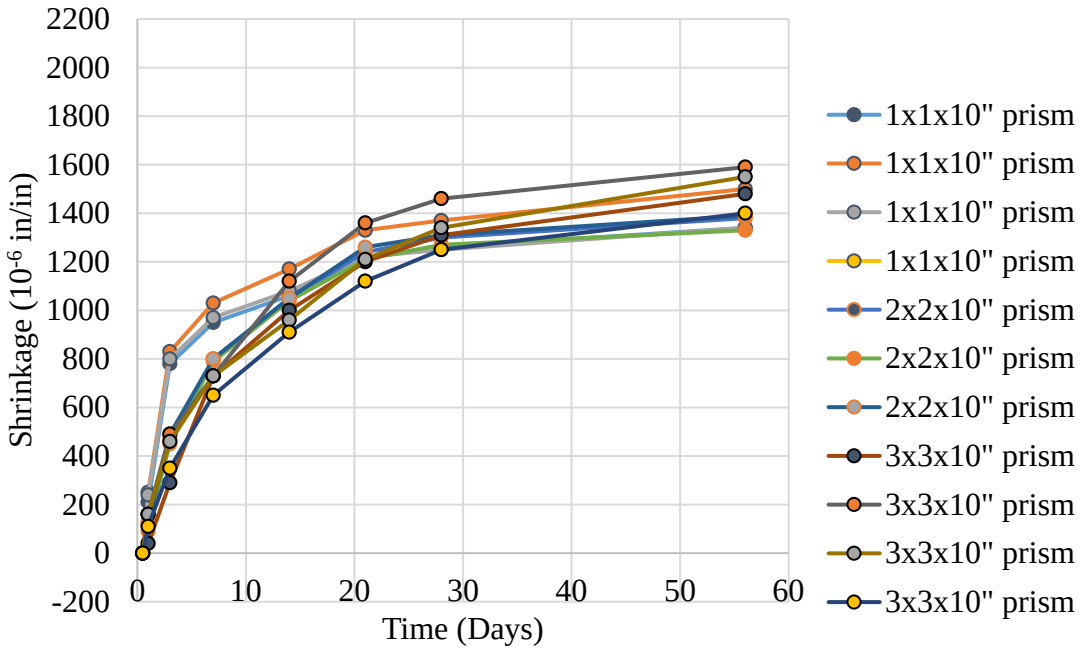

Figure 44. Shrinkage versus Time Stored in Humidity Chamber (Mix 2)

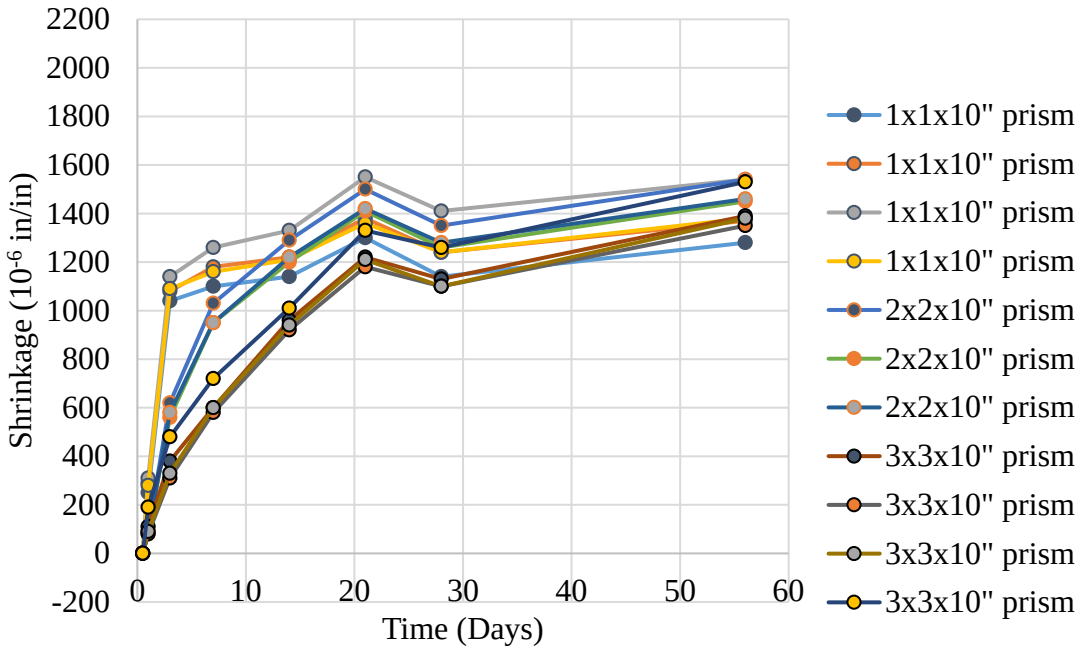

Figure 45. Shrinkage versus Time Stored in Fume Hood (Mix 2)

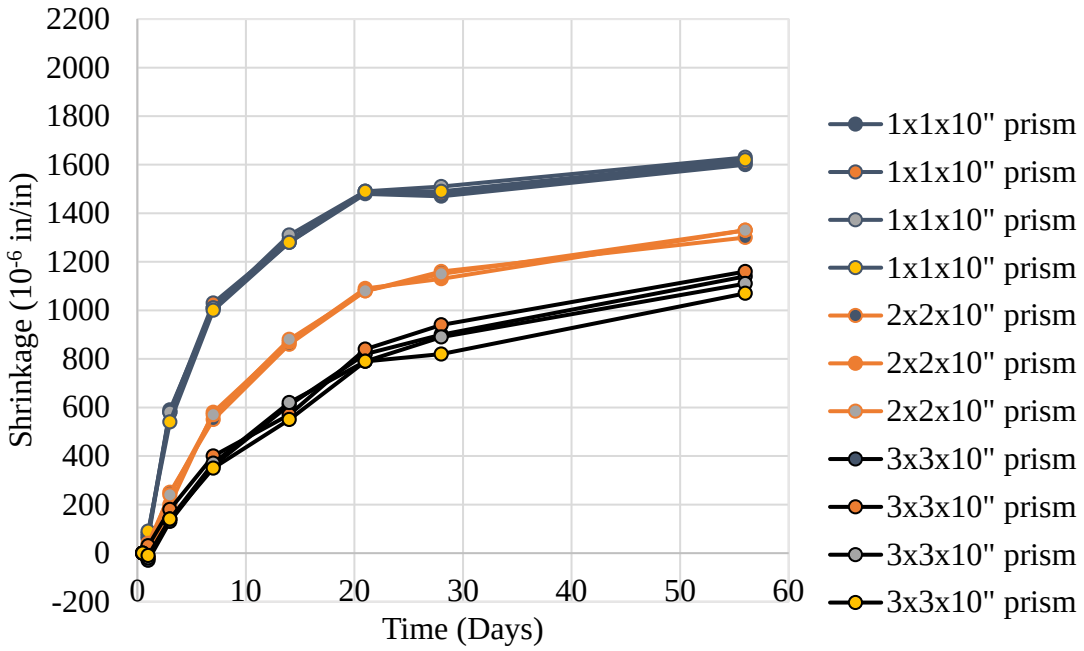

Figure 46. Shrinkage versus Time Stored in Storage Room 130C (Mix 2)

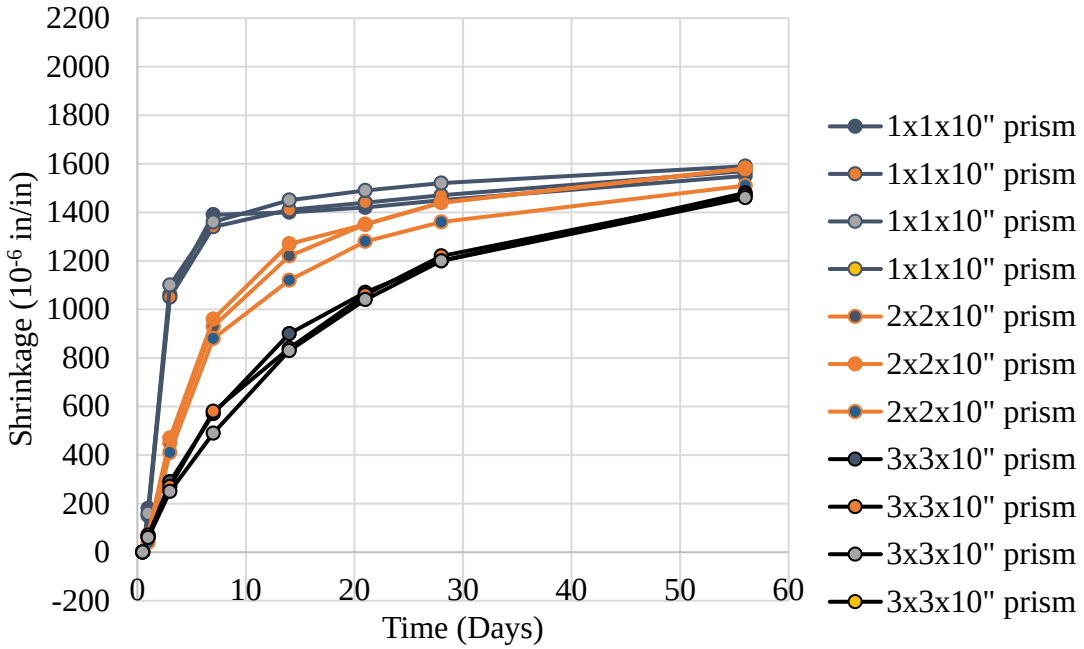

Figure 47. Shrinkage versus Time Stored in Room 110A (Mix 2)

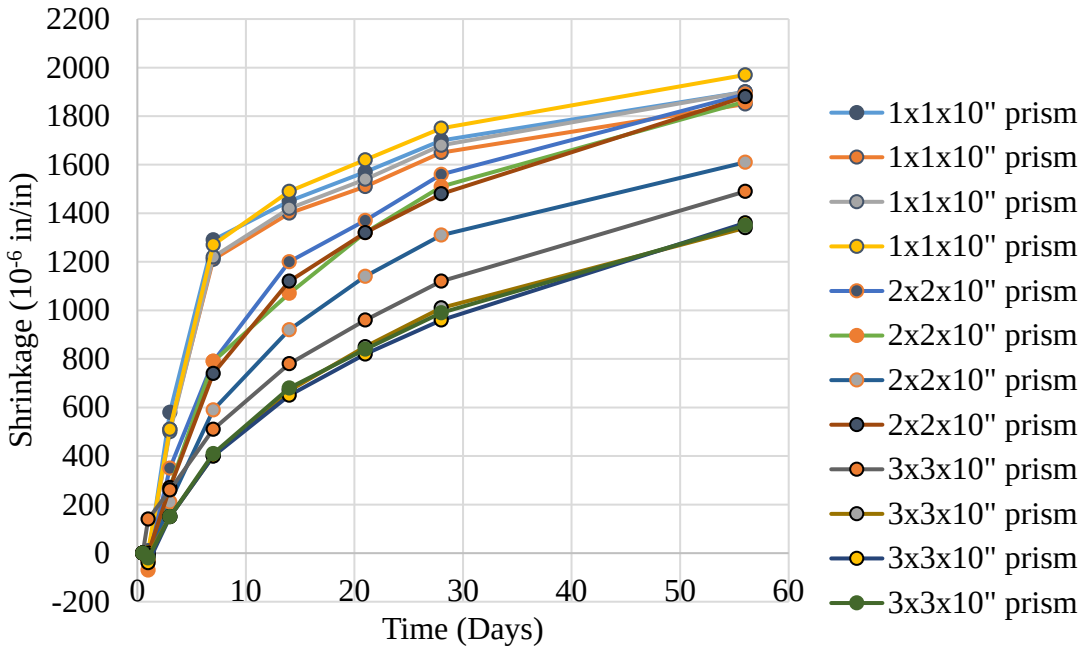

Figure 48. Shrinkage versus Time Stored in UDOT Lab (Mix 2)

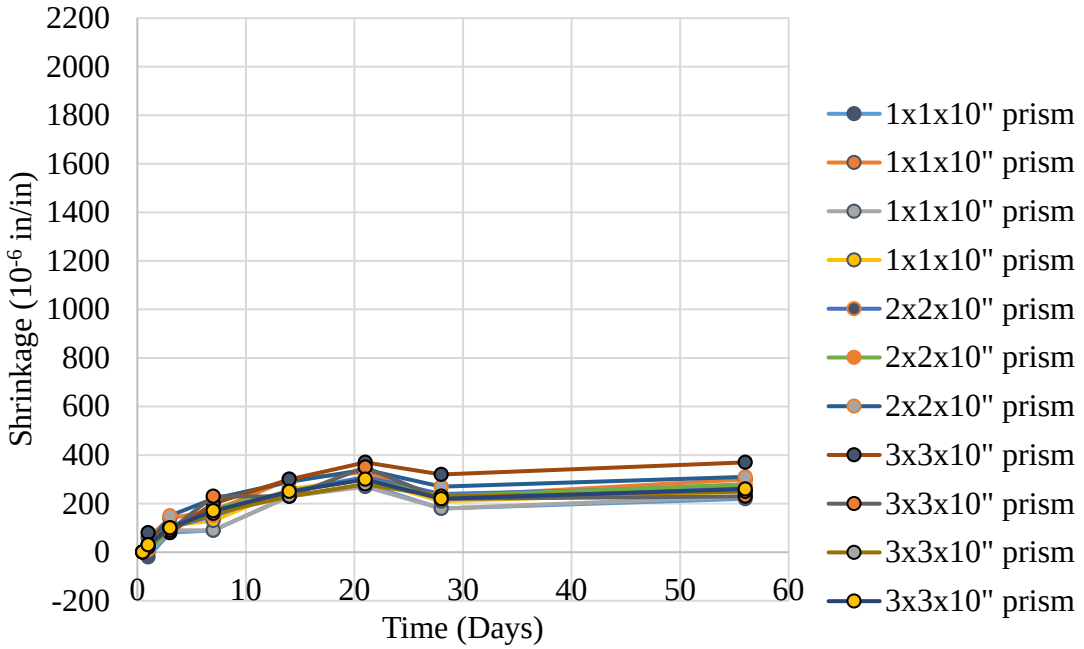

Figure 49. Shrinkage versus Time Stored in Fog Room (Mix 2)

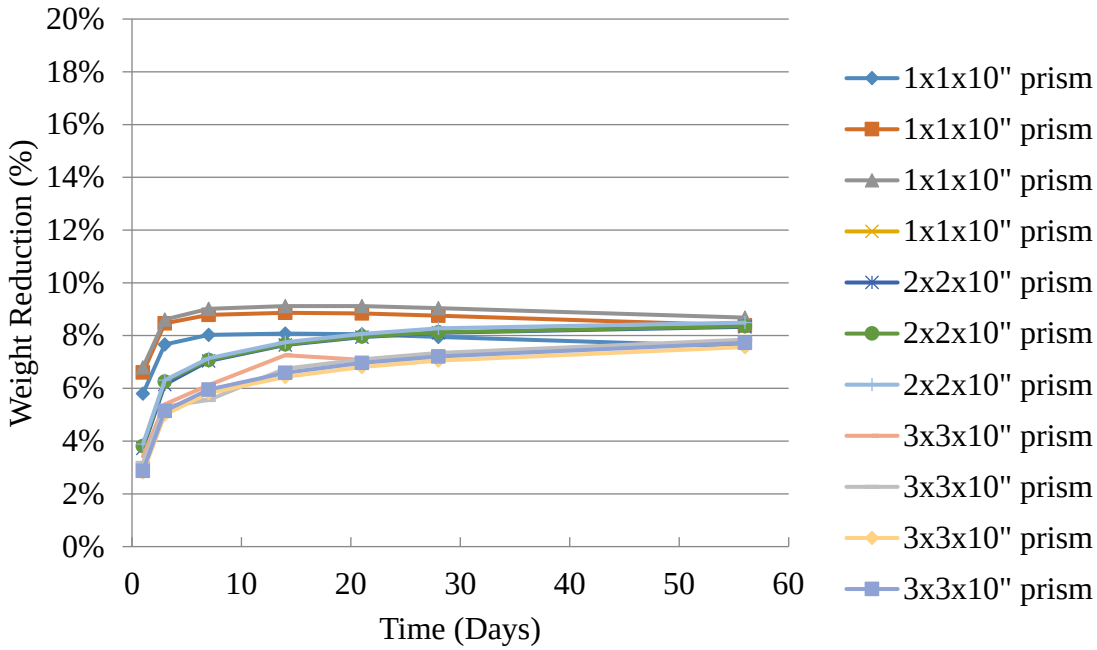

Figure 50. Weight Reduction for Mix 1 Stored in Humidity Chamber

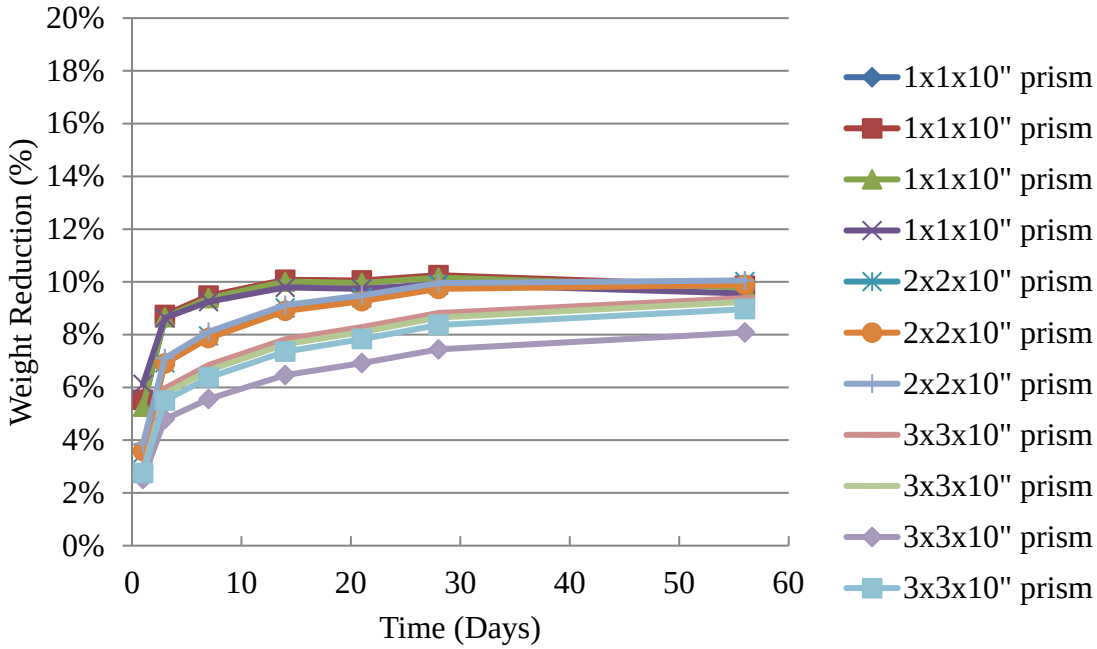

Figure 51. Weight Reduction for Mix 1 Stored in Fume Hood

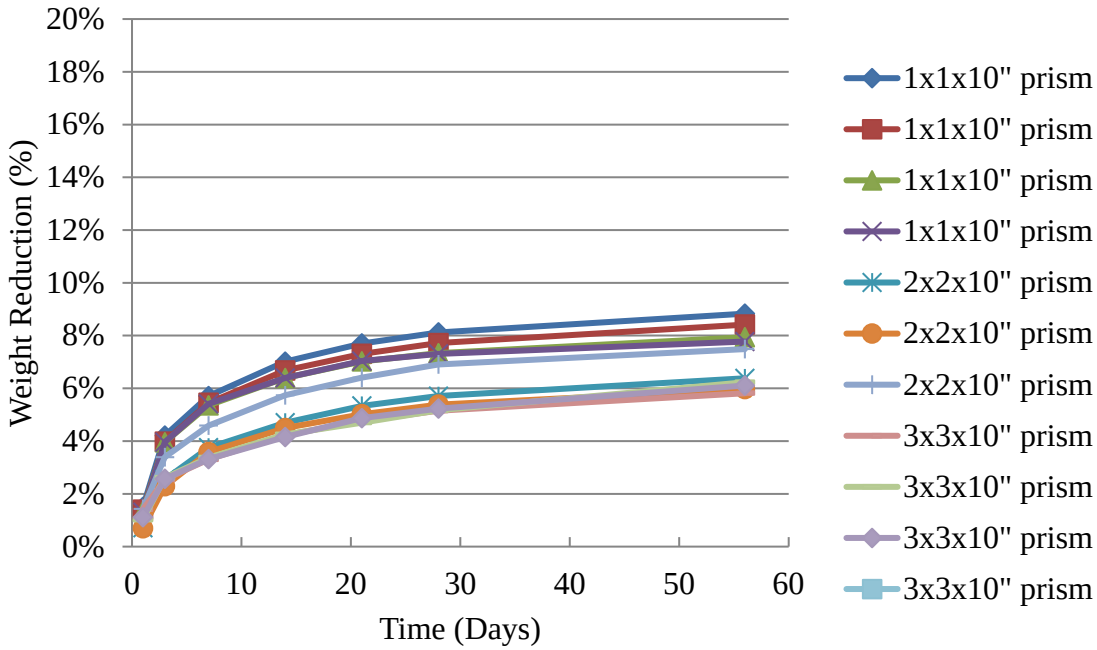

Figure 52. Weight Reduction for Samples Stored in Refrigerator (Mix 2)

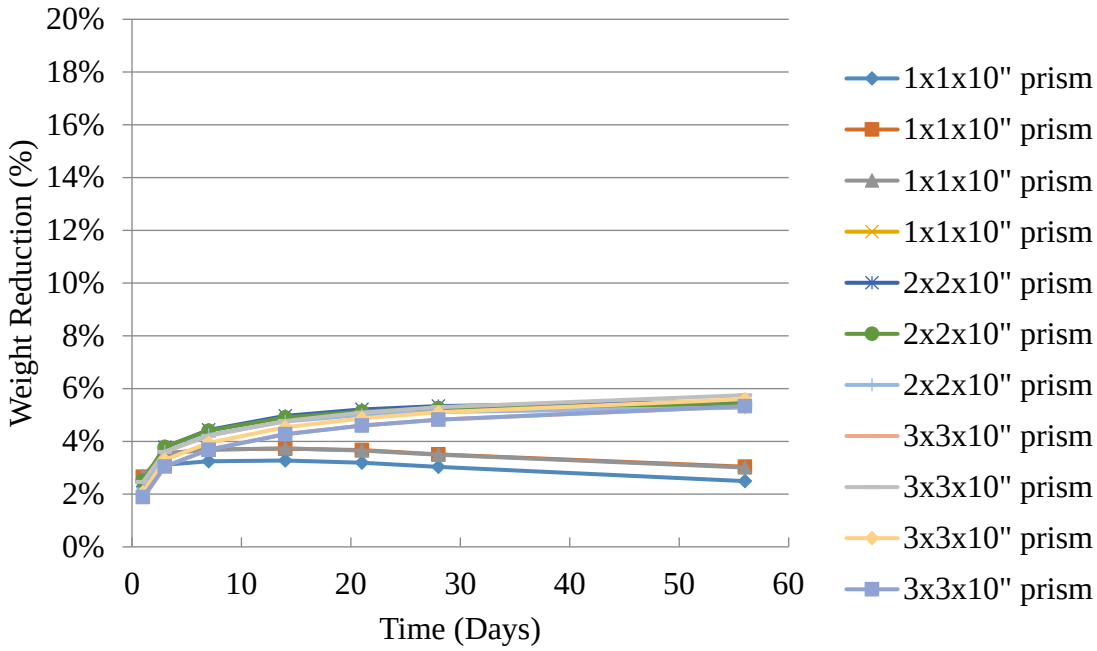

Figure 53. Weight Reduction for Samples Stored in Humidity Chamber (Mix 2)

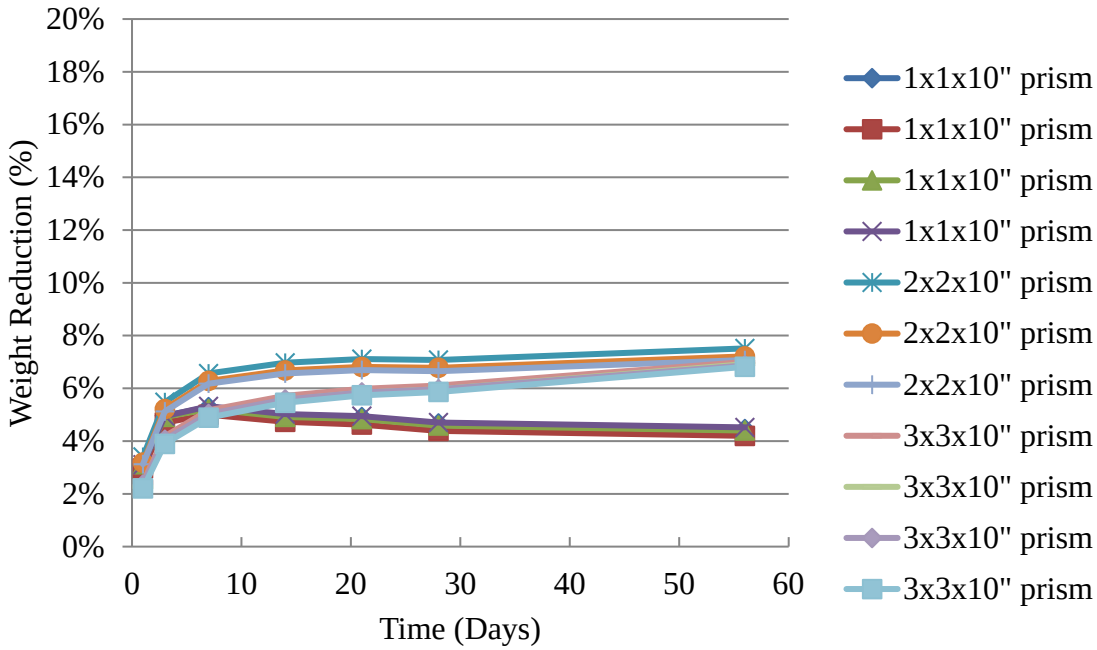

Figure 54. Weight Reduction for Samples Stored in Fume Hood (Mix 2)

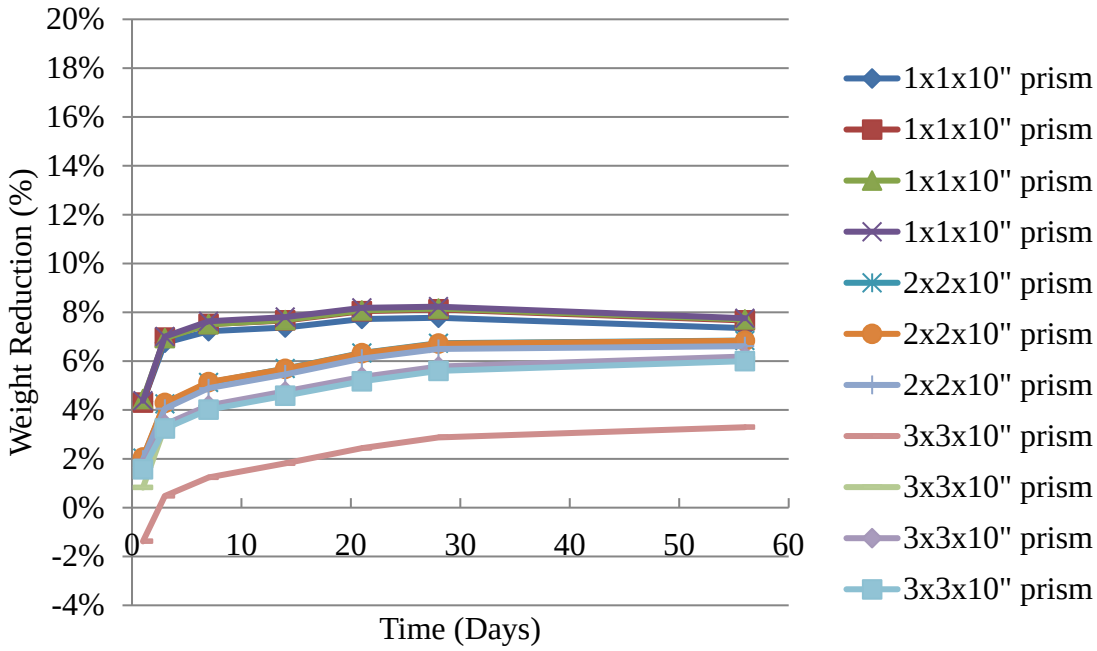

Figure 55. Weight Reduction for Samples Stored in Storage Room 130C (Mix 2)

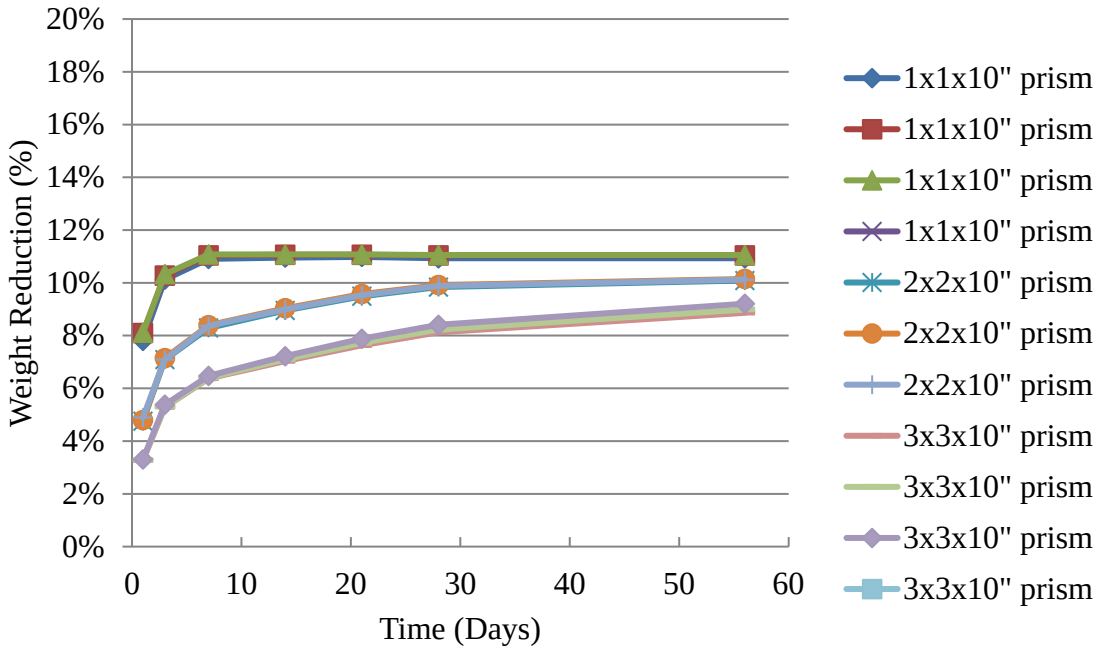

Figure 56. Weight Reduction for Samples Stored in Room 110A (Mix 2)

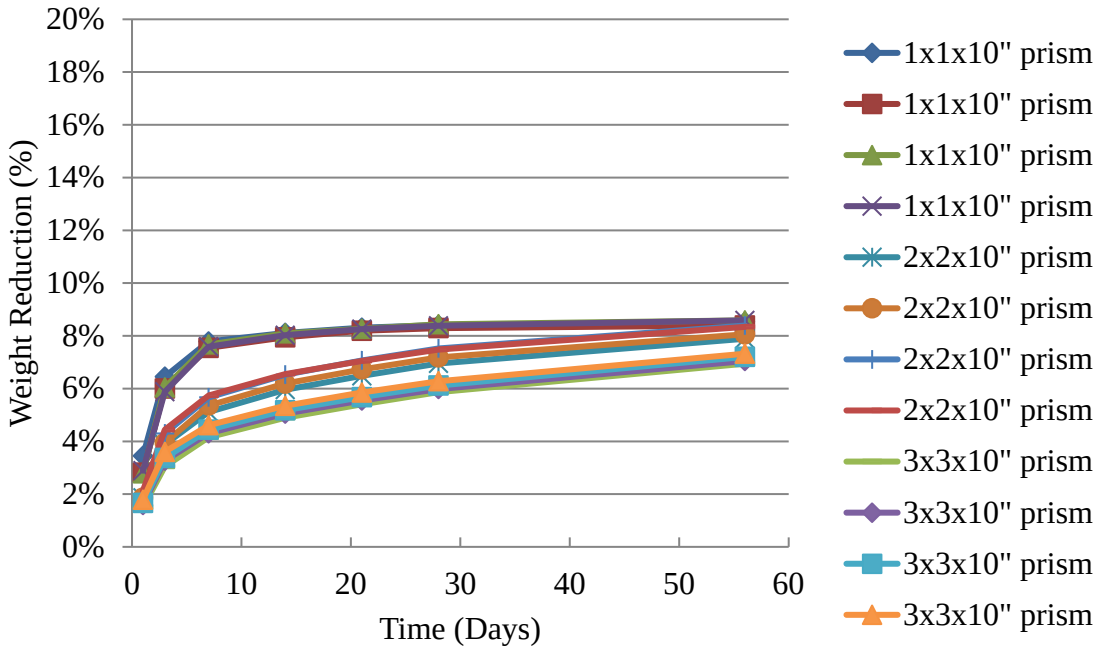

Figure 57. Weight Reduction for Samples Stored in UDOT Lab (Mix 2)

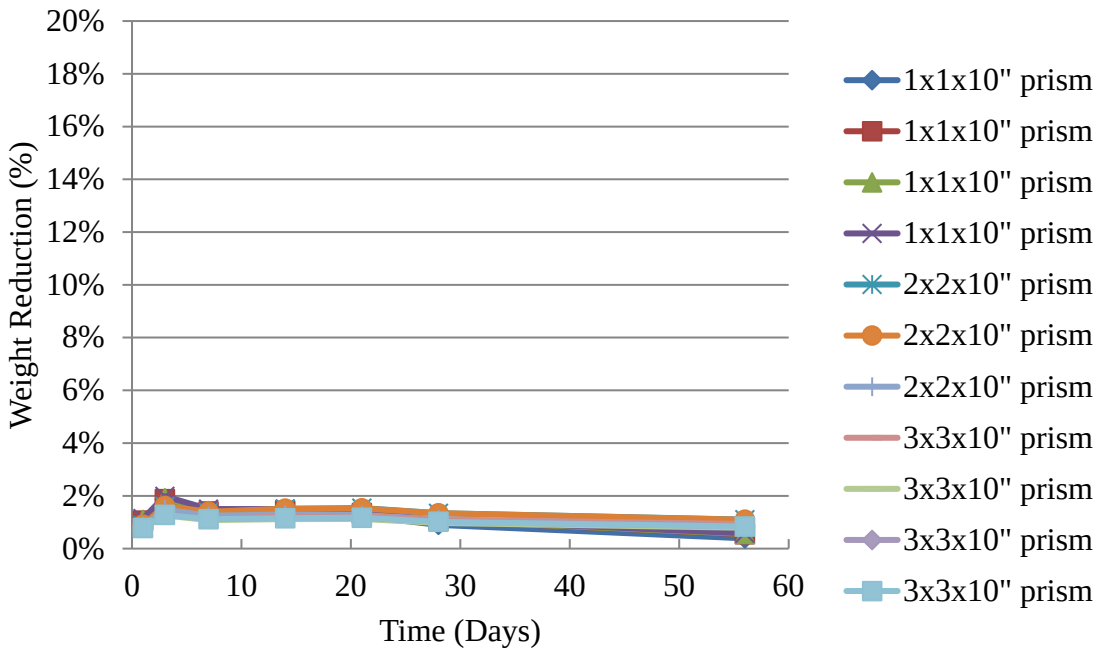

Figure 58. Weight Reduction for Samples Stored in Fog Room (Mix 2)

APPENDIX F

SHRINKAGE PREDICTION PER ACI COMMITTEE 209

In this appendix, shrinkage prediction parameters and comparison between predicted and measured shrinkage values will be listed by following ACI Committee 209 equations.

Table 22 Prediction Parameters Per ACI Committee 209

Mix	Locations	Dimensions	γ_h	γ_{cp}	γ_{th}	γ_s	γ_f	γ_e	γ_c	$\gamma_{V/S}$	γ_{sh}
Mix 1	Fume Hood	1”	1	2	1.43	1	1.1	1	1.36	1.17	4.99
		2”	1	2	1.30	1	1.1	1	1.36	1.14	4.42
		3”	1	2	1.17	1	1.1	1	1.36	1.11	3.88
	Humidity Chamber	1”	0.89	2	1.43	1	1.1	1	1.36	1.17	4.44
		2”	0.89	2	1.30	1	1.1	1	1.36	1.14	3.93
		3”	0.89	2	1.17	1	1.1	1	1.36	1.11	3.46
Mix 2	Refrigerator	1”	1	2	1.43	1	1.1	1	1.22	1.17	4.48
		2”	1	2	1.30	1	1.1	1	1.22	1.14	3.96
		3”	1	2	1.17	1	1.1	1	1.22	1.11	3.48
	Humidity Chamber	1”	0.89	2	1.43	1	1.1	1	1.22	1.17	3.98
		2”	0.89	2	1.30	1	1.1	1	1.22	1.14	3.53
		3”	0.89	2	1.17	1	1.1	1	1.22	1.11	3.10
	Fume Hood	1”	1	2	1.43	1	1.1	1	1.22	1.17	4.48
		2”	1	2	1.30	1	1.1	1	1.22	1.14	3.96
		3”	1	2	1.17	1	1.1	1	1.22	1.11	3.48
	Storage Room 130C	1”	0.84	2	1.43	1	1.1	1	1.22	1.17	3.76
		2”	0.84	2	1.30	1	1.1	1	1.22	1.14	3.33
		3”	0.84	2	1.17	1	1.1	1	1.22	1.11	2.92
	Room 110A	1”	1	2	1.43	1	1.1	1	1.22	1.17	4.48
		2”	1	2	1.30	1	1.1	1	1.22	1.14	3.96
		3”	1	2	1.17	1	1.1	1	1.22	1.11	3.48
	UDOT	1”	0.96	2	1.43	1	1.1	1	1.22	1.17	4.30
		2”	0.96	2	1.30	1	1.1	1	1.22	1.14	3.81
		3”	0.96	2	1.17	1	1.1	1	1.22	1.11	3.35
	Fog Room	1”	0	2	1.43	1	1.1	1	1.22	1.17	0.00
		2”	0	2	1.30	1	1.1	1	1.22	1.14	0.00
		3”	0	2	1.17	1	1.1	1	1.22	1.11	0.00

Table 23 Predicted Values, Measured Values, Error, and Squared Error for All Samples at All Ages (ACI Committee 209 Equations)

		Ages	3				7			
Mix	Locations	Sizes	P*	M	E	SE	P	M	E	SE
1	Fume Hood	1"	307	865	558	310897	649	1465	816	665864
		2"	272	263	-9	79	575	817	242	58579
		3"	239	183	-57	3203	505	510	5	28
	Humidity Chamber	1"	274	787	513	263235	578	983	406	164615
		2"	242	247	4	19	511	620	109	11788
		3"	213	128	-85	7275	449	385	-64	4125
2	Refrigerator	1"	276	210	-66	4317	582	735	153	23396
		2"	244	193	-51	2579	515	437	-79	6192
		3"	214	150	-64	4151	453	320	-133	17604
	Humidity Chamber	1"	245	803	558	311316	518	983	465	216520
		2"	217	470	253	63876	459	797	338	114246
		3"	191	398	207	42708	403	710	307	94320
	Fume Hood	1"	276	1088	812	659013	582	1175	593	351600
		2"	244	587	343	117342	515	977	461	212810
		3"	214	375	161	25784	453	625	172	29695
	Storage Room 130C	1"	231	573	341	116407	488	1013	524	274751
		2"	205	230	25	634	432	567	134	18033
		3"	180	147	-32	1050	380	370	-10	96
	Room 110A	1"	276	1070	794	630906	582	1363	781	610417
		2"	244	443	199	39688	515	923	408	166448
		3"	214	270	56	3088	453	547	94	8834
	UDOT	1"	265	525	260	67568	560	1248	688	473241
		2"	235	277	42	1762	495	723	228	51926
		3"	206	178	-29	821	435	430	-5	27
	Fog Room	1"	0	105	105	11025	0	120	120	14400
		2"	0	113	113	12844	0	183	183	33611
		3"	0	92	92	8556	0	190	190	36100

* P, M, E, SE stand for predicted values, measured values, error, and squared error.

Table 23 Continued

		Ages	14				21			
Mix	Locations	Sizes	P	M	E	SE	P	M	E	SE
1	Fume Hood	1"	1113	1628	515	265160	1460	1598	137	18841
		2"	985	1197	212	44765	1293	1290	-3	9
		3"	865	910	45	1999	1136	1085	-51	2570
	Humidity Chamber	1"	990	1210	220	48320	1300	1253	-46	2142
		2"	877	953	77	5868	1151	1067	-84	7063
		3"	770	687	-83	6824	1011	843	-168	28313
2	Refrigerator	1"	998	1363	365	133017	1310	1655	345	119306
		2"	883	750	-133	17812	1160	1070	-90	8018
		3"	776	527	-249	62177	1019	747	-272	73908
	Humidity Chamber	1"	888	1103	215	46356	1166	1257	91	8304
		2"	786	1047	260	67800	1032	1237	205	41891
		3"	691	998	307	94152	906	1223	316	99863
	Fume Hood	1"	998	1225	227	51627	1310	1398	88	7728
		2"	883	1237	353	124753	1160	1443	284	80536
		3"	776	958	181	32935	1019	1235	216	46861
	Storage Room 130C	1"	837	1290	453	205081	1099	1488	389	151128
		2"	741	870	129	16583	973	1083	110	12205
		3"	651	588	-64	4043	855	810	-45	1984
	Room 110A	1"	998	1420	422	178265	1310	1450	140	19714
		2"	883	1203	320	102317	1160	1327	167	27930
		3"	776	857	81	6504	1019	1057	38	1455
	UDOT	1"	959	1440	481	231101	1259	1560	301	90575
		2"	849	1063	214	45784	1115	1277	162	26205
		3"	746	695	-51	2608	979	868	-112	12479
	Fog Room	1"	0	255	255	65025	0	295	295	87025
		2"	0	263	263	69344	0	317	317	100278
		3"	0	253	253	63756	0	325	325	105625

Table 23 Continued

		Ages	28				56			
Mix	Locations	Sizes	P	M	E	SE	P	M	E	SE
1	Fume Hood	1"	1731	1713	-18	330	2396	1670	-726	527497
		2"	1532	1397	-136	18413	2122	1420	-702	492428
		3"	1346	1213	-134	17823	1864	1388	-476	226765
	Humidity Chamber	1"	1540	1343	-197	38789	2133	1413	-719	517486
		2"	1364	1170	-194	37559	1888	1257	-632	399013
		3"	1198	1005	-193	37227	1659	1190	-469	219671
2	Refrigerator	1"	1552	1768	215	46393	2149	1918	-232	53627
		2"	1374	1290	-84	7102	1903	1703	-200	39804
		3"	1207	920	-287	82451	1671	1390	-281	79202
	Humidity Chamber	1"	1381	1293	-88	7752	1913	1393	-519	269718
		2"	1223	1293	70	4932	1694	1367	-327	106840
		3"	1074	1340	266	70566	1488	1505	17	304
	Fume Hood	1"	1552	1258	-295	86795	2149	1393	-757	572407
		2"	1374	1297	-78	6023	1903	1483	-420	175988
		3"	1207	1148	-60	3557	1671	1413	-259	67044
	Storage Room 130C	1"	1302	1488	185	34329	1803	1615	-188	35372
		2"	1153	1147	-6	40	1596	1320	-276	76444
		3"	1013	888	-125	15698	1402	1120	-282	79709
	Room 110A	1"	1552	1480	-72	5200	2149	1570	-579	335329
		2"	1374	1413	39	1526	1903	1557	-346	119838
		3"	1207	1207	0	0	1671	1470	-201	40573
	UDOT	1"	1492	1695	203	41128	2066	1905	-161	25960
		2"	1321	1460	139	19258	1829	1787	-43	1826
		3"	1161	1020	-141	19754	1607	1385	-222	49245
	Fog Room	1"	0	200	200	40000	0	250	250	62500
		2"	0	247	247	60844	0	287	287	82178
		3"	0	247	247	61256	0	277	277	77006

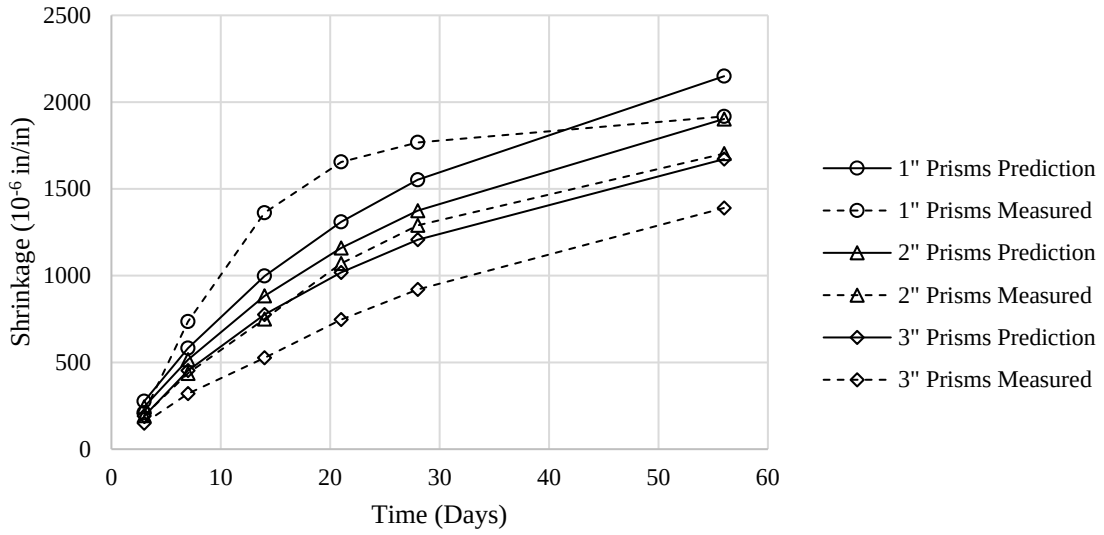

Figure 59. Comparison Between Predicted and Measured Shrinkage Values for Mix 2 Samples Stored in Refrigerator at All Ages (ACI Committee 209)

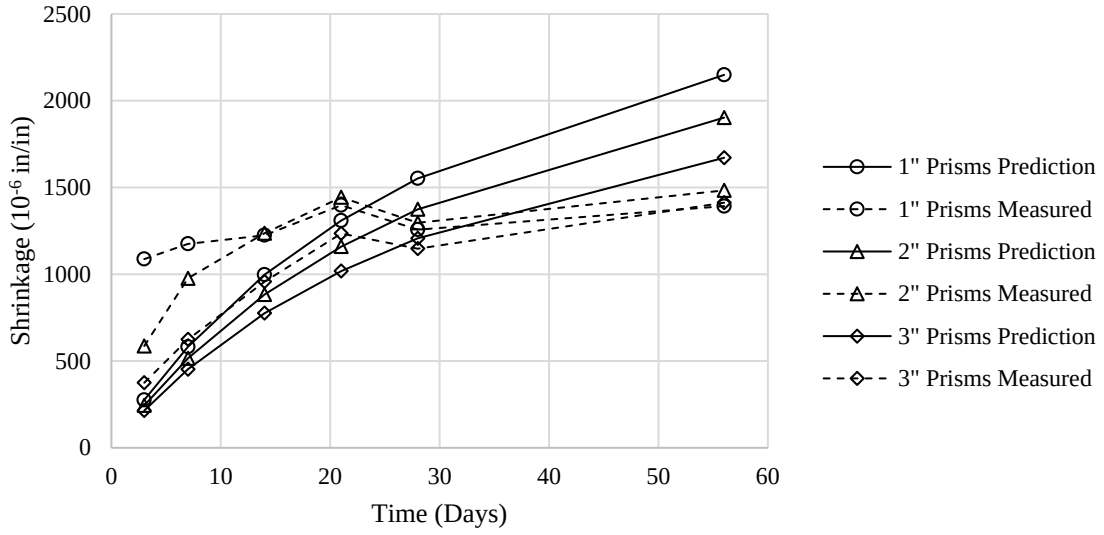

Figure 60. Comparison Between Predicted and Measured Shrinkage Values for Mix 2 Samples Stored in Fume Hood at All Ages (ACI Committee 209)

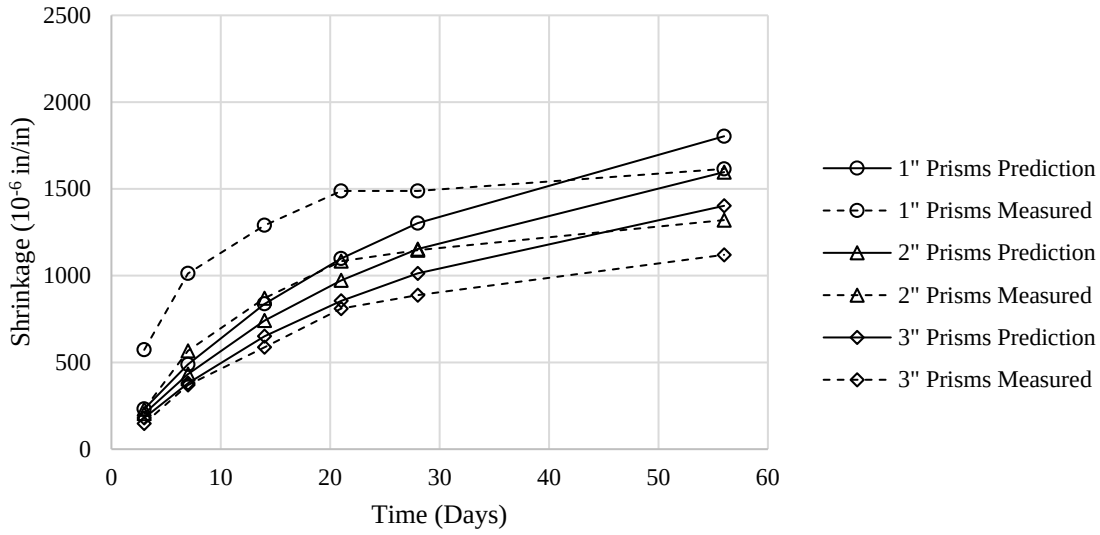

Figure 61. Comparison Between Predicted and Measured Shrinkage Values for Mix 2 Samples Stored in Storage Room 130C at All Ages (ACI Committee 209)

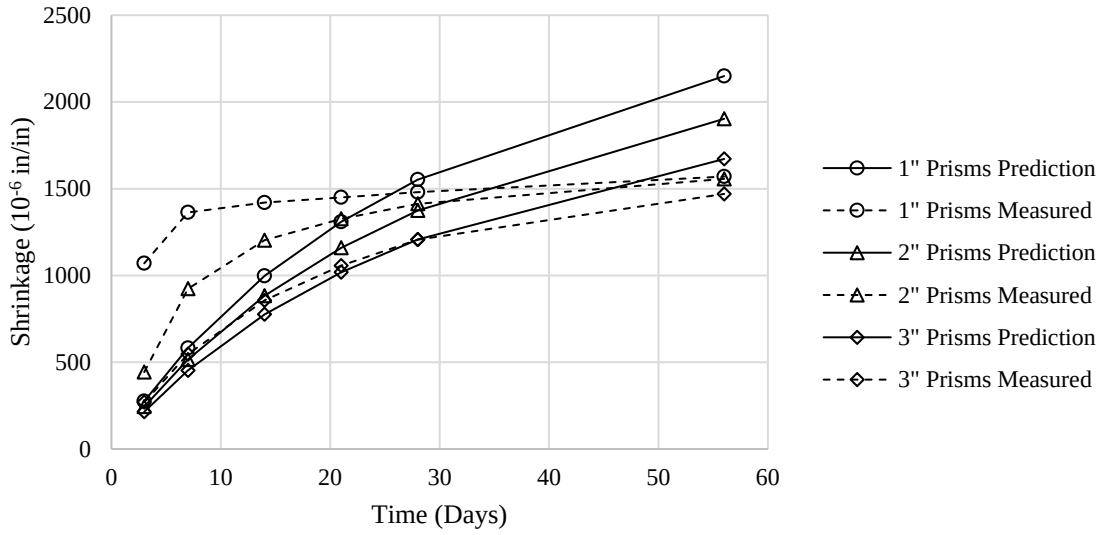

Figure 62. Comparison Between Predicted and Measured Shrinkage Values for Mix 2 Samples Stored in Room 110A at All Ages (ACI Committee 209)

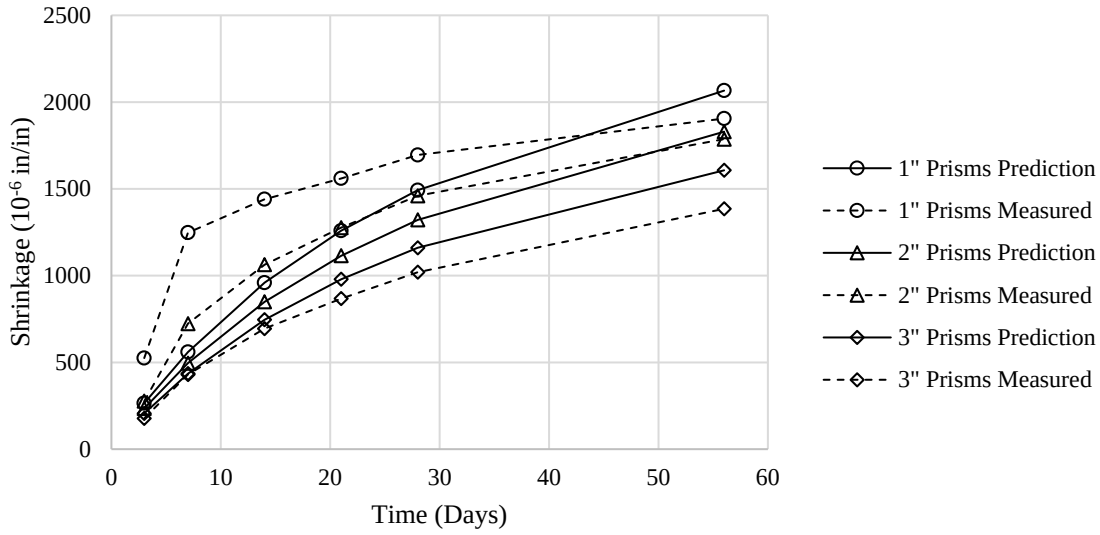

Figure 63. Comparison Between Predicted and Measured Shrinkage Values for Mix 2 Samples Stored in Room 110A at All Ages (ACI Committee 209)

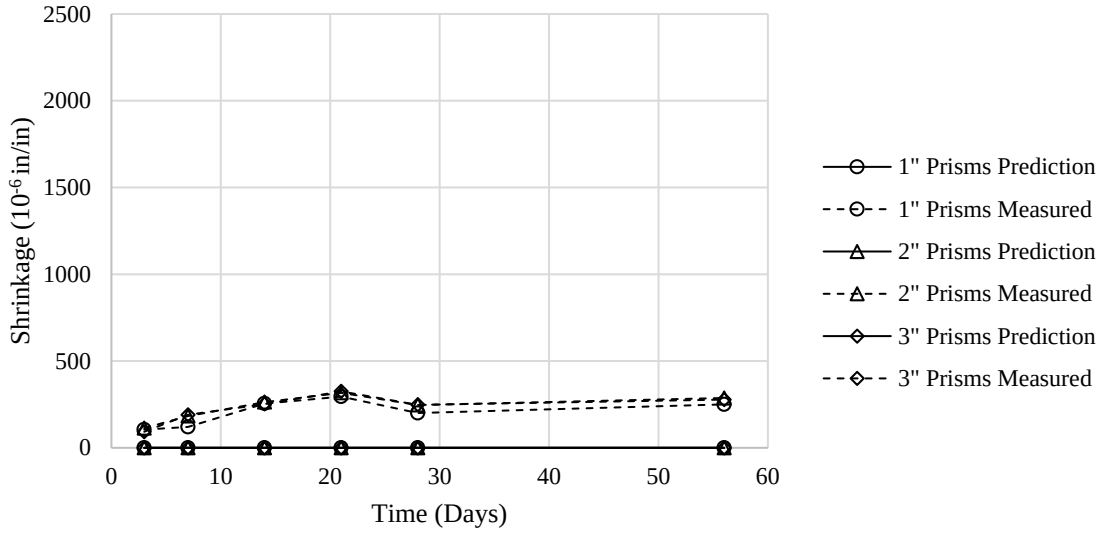

Figure 64. Comparison Between Predicted and Measured Shrinkage Values for Mix 2 Samples Stored in Fog Room at All Ages (ACI Committee 209)

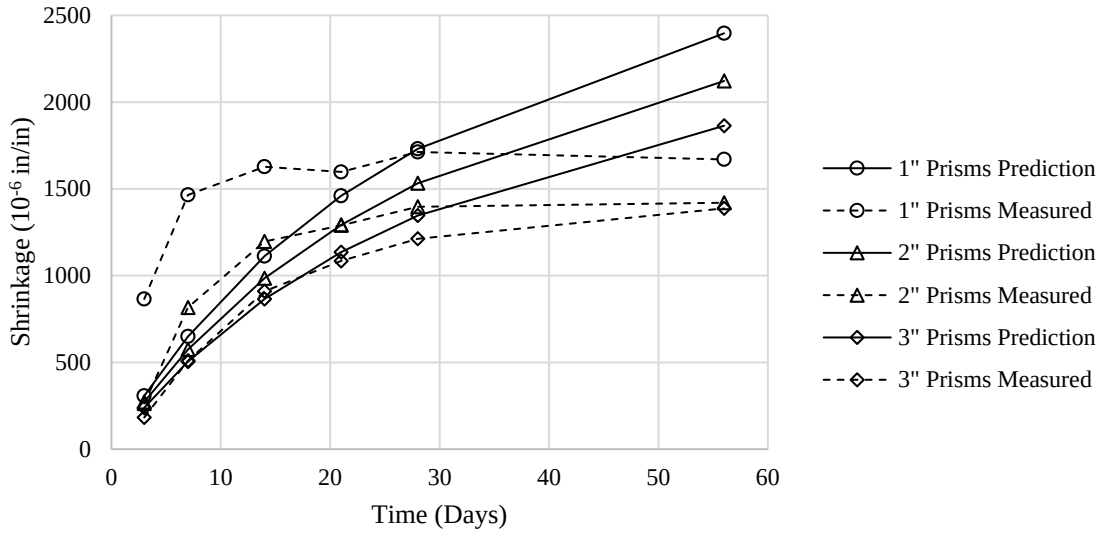

Figure 65. Comparison Between Predicted and Measured Shrinkage Values for Mix 1 Samples Stored in Fume Hood at All Ages (ACI Committee 209)

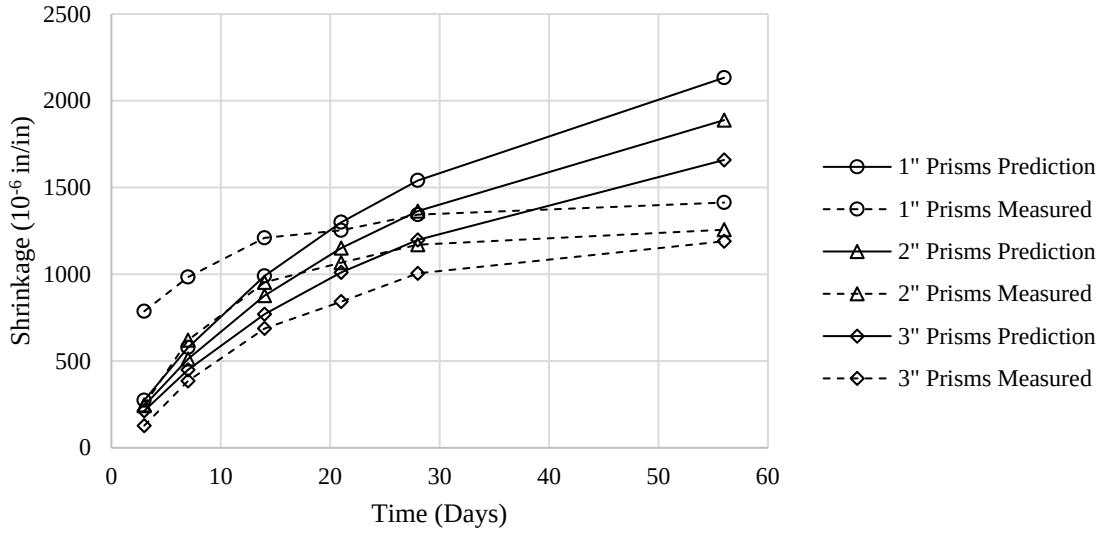

Figure 66. Comparison Between Predicted and Measured Shrinkage Values for Mix 1 Samples Stored in Humidity Chamber at All Ages (ACI Committee 209)

APPENDIX G

SHRINKAGE PREDICTION PER MOON AND WEISS

In this appendix, shrinkage prediction parameters and comparison between predicted and measured shrinkage values will be listed by following Moon and Weiss diffusion equations.

Table 24 Prediction Parameters (Moon and Weiss)

Mix	Locations	γ_h	γ_{cp}	γ_s	γ_f	γ_e	γ_c	Shrinkage Coefficient
1	Fume Hood	1	2	1	1.1	1	1.36	2335
		1	2	1	1.1	1	1.36	2335
		1	2	1	1.1	1	1.36	2335
	Humidity Chamber	0.89	2	1	1.1	1	1.36	2335
		0.89	2	1	1.1	1	1.36	2335
		0.89	2	1	1.1	1	1.36	2335
2	Refrigerator	1	2	1	1.1	1	1.22	2094
		1	2	1	1.1	1	1.22	2094
		1	2	1	1.1	1	1.22	2094
	Humidity Chamber	0.89	2	1	1.1	1	1.22	2094
		0.89	2	1	1.1	1	1.22	2094
		0.89	2	1	1.1	1	1.22	2094
	Fume Hood	1	2	1	1.1	1	1.22	2094
		1	2	1	1.1	1	1.22	2094
		1	2	1	1.1	1	1.22	2094
	Storage Room 130C	0.839	2	1	1.1	1	1.22	2094
		0.839	2	1	1.1	1	1.22	2094
		0.839	2	1	1.1	1	1.22	2094
	Room 110A	1	2	1	1.1	1	1.22	2094
		1	2	1	1.1	1	1.22	2094
		1	2	1	1.1	1	1.22	2094
	UDOT	0.9614	2	1	1.1	1	1.22	2094
		0.9614	2	1	1.1	1	1.22	2094
		0.9614	2	1	1.1	1	1.22	2094
	Fog Room	0	2	1	1.1	1	1.22	2094
		0	2	1	1.1	1	1.22	2094
		0	2	1	1.1	1	1.22	2094

Table 25 Internal RH and Delta RH at Specific Depths and Ages

		Age		3		7		14	
Mix	Locations	Sizes	Depth	RH(x,t)	ΔRH	RH(x,t)	ΔRH	RH(x,t)	ΔRH
1	Fume Hood	1"	0.5	0.899	0.101	0.771	0.229	0.668	0.332
		2"	1	0.997	0.003	0.959	0.041	0.878	0.122
		3"	1.5	1.000	0.000	0.997	0.003	0.969	0.031
	Humidity Chamber	1"	0.5	0.922	0.078	0.824	0.176	0.745	0.255
		2"	1	0.998	0.002	0.969	0.031	0.906	0.094
		3"	1.5	1.000	0.000	0.997	0.003	0.976	0.024
2	Refrigerator	1"	0.5	0.853	0.147	0.666	0.334	0.515	0.485
		2"	1	0.996	0.004	0.940	0.060	0.821	0.179
		3"	1.5	1.000	0.000	0.995	0.005	0.954	0.046
	Humidity Chamber	1"	0.5	0.922	0.078	0.824	0.176	0.745	0.255
		2"	1	0.998	0.002	0.969	0.031	0.906	0.094
		3"	1.5	1.000	0.000	0.997	0.003	0.976	0.024
	Fume Hood	1"	0.5	0.899	0.101	0.771	0.229	0.668	0.332
		2"	1	0.997	0.003	0.959	0.041	0.878	0.122
		3"	1.5	1.000	0.000	0.997	0.003	0.969	0.031
	Storage Room 130C	1"	0.5	0.930	0.070	0.842	0.158	0.770	0.230
		2"	1	0.998	0.002	0.972	0.028	0.915	0.085
		3"	1.5	1.000	0.000	0.998	0.002	0.978	0.022
	Room 110A	1"	0.5	0.890	0.110	0.750	0.250	0.638	0.362
		2"	1	0.997	0.003	0.955	0.045	0.866	0.134
		3"	1.5	1.000	0.000	0.996	0.004	0.966	0.034
	UDOT	1"	0.5	0.912	0.088	0.799	0.201	0.709	0.291
		2"	1	0.997	0.003	0.964	0.036	0.893	0.107
		3"	1.5	1.000	0.000	0.997	0.003	0.972	0.028
	Fog Room	1"	0.5	1.000	0.000	1.000	0.000	1.000	0.000
		2"	1	1.000	0.000	1.000	0.000	1.000	0.000
		3"	1.5	1.000	0.000	1.000	0.000	1.000	0.000

Table 25 Continued

		Age		21		28		56	
Mix	Locations	Sizes	Depth	RH(x,t)	ΔRH	RH(x,t)	ΔRH	RH(x,t)	ΔRH
1	Fume Hood	1"	0.5	0.616	0.384	0.583	0.417	0.518	0.482
		2"	1	0.816	0.184	0.771	0.229	0.668	0.332
		3"	1.5	0.930	0.070	0.894	0.106	0.790	0.210
	Humidity Chamber	1"	0.5	0.704	0.296	0.679	0.321	0.629	0.371
		2"	1	0.859	0.141	0.824	0.176	0.745	0.255
		3"	1.5	0.947	0.053	0.919	0.081	0.838	0.162
2	Refrigerator	1"	0.5	0.439	0.561	0.390	0.610	0.295	0.705
		2"	1	0.732	0.268	0.666	0.334	0.515	0.485
		3"	1.5	0.898	0.102	0.845	0.155	0.693	0.307
	Humidity Chamber	1"	0.5	0.704	0.296	0.679	0.321	0.629	0.371
		2"	1	0.859	0.141	0.824	0.176	0.745	0.255
		3"	1.5	0.947	0.053	0.919	0.081	0.838	0.162
	Fume Hood	1"	0.5	0.616	0.384	0.583	0.417	0.518	0.482
		2"	1	0.816	0.184	0.771	0.229	0.668	0.332
		3"	1.5	0.930	0.070	0.894	0.106	0.790	0.210
	Storage Room 130C	1"	0.5	0.734	0.266	0.711	0.289	0.666	0.334
		2"	1	0.873	0.127	0.842	0.158	0.770	0.230
		3"	1.5	0.952	0.048	0.927	0.073	0.854	0.146
	Room 110A	1"	0.5	0.580	0.420	0.544	0.456	0.473	0.527
		2"	1	0.799	0.201	0.750	0.250	0.638	0.362
		3"	1.5	0.924	0.076	0.884	0.116	0.770	0.230
	UDOT	1"	0.5	0.663	0.337	0.634	0.366	0.577	0.423
		2"	1	0.839	0.161	0.799	0.201	0.709	0.291
		3"	1.5	0.939	0.061	0.907	0.093	0.816	0.184
	Fog Room	1"	0.5	1.000	0.000	1.000	0.000	1.000	0.000
		2"	1	1.000	0.000	1.000	0.000	1.000	0.000
		3"	1.5	1.000	0.000	1.000	0.000	1.000	0.000

Table 26 Predicted Values, Measured Values, Error, and Squared Error for All Samples at All Ages (Moon and Weiss)

		Ages	3				7			
Mix	Locations	Sizes	P*	M	E	SE	P	M	E	SE
1	Fume Hood	1"	235	865	630	396315	534	1465	931	866146
		2"	7	263	257	65822	95	817	722	520581
		3"	0	183	182	33295	8	510	502	252056
	Humidity Chamber	1"	181	787	606	366679	411	983	572	327539
		2"	5	247	241	58300	73	620	547	298996
		3"	0	128	127	16250	6	385	379	143554
2	Refrigerator	1"	309	210	-99	9729	700	735	35	1199
		2"	9	193	184	34022	125	437	312	97309
		3"	0	150	150	22488	10	320	310	95841
	Humidity Chamber	1"	162	803	641	410744	369	983	615	377873
		2"	5	470	465	216528	66	797	731	534394
		3"	0	398	397	157990	5	710	705	496344
	Fume Hood	1"	211	1088	876	767950	479	1175	696	484129
		2"	6	587	581	337084	85	977	891	794469
		3"	0	375	375	140605	7	625	618	381765
	Storage Room 130C	1"	146	573	426	181735	332	1013	681	463410
		2"	4	230	226	50982	59	567	508	257645
		3"	0	147	147	21751	5	370	365	133272
	Room 110A	1"	231	1070	839	704482	523	1363	840	705420
		2"	7	443	437	190703	93	923	830	689098
		3"	0	270	270	72884	8	547	539	290392
	UDOT	1"	185	525	340	115476	420	1248	827	684381
		2"	5	277	271	73624	75	723	648	420552
		3"	0	178	177	31498	6	430	424	179563
	Fog Room	1"	0	105	105	11025	0	120	120	14400
		2"	0	113	113	12844	0	183	183	33611
		3"	0	92	92	8556	0	190	190	36100

* P, M, E, SE stand for predicted values, measured values, error, and squared error.

Table 26 Continued

		Ages	14				21			
Mix	Locations	Sizes	P	M	E	SE	P	M	E	SE
1	Fume Hood	1"	775	1628	853	726974	897	1598	700	490471
		2"	286	1197	911	830173	429	1290	861	741587
		3"	73	910	837	699926	162	1085	923	851279
	Humidity Chamber	1"	596	1210	614	376928	690	1253	563	317203
		2"	220	953	734	538310	330	1067	737	542853
		3"	56	687	631	398225	125	843	718	514969
2	Refrigerator	1"	1016	1363	347	120291	1176	1655	479	229475
		2"	374	750	376	141181	562	1070	508	257949
		3"	96	527	430	185311	213	747	534	285009
	Humidity Chamber	1"	535	1103	569	323499	619	1257	638	406710
		2"	197	1047	850	721970	296	1237	941	885138
		3"	51	998	947	896571	112	1223	1110	1233205
	Fume Hood	1"	695	1225	530	280972	805	1398	593	351522
		2"	256	1237	981	961566	385	1443	1059	1120909
		3"	66	958	892	795105	146	1235	1089	1186785
	Storage Room 130C	1"	481	1290	809	654308	557	1488	930	865764
		2"	177	870	693	479860	266	1083	817	667602
		3"	46	588	542	293696	101	810	709	502962
	Room 110A	1"	759	1420	661	436815	879	1450	571	326179
		2"	280	1203	924	853081	420	1327	907	821853
		3"	72	857	785	615877	159	1057	898	805727
	UDOT	1"	609	1440	831	689893	706	1560	854	730036
		2"	225	1063	839	703549	337	1277	939	882470
		3"	58	695	637	406134	128	868	740	547329
	Fog Room	1"	0	255	255	65025	0	295	295	87025
		2"	0	263	263	69344	0	317	317	100278
		3"	0	253	253	63756	0	325	325	105625

Table 26 Continued

		Age	28				56			
Mix	Locations	Size	P	M	E	SE	P	M	E	SE
1	Fume Hood	1"	974	1713	738	545314	1127	1670	543	295386
		2"	534	1397	862	743624	775	1420	645	416189
		3"	247	1213	966	932257	491	1388	896	803434
	Humidity Chamber	1"	749	1343	594	352915	867	1413	547	298980
		2"	411	1170	759	576046	596	1257	661	436407
		3"	190	1005	815	664268	378	1190	812	659650
2	Refrigerator	1"	1277	1768	491	240846	1477	1918	441	194413
		2"	700	1290	590	347654	1016	1703	688	472880
		3"	324	920	596	355559	644	1390	746	556836
	Humidity Chamber	1"	672	1293	621	386095	777	1393	616	379687
		2"	369	1293	925	855095	535	1367	832	692396
		3"	170	1340	1170	1368023	339	1505	1166	1359942
	Fume Hood	1"	874	1258	384	147411	1010	1393	382	146085
		2"	479	1297	817	668242	695	1483	788	621576
		3"	221	1148	926	857500	440	1413	972	944814
	Storage Room 130C	1"	605	1488	883	779210	699	1615	916	838266
		2"	332	1147	815	664076	481	1320	839	703741
		3"	153	888	734	538995	305	1120	815	664305
	Room 110A	1"	954	1480	526	276471	1104	1570	466	217578
		2"	523	1413	890	791910	759	1557	798	636145
		3"	242	1207	965	930713	481	1470	989	977835
	UDOT	1"	766	1695	929	862960	886	1905	1019	1038471
		2"	420	1460	1040	1081129	609	1787	1177	1385952
		3"	194	1020	826	681901	386	1385	999	997459
	Fog Room	1"	0	200	200	40000	0	250	250	62500
		2"	0	247	247	60844	0	287	287	82178
		3"	0	247	247	61256	0	277	277	77006

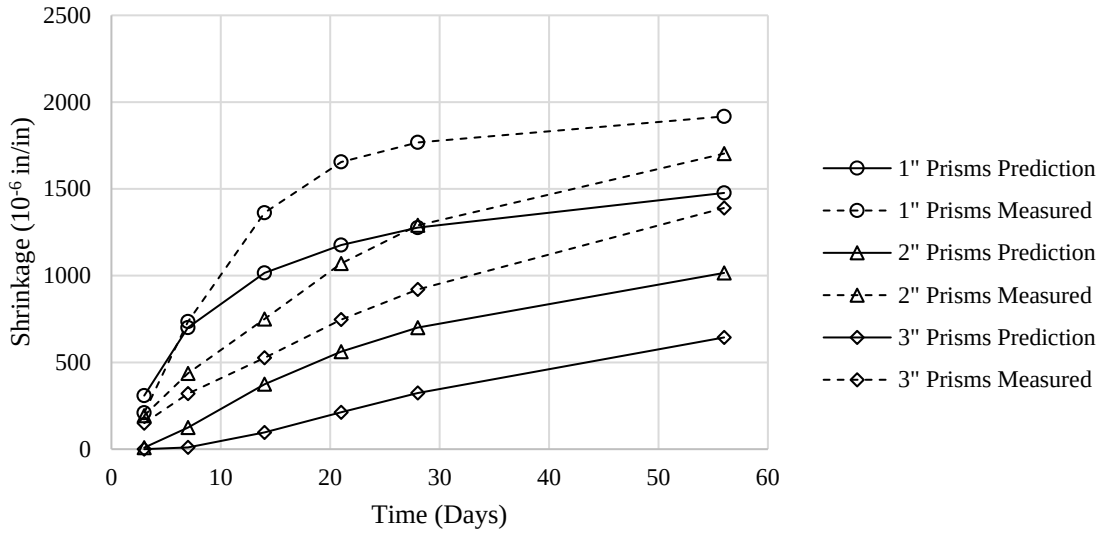

Figure 67. Comparison Between Predicted and Measured Shrinkage Values for Mix 2 Samples Stored in Refrigerator at All Ages (Moon and Weiss)

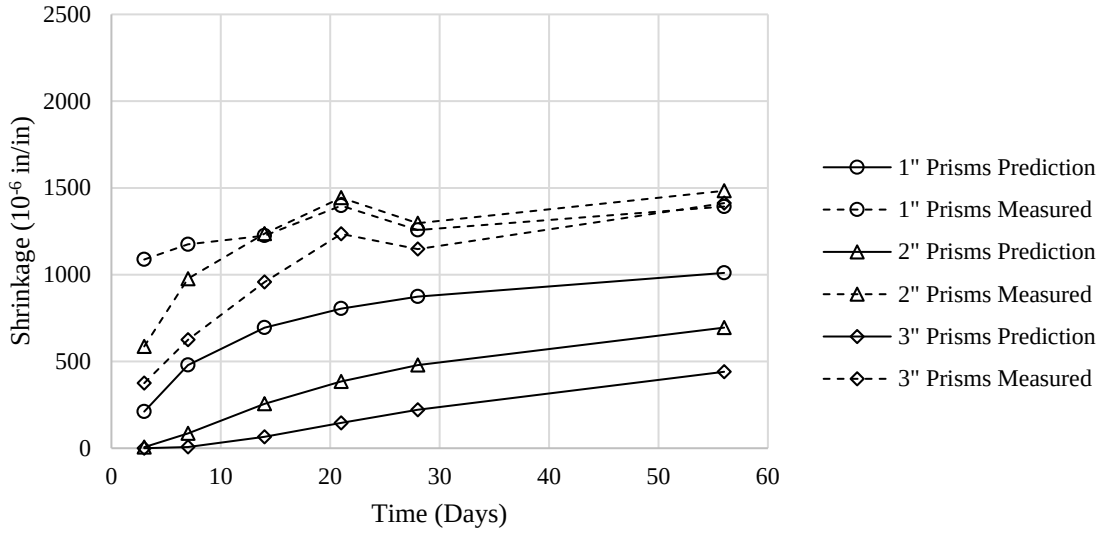

Figure 68. Comparison Between Predicted and Measured Shrinkage Values for Mix 2 Samples Stored in Fume Hood at All Ages (Moon and Weiss)

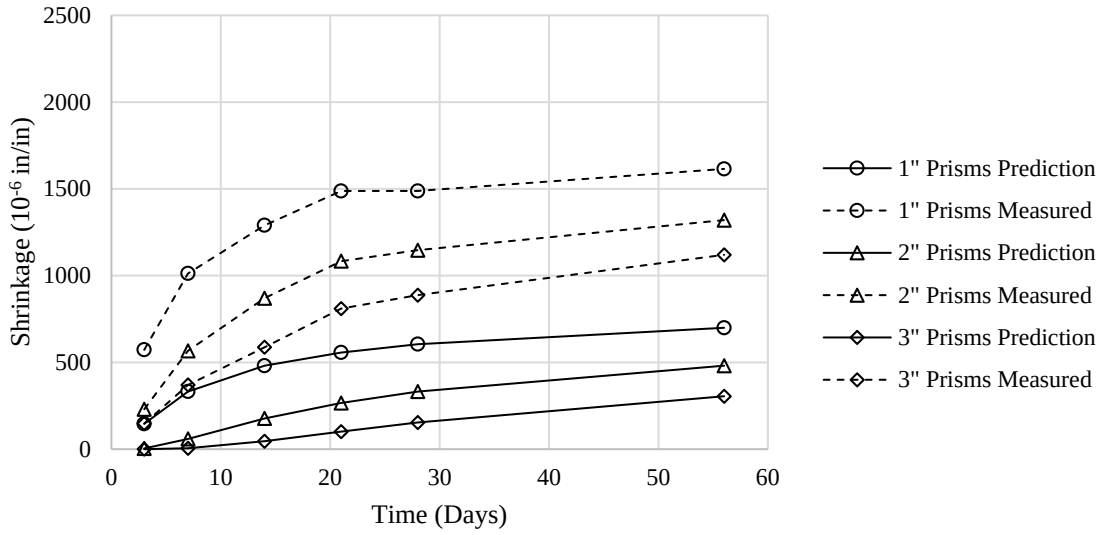

Figure 69. Comparison Between Predicted and Measured Shrinkage Values for Mix 2 Samples Stored in Storage Room 130C at All Ages (Moon and Weiss)

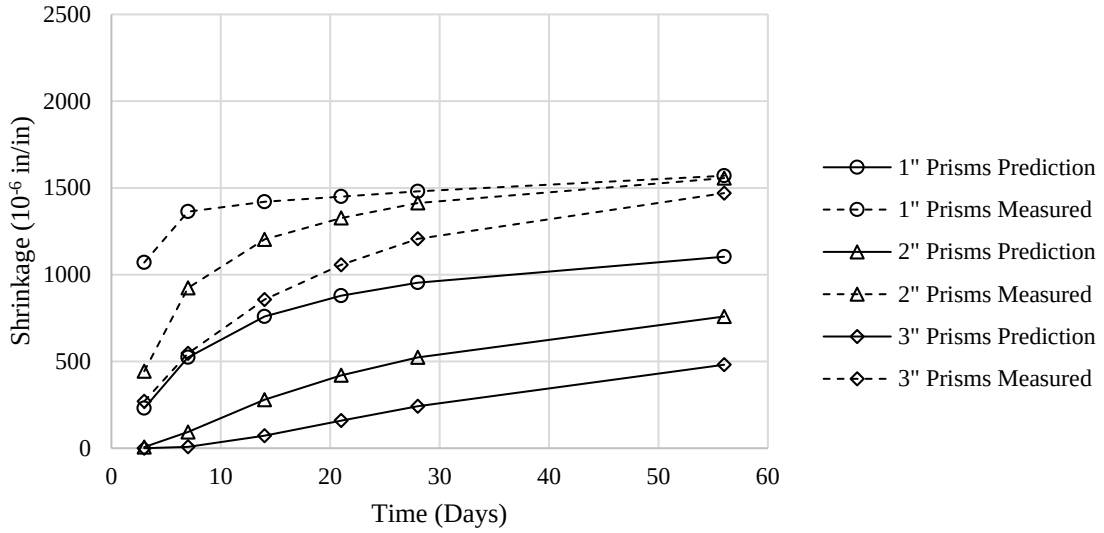

Figure 70. Comparison Between Predicted and Measured Shrinkage Values for Mix 2 Samples Stored in Room 110A at All Ages (Moon and Weiss)

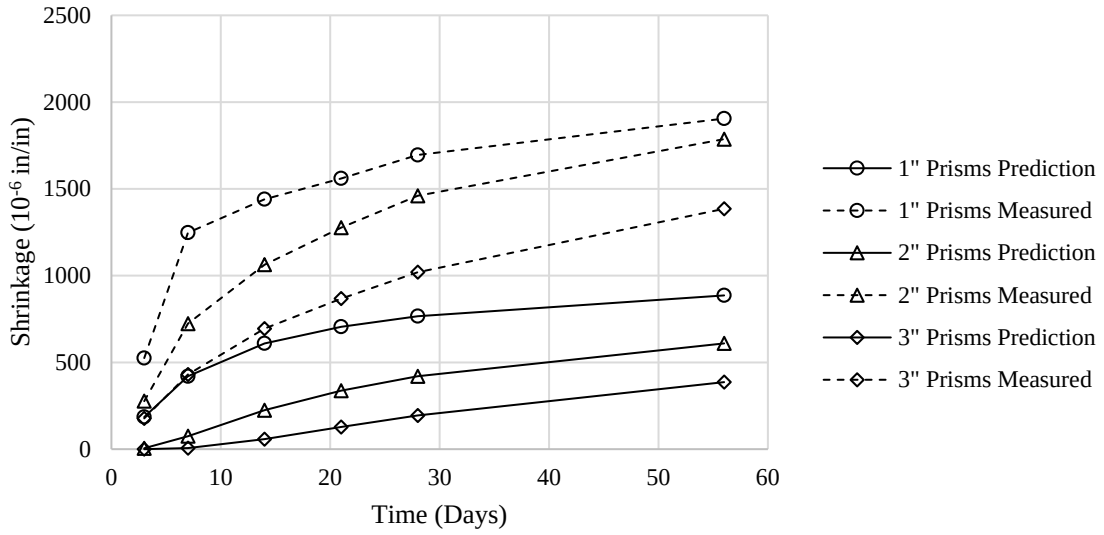

Figure 71. Comparison Between Predicted and Measured Shrinkage Values for Mix 2 Samples Stored in UDOT at All Ages (Moon and Weiss)

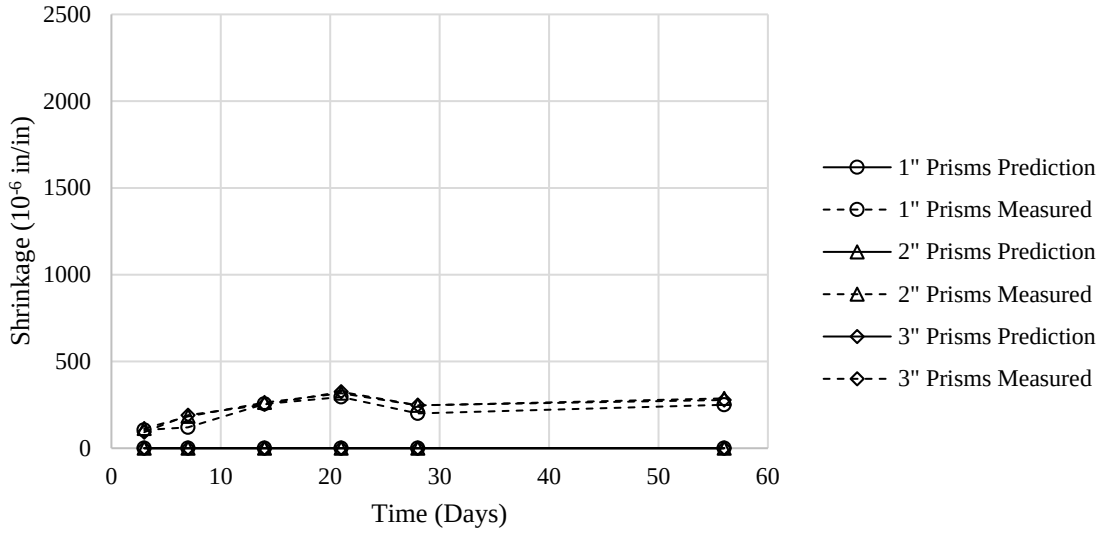

Figure 72. Comparison Between Predicted and Measured Shrinkage Values for Mix 2 Samples Stored in Fog Room at All Ages (Moon and Weiss)

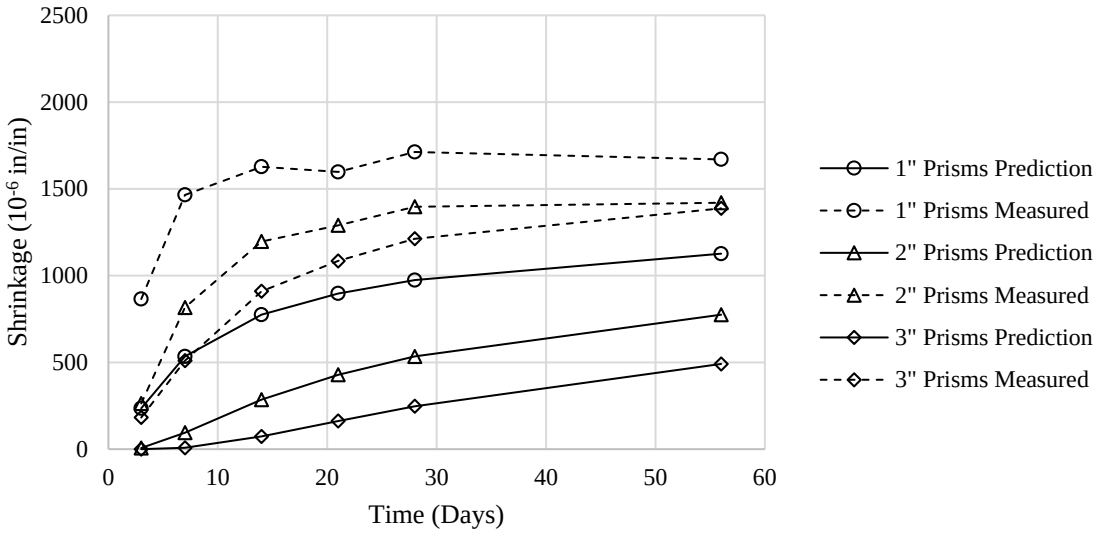

Figure 73. Comparison Between Predicted and Measured Shrinkage Values for Mix 1 Samples Stored in Fume Hood at All Ages (Moon and Weiss)

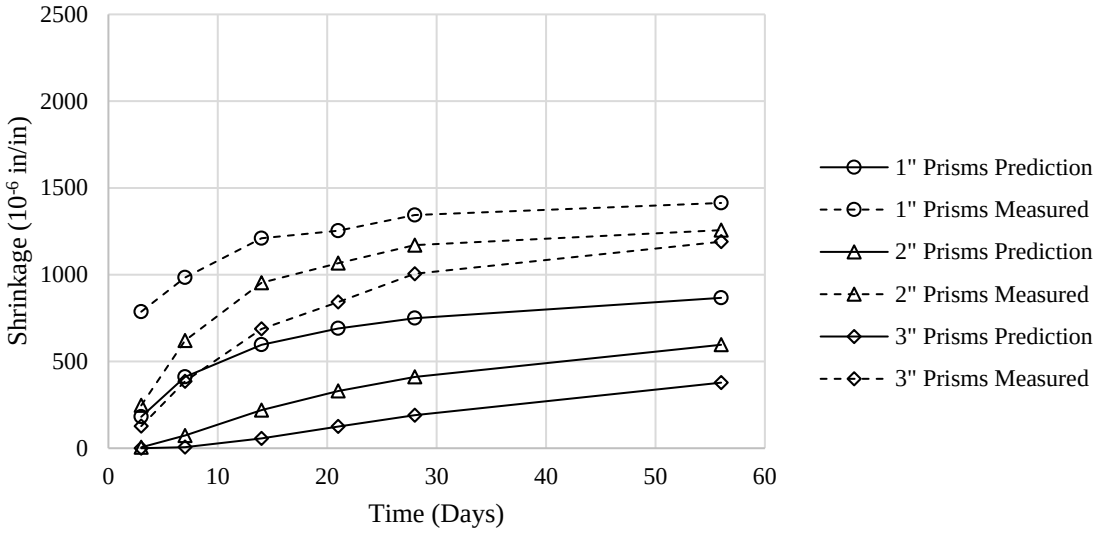

Figure 74. Comparison Between Predicted and Measured Shrinkage Values for Mix 1 Samples Stored in Humidity Chamber at All Ages (Moon and Weiss)

APPENDIX H

SEM/EDS SAMPLE PREPARATION

The concrete sample preparation steps for the analysis under SEM/EDS were based on the FHWA manual, and are detailed below:

Part I: Epoxy

Samples were all put into epoxy before flatting and polishing.

1. The appropriate molds were selected based on samples' dimensions;
2. One mold for one sample each time;
3. Acrylic powder and liquid with a liquid/powder ratio of ½ were used as epoxy material;
4. The acrylic liquid was poured into the specific mixing cup firstly, then the powder was added. The mixture was stirred to a "jelly" status, then poured into the mold;
5. A 40-psi pressure was put to the mold by using a pump, then remained for about 10 minutes to a complete solid status to avoid air voids.

Part II: Flat and Polishing

When samples were all in epoxy, they were flatted and polished to have a better image quality by Gatan 691 Precision Ion Polishing System in University of Utah Nanofab.

1. The RPM number was set to 100 for polishing machine;

2. A 60-grade sand paper was used to flat the sample, checked every 5 minutes to see if the tested sample surface is in the same plane with the epoxy surface, which usually takes 1-2 hours.
3. A 180-grade sand paper was used to polish for approximately 30 minutes.

Part III: Carbon Coating

To avoid changing in SEM, all samples were carbon coated by Gatan 682 Precision Etching Coating System in University of Utah Nanofab Lab after polishing.

1. The Argon gas was turned on for protection;
2. The left and right guns were turned on for approximately 10 minutes for warming up;
3. The chamber and stand were popped out by turning the middle switch to “off” and pushing the “Vent” button;
4. The sample was put on the stand, which was pushed back into the chamber;
5. The “VAC” button was pushed when the Torr number drops;
6. The middle switch was turned to “On”;
7. The rotation wire was turned on;
8. Carbon was selected as the coating material;
9. The left and right guns were turned on;
10. Coating time was set to 20 minutes, then turn on the coating button.

The sample was fully carbon-coated when it finished and ready for SEM/EDS analysis.

APPENDIX I

RAW EDS NUMBER

In this section, tables showed the raw data of weight percentage for each of the three randomly selected spots for each chemical element from SEM/EDS and its normalized percentage weight.

Table 27 EDS Number for PURETi Sample 09/17/15

Sample 1: PureTi 09/17/15							
Element	**%Weight (Reading)**			**%Weight (Normalized)**			
	Spot 1	**Spot 2**	**Spot 3**	**Spot 1**	**Spot 2**	**Spot 3**	**Average**
C	16.72	21.14	15.61	16.72	21.58	15.69	18.00
O	30.44	26.29	30.12	30.44	26.84	30.27	29.18
Na	1.08	0.98	0.95	1.08	1.00	0.95	1.01
Mg	1.31	1.60	1.63	1.31	1.63	1.64	1.53
Al	1.75	1.84	1.83	1.75	1.88	1.84	1.82
Si	13.85	9.70	10.70	13.85	9.90	10.75	11.50
S	1.07	0.93	1.00	1.07	0.95	1.01	1.01
K	1.66	1.46	2.37	1.66	1.49	2.38	1.84
Ca	29.89	31.71	32.43	29.89	32.37	32.59	31.62
Fe	2.24	2.30	2.86	2.24	2.35	2.87	2.49
Sum	100.01	97.95	99.50	100.00	100.00	100.00	100.00

Table 28 EDS Number for TiO_2 Sample 09/17/15

Sample 2: 1% TiO_2 09/17/15							
Element	**%Weight (Reading)**			**%Weight (Normalized)**			
	Spot 1	**Spot 2**	**Spot 3**	**Spot 1**	**Spot 2**	**Spot 3**	**Average**
C	9.98	13.03	13.30	9.98	13.03	13.65	12.22
O	30.42	32.16	31.17	30.42	32.16	31.99	31.53
Na	-	0.62	0.62	-	0.62	0.64	0.63
Mg	1.49	1.36	2.63	1.49	1.36	2.70	1.85
Al	2.14	1.55	1.83	2.14	1.55	1.88	1.86
Si	10.79	11.72	9.89	10.79	11.72	10.15	10.89
S	1.18	1.26	-	1.18	1.26	-	1.22
K	0.81	1.79	1.03	0.81	1.79	1.06	1.22
Ca	39.44	33.53	33.59	39.44	33.53	34.48	35.82
Ti	0.74	0.65	0.77	0.74	0.65	0.79	0.73
Fe	3.00	2.33	2.60	3.00	2.33	2.67	2.67
Sum	99.99	100.00	97.43	100.00	100.00	100.00	100.00

Table 29 EDS Number for Plain Concrete Sample 09/17/15

Sample 3: Plain Concrete 09/17/15							
Element	**%Weight (Reading)**			**%Weight (Normalized)**			
	Spot 1	**Spot 2**	**Spot 3**	**Spot 1**	**Spot 2**	**Spot 3**	**Average**
C	15.54	17.15	19.98	15.72	17.33	20.09	17.71
O	35.70	37.40	30.32	36.11	37.79	30.49	34.80
Na	0.68	-	1.01	0.69	-	1.02	0.85
Mg	1.51	1.26	1.20	1.53	1.27	1.21	1.34
Al	2.01	2.25	1.96	2.03	2.27	1.97	2.09
Si	10.83	10.03	8.70	10.95	10.14	8.75	9.95
S	0.64	0.87	1.26	0.65	0.88	1.27	0.93
K	1.56	1.20	1.06	1.58	1.21	1.07	1.29
Ca	28.01	26.32	30.75	28.33	26.60	30.92	28.62
Fe	2.38	2.48	3.20	2.41	2.51	3.22	2.71
Sum	98.86	98.96	99.44	100.00	100.00	100.00	100.00

Table 30 EDS Number for PURETi Sample 10/28/15

Sample 4: PureTi 10/28/15							
Element	**%Weight (Reading)**			**%Weight (Normalized)**			
	Spot 1	**Spot 2**	**Spot 3**	**Spot 1**	**Spot 2**	**Spot 3**	**Average**
C	12.82	-	14.85	12.82	-	14.95	13.89
O	31.19	40.17	33.24	31.19	40.17	33.47	34.94
Na	-	-	0.48	-	-	0.48	0.48
Mg	1.68	1.00	1.01	1.68	1.00	1.02	1.23
Al	1.85	1.62	1.78	1.85	1.62	1.79	1.75
Si	12.62	25.61	9.80	12.62	25.61	9.87	16.03
S	1.05	-	1.01	1.05	-	1.02	1.03
K	0.75	1.26	0.95	0.75	1.26	0.96	0.99
Ca	35.00	27.95	33.48	35.00	27.95	33.71	32.22
Fe	3.03	2.40	2.71	3.03	2.40	2.73	2.72
Sum	99.99	100.01	99.31	100.00	100.00	100.00	100.00

Table 31 EDS Number for TiO_2 Sample 10/28/15

Sample 5: 1% TiO_2 10/28/15							
Element	**%Weight (Reading)**			**%Weight (Normalized)**			
	Spot 1	**Spot 2**	**Spot 3**	**Spot 1**	**Spot 2**	**Spot 3**	**Average**
C	13.04	12.50	11.74	13.25	12.67	11.84	12.59
O	28.87	30.86	30.17	29.34	31.28	30.42	30.34
Na	0.56	0.39	-	0.57	0.40	-	0.48
Mg	1.09	1.43	1.44	1.11	1.45	1.45	1.34
Al	1.90	1.96	2.01	1.93	1.99	2.03	1.98
Si	13.16	14.87	11.84	13.37	15.07	11.94	13.46
S	0.91	0.99	1.08	0.92	1.00	1.09	1.01
K	1.29	0.67	0.64	1.31	0.68	0.65	0.88
Ca	34.06	31.46	36.20	34.61	31.89	36.50	34.33
Ti	0.73	0.83	0.95	0.74	0.84	0.96	0.85
Fe	2.79	2.70	3.12	2.84	2.74	3.15	2.91
Sum	98.40	98.66	99.19	100.00	100.00	100.00	100.00

Table 32 EDS Number for Plain Concrete Sample 10/28/15

Sample 6: Plain Concrete 10/28/15							
Element	**%Weight (Reading)**			**%Weight (Normalized)**			
	Spot 1	**Spot 2**	**Spot 3**	**Spot 1**	**Spot 2**	**Spot 3**	**Average**
C	11.33	8.89	8.21	11.33	8.91	8.21	9.48
O	40.57	36.40	35.09	40.57	36.46	35.09	37.37
Na	-	0.49	0.57	-	0.49	0.57	0.53
Mg	0.39	2.05	1.95	0.39	2.05	1.95	1.46
Al	6.48	2.99	3.07	6.48	3.00	3.07	4.18
Si	24.15	12.87	12.07	24.15	12.89	12.07	16.37
S	-	0.58	0.60	-	0.58	0.60	0.59
K	1.72	0.94	0.91	1.72	0.94	0.91	1.19
Ca	13.61	30.92	33.22	13.61	30.97	33.22	25.93
Fe	1.76	3.70	4.32	1.76	3.71	4.32	3.26
Sum	100.01	99.83	100.01	100.00	100.00	100.00	100.00

APPENDIX J

RAW TGA

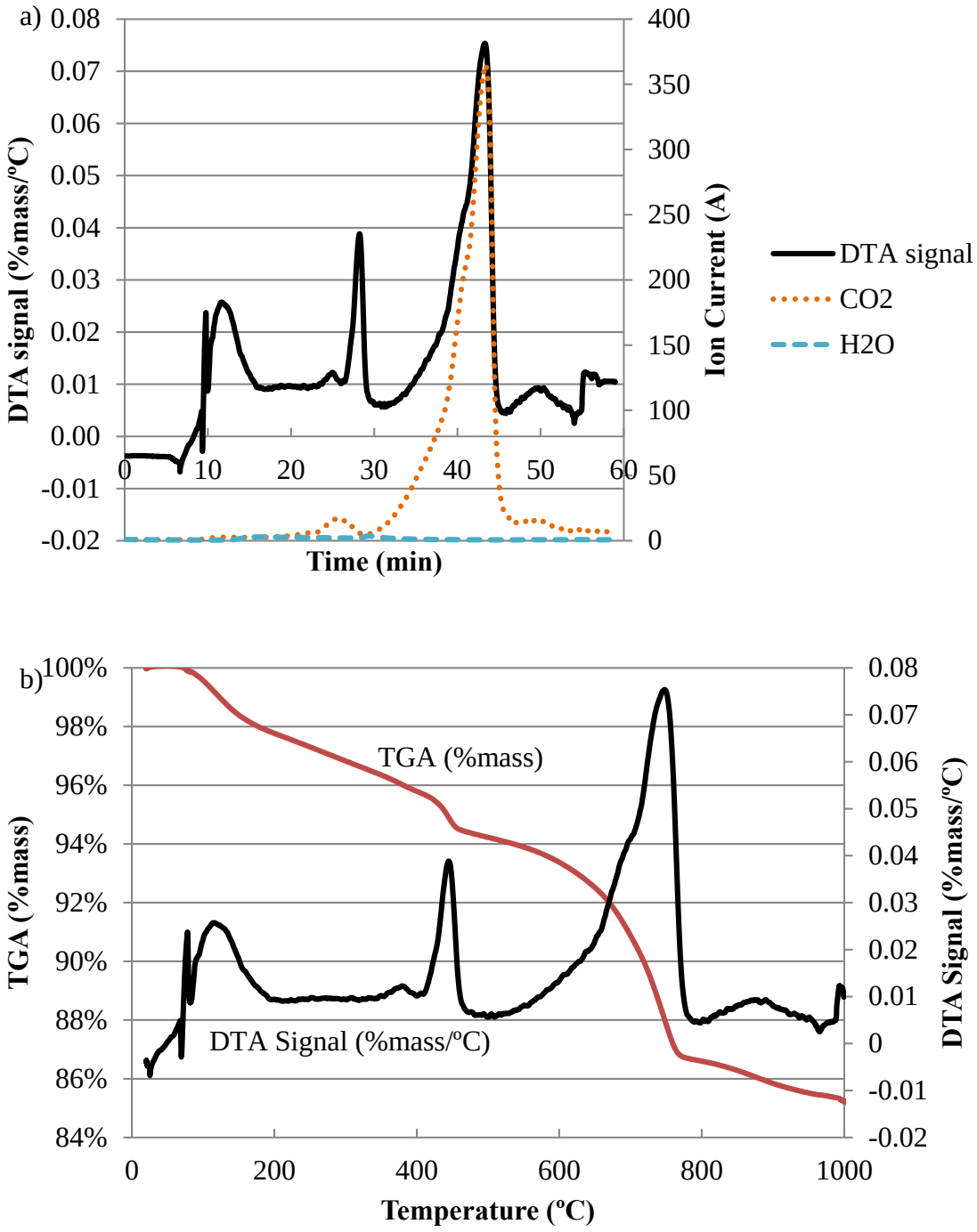

Figure 75. Plain Concrete 08/12/15 at 5 mm Depth a) MS; b) TGA

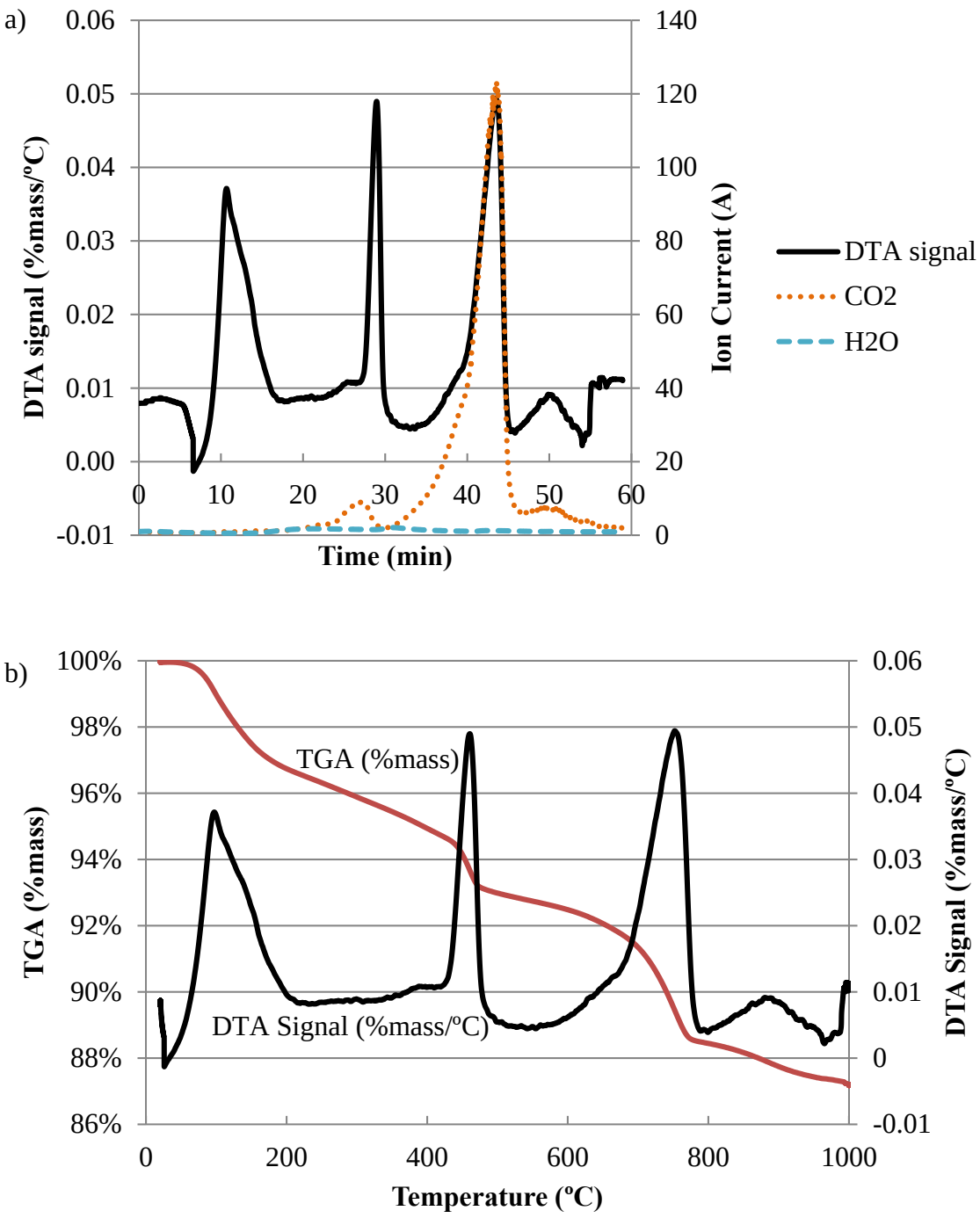

Figure 76. Plain Concrete 08/12/15 at 10 mm Depth a) DTA-MS; b) TGA

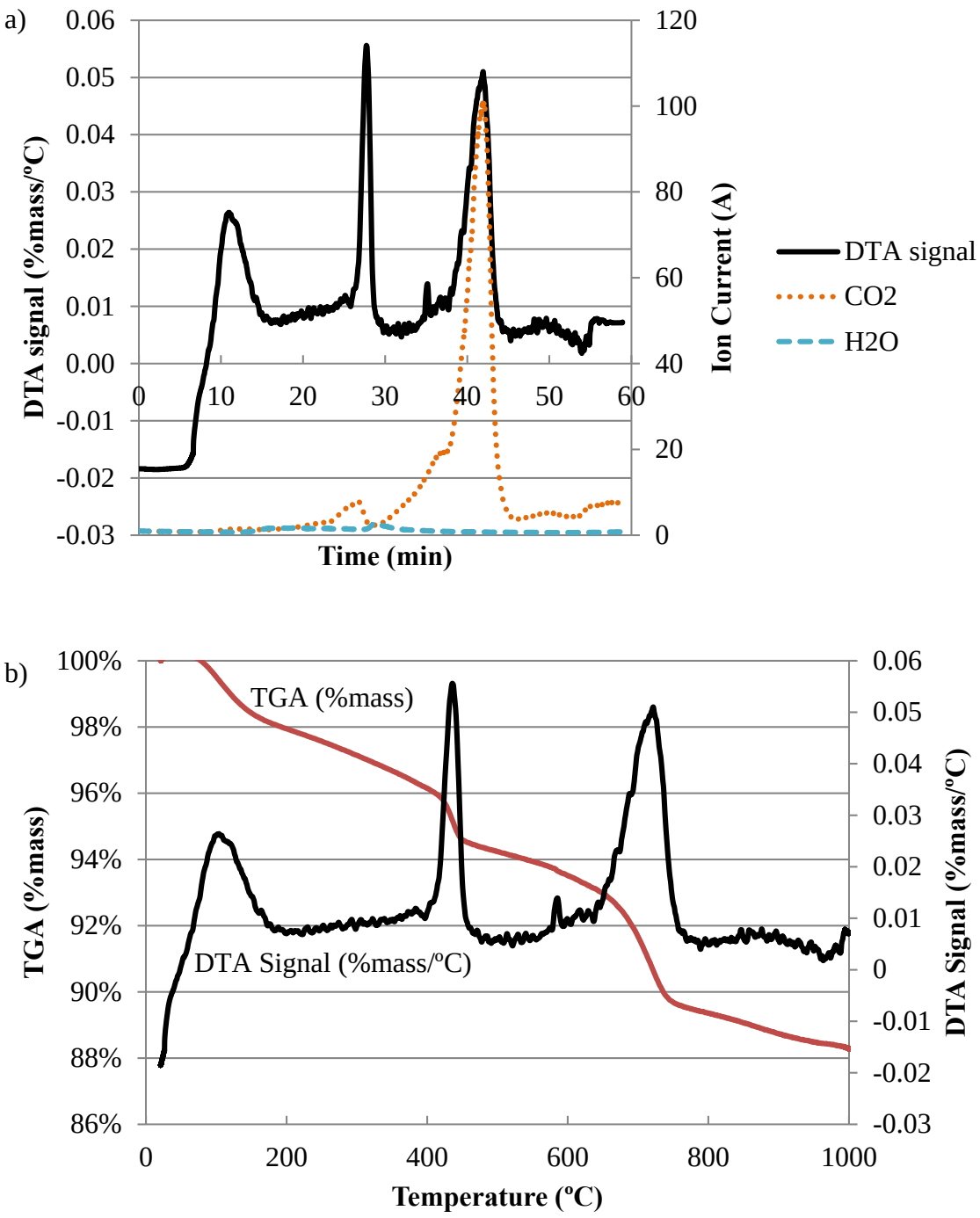

Figure 77. Plain Concrete 08/12/15 at 15 mm Depth a) DTA-MS; b) TGA

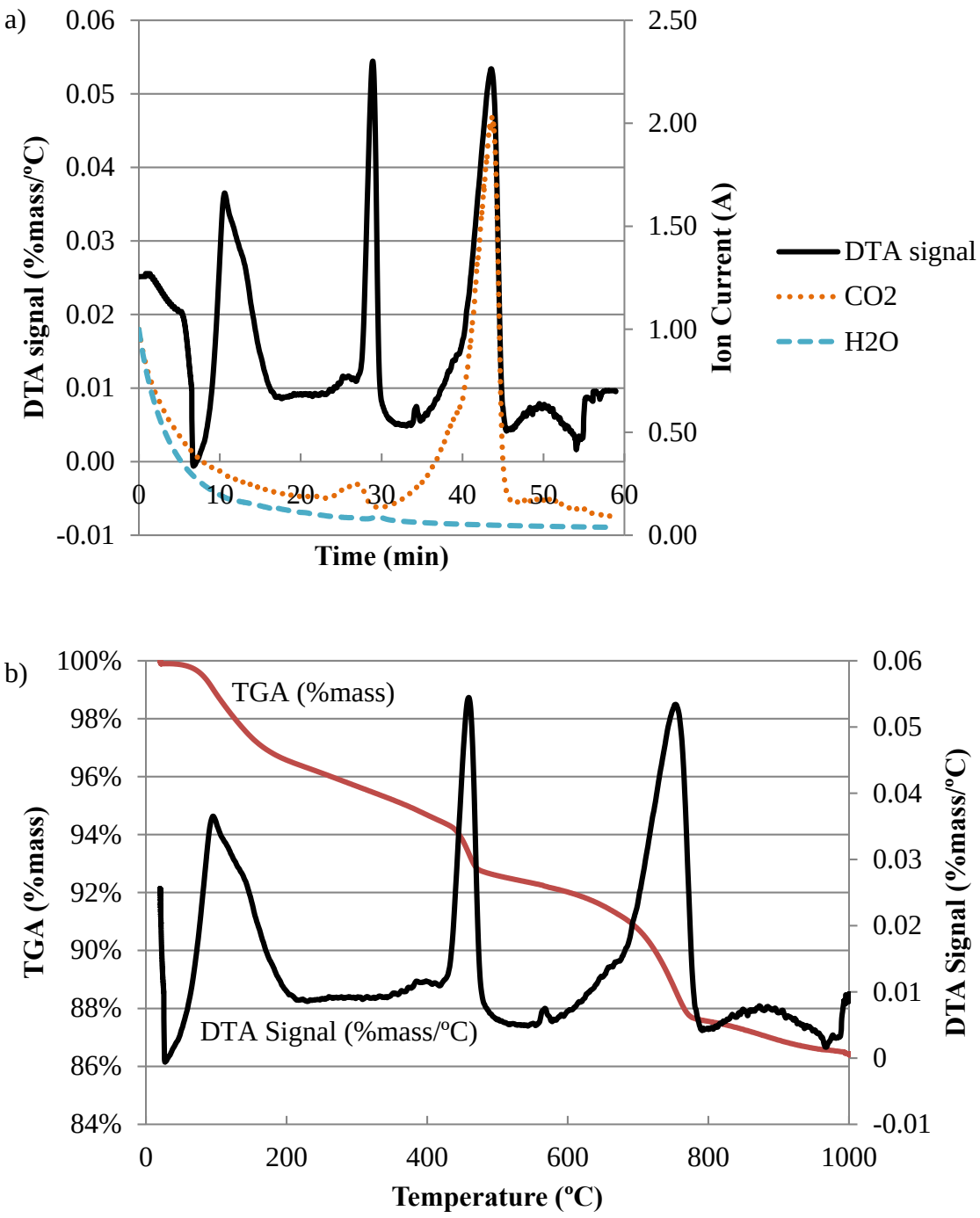

Figure 78. Plain Concrete 09/17/15 at 10 mm Depth a) DTA-MS; b) TGA

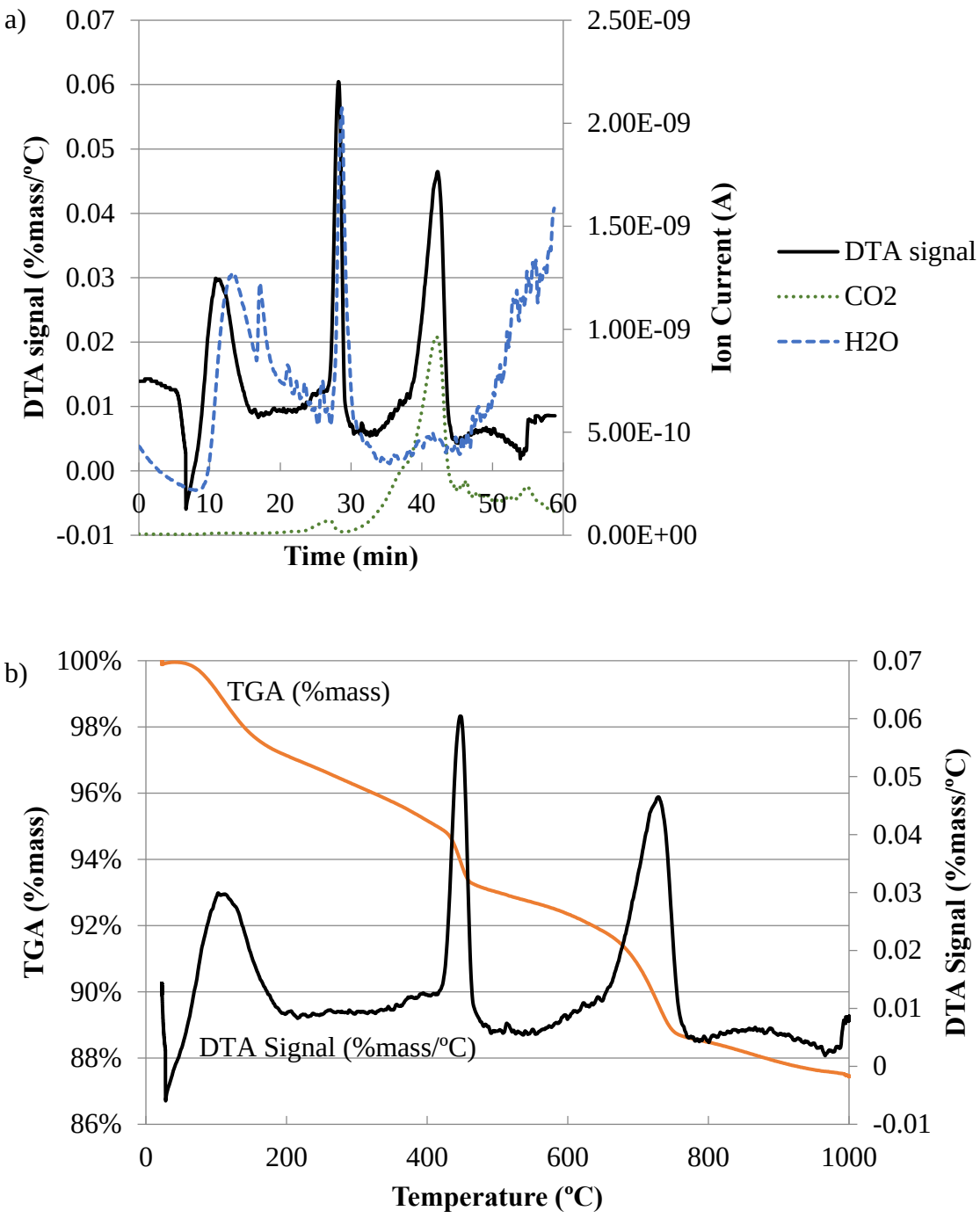

Figure 79. Plain Concrete 09/17/15 at 15 mm Depth a) DTA-MS; b) TGA

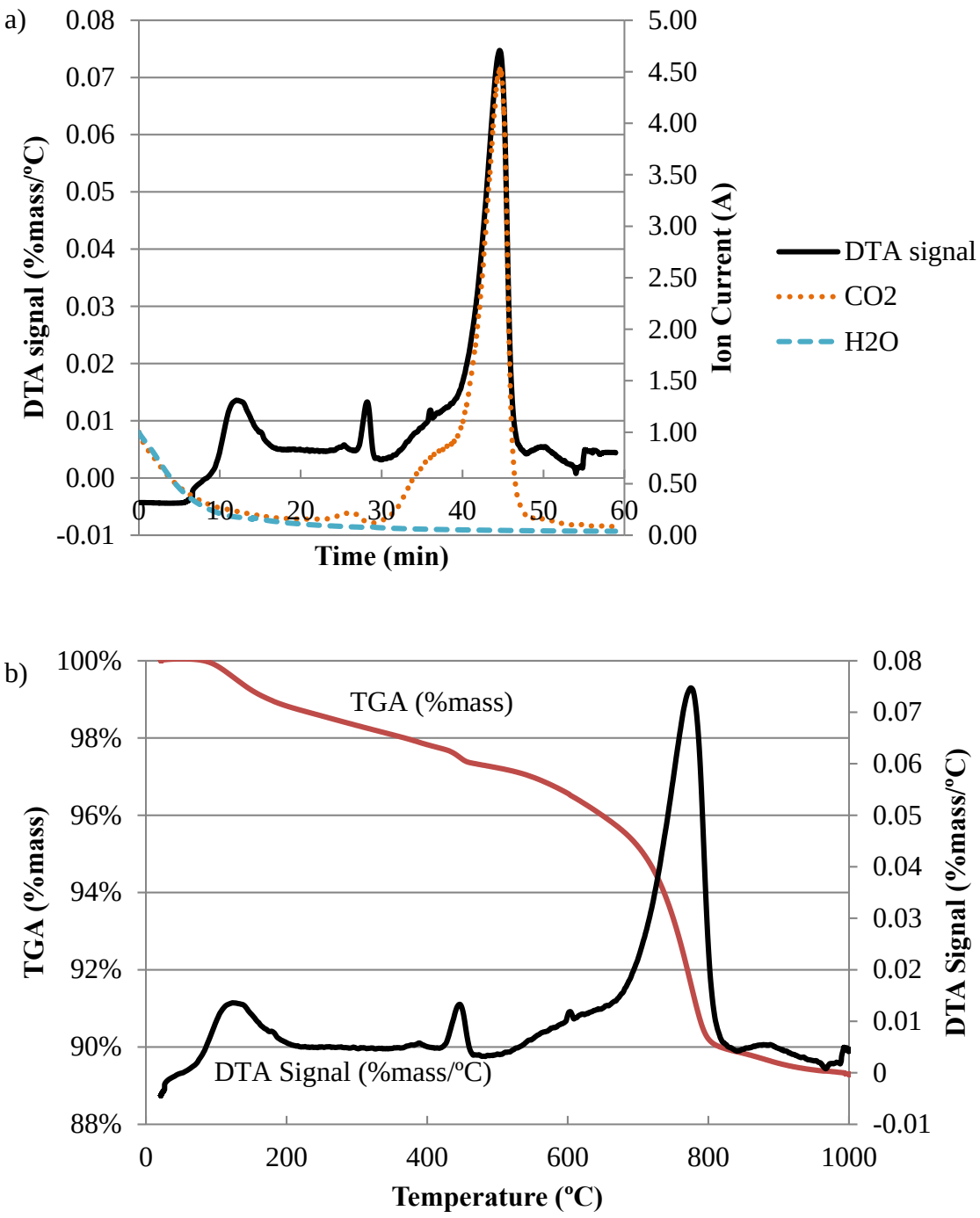

Figure 80. Plain Concrete 10/28/15 at 5 mm Depth a) DTA-MS; b) TGA

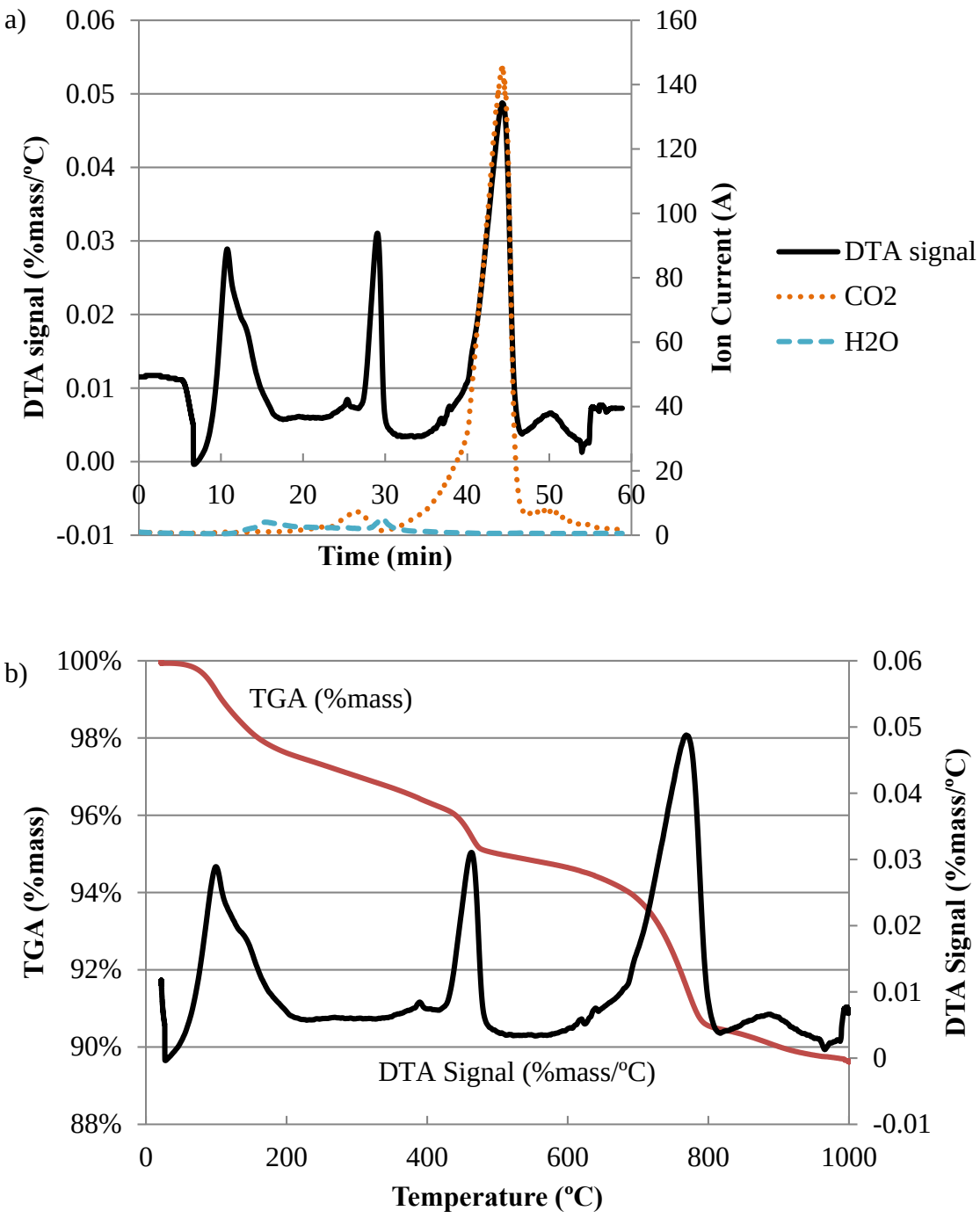

Figure 81. Plain Concrete 10/28/15 at 10 mm Depth a) DTA-MS; b) TGA

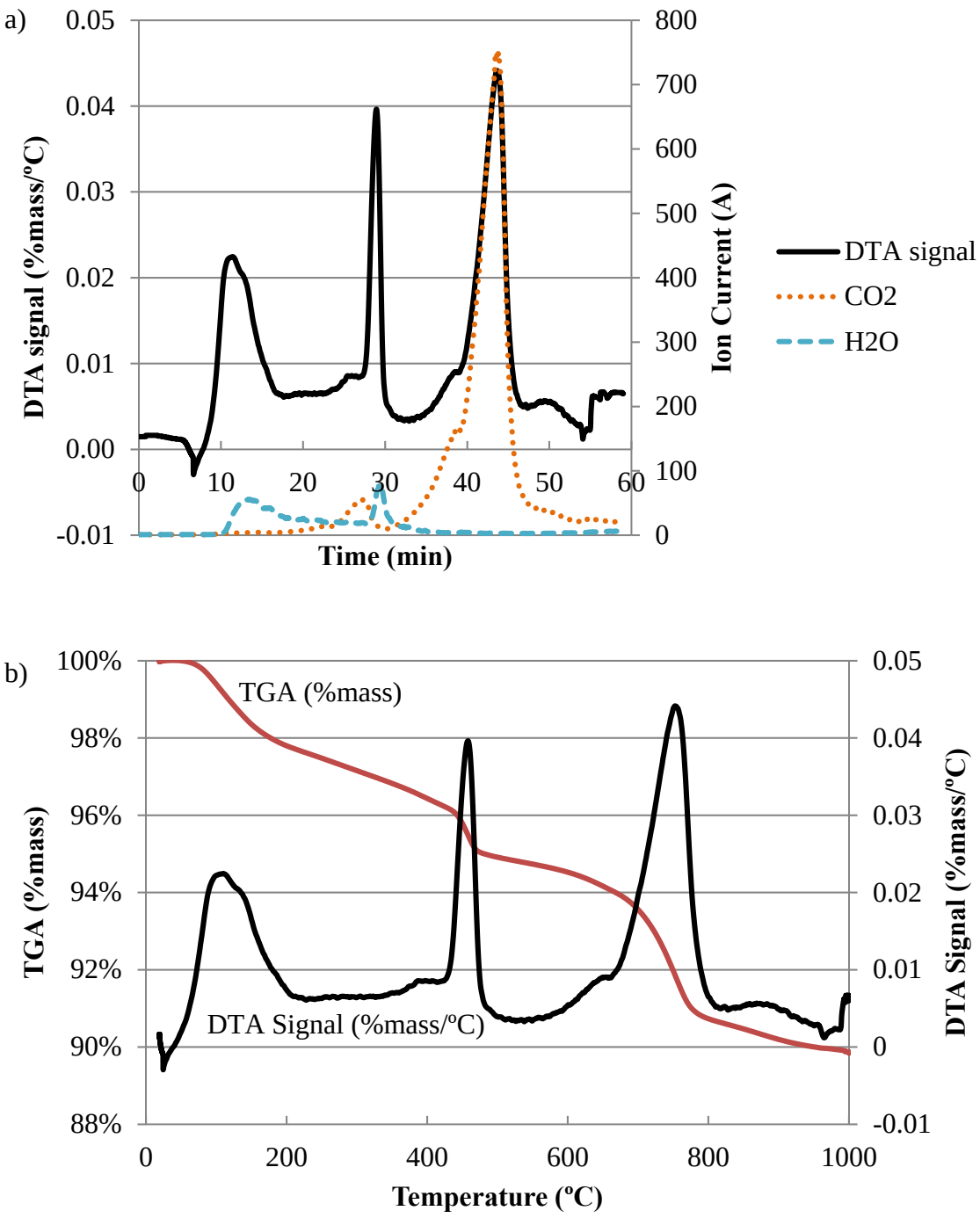

Figure 82. Plain Concrete 10/28/15 at 15 mm Depth a) DTA-MS; b) TGA

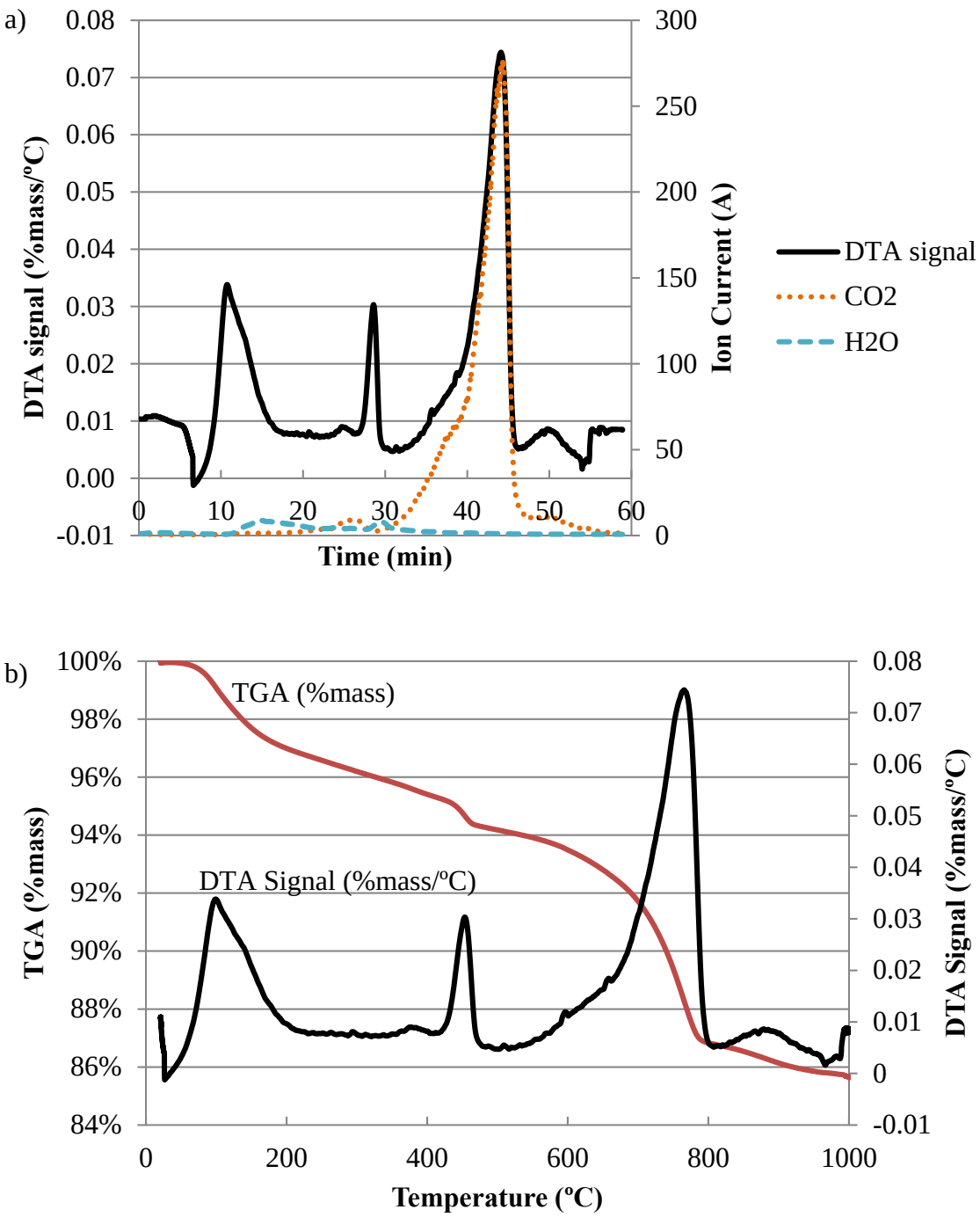

Figure 83. PureTi 08/12/15 at 5 mm Depth a) DTA-MS; b) TGA

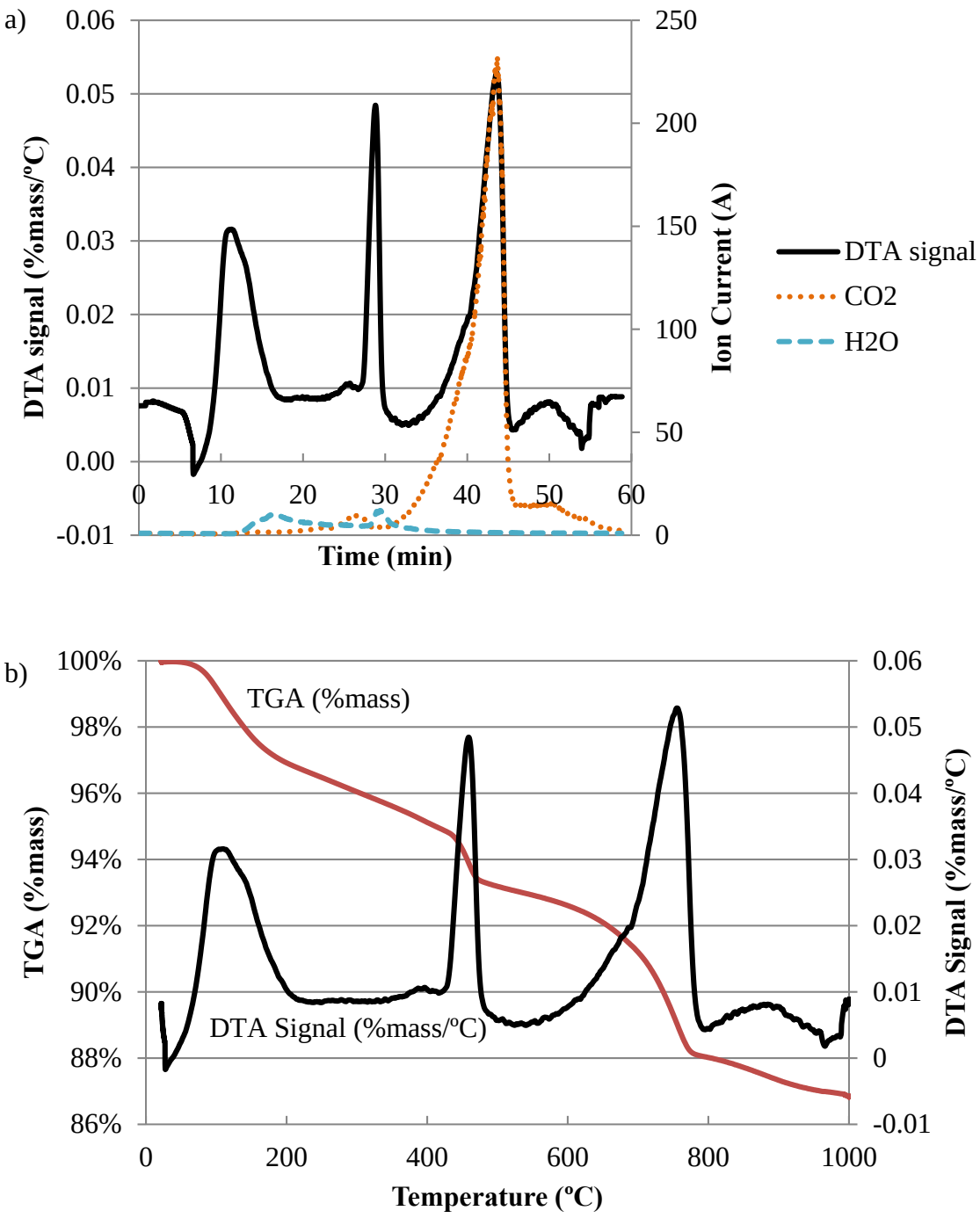

Figure 84. PureTi 08/12/15 at 10 mm Depth a) DTA-MS; b) TGA

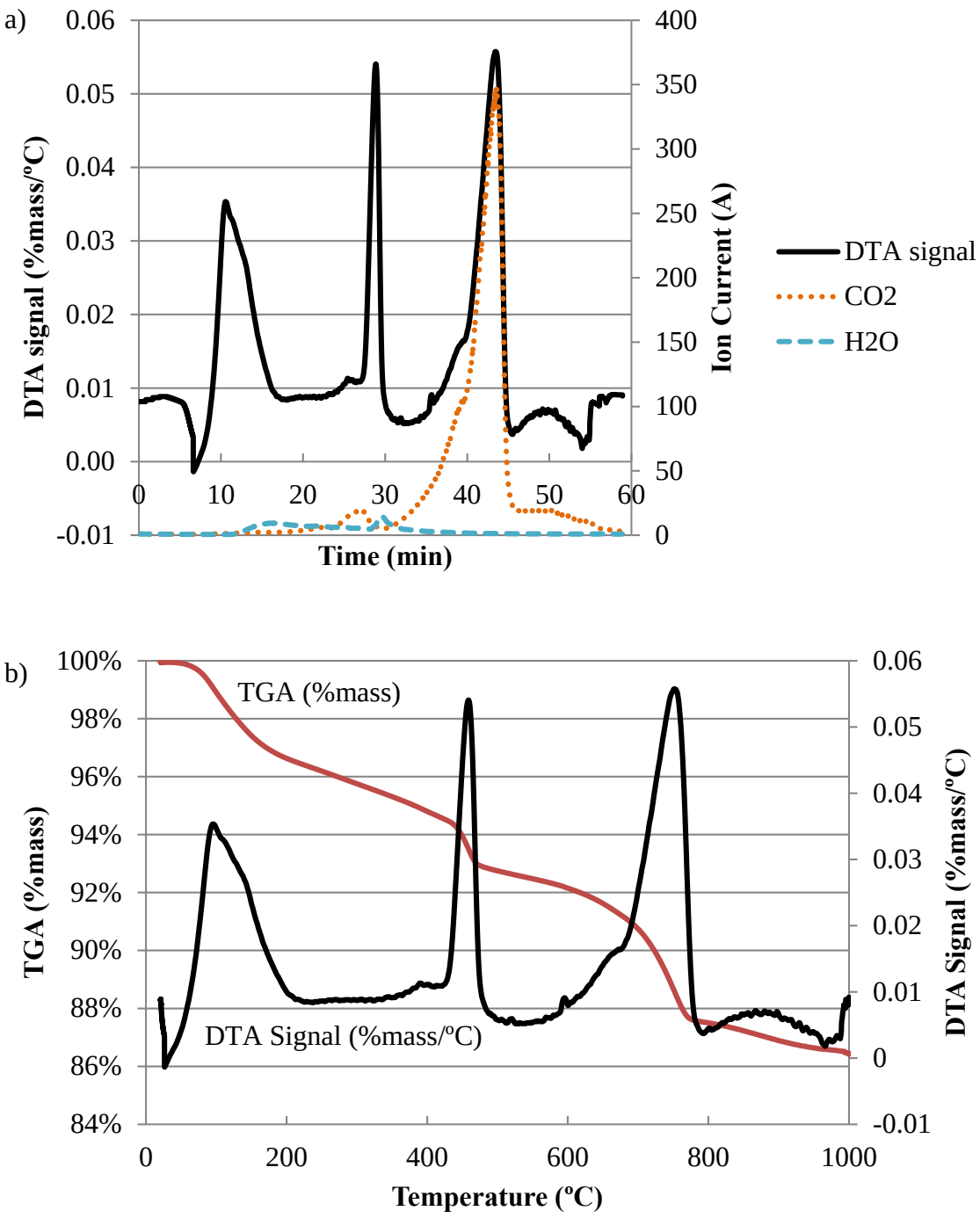

Figure 85. PureTi 08/12/15 at 15 mm Depth a) DTA-MS; b) TGA

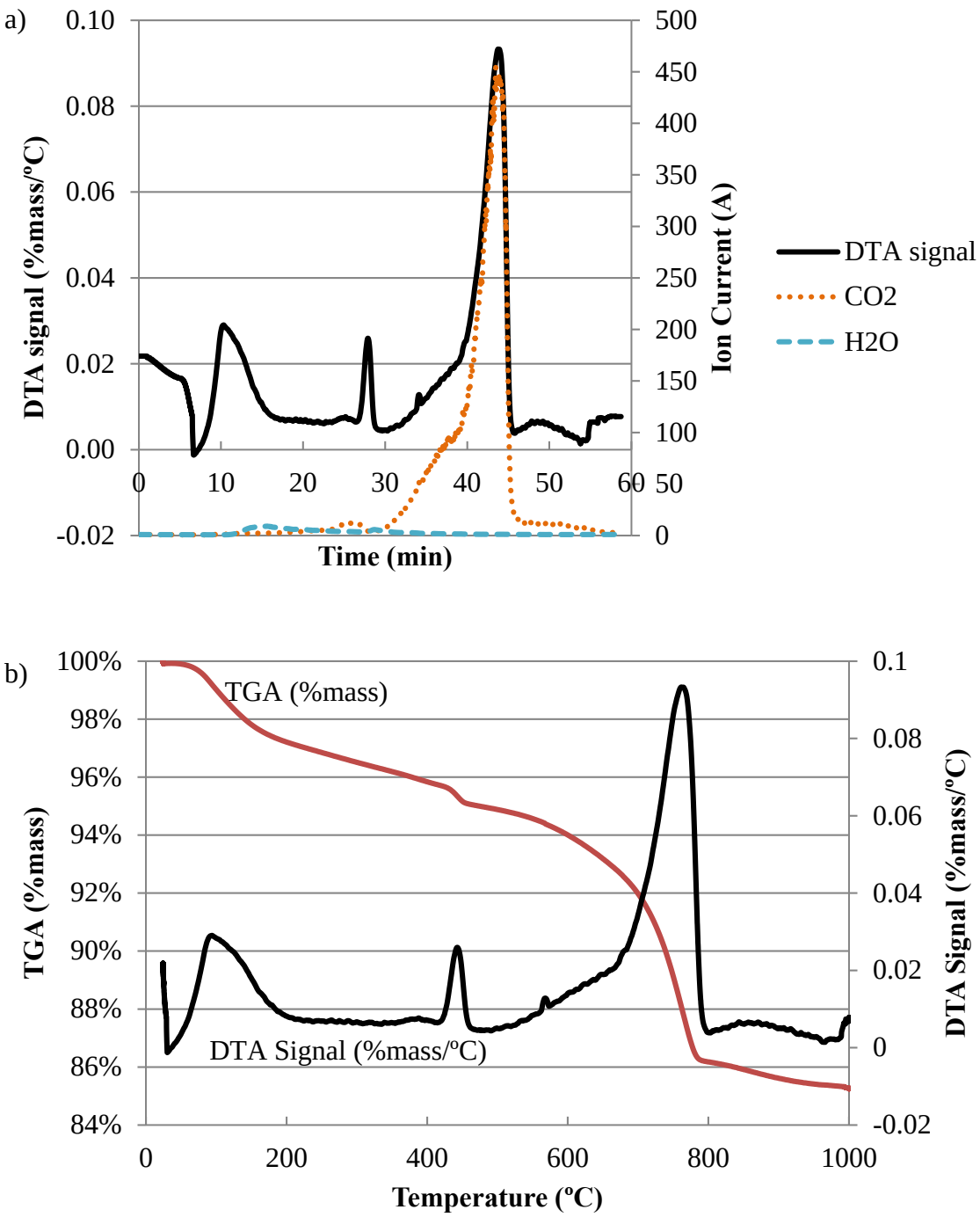

Figure 86. PureTi 09/17/15 at 5 mm Depth a) DTA-MS; b) TGA

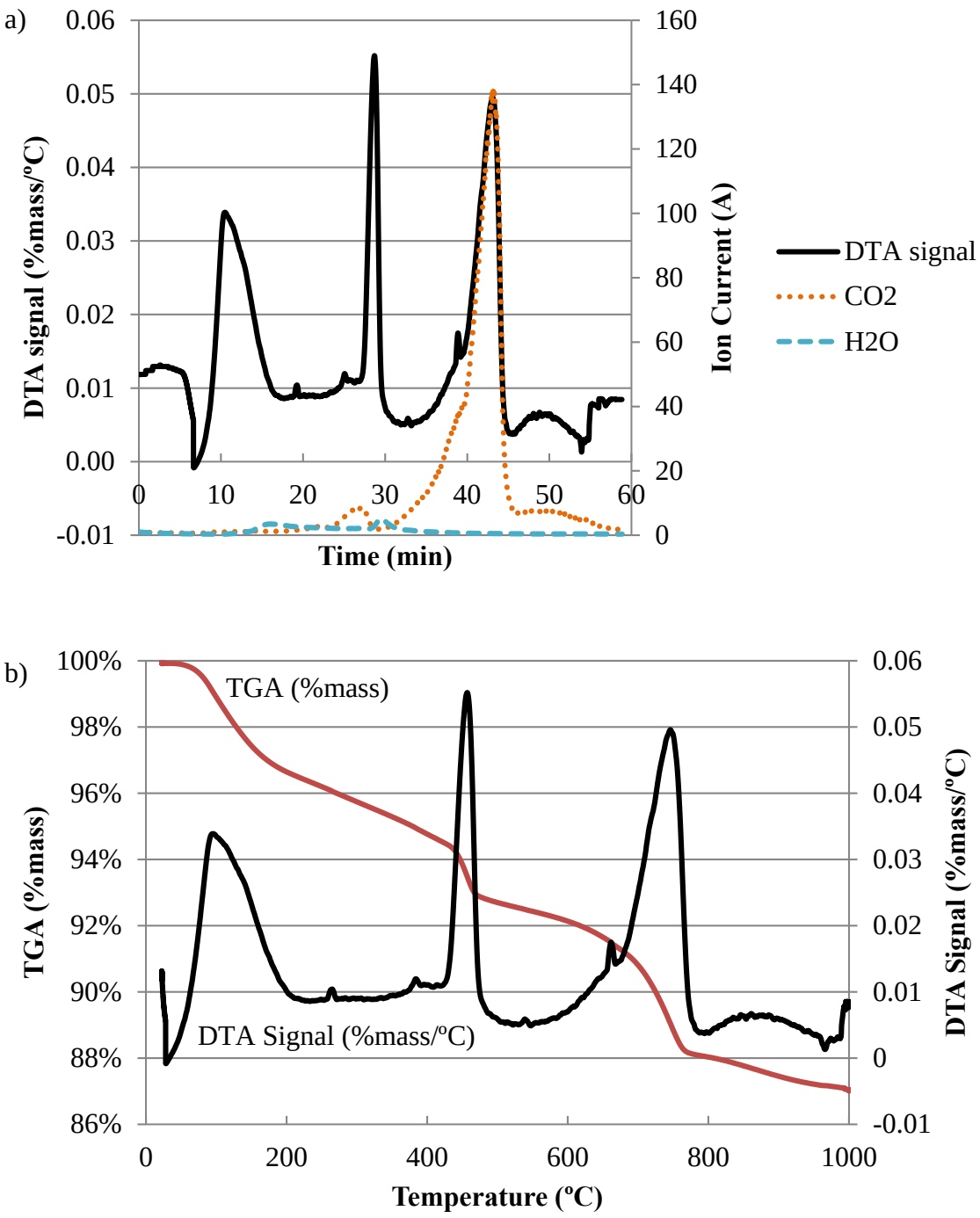

Figure 87. PureTi 09/17/15 at 10 mm Depth a) DTA-MS; b) TGA

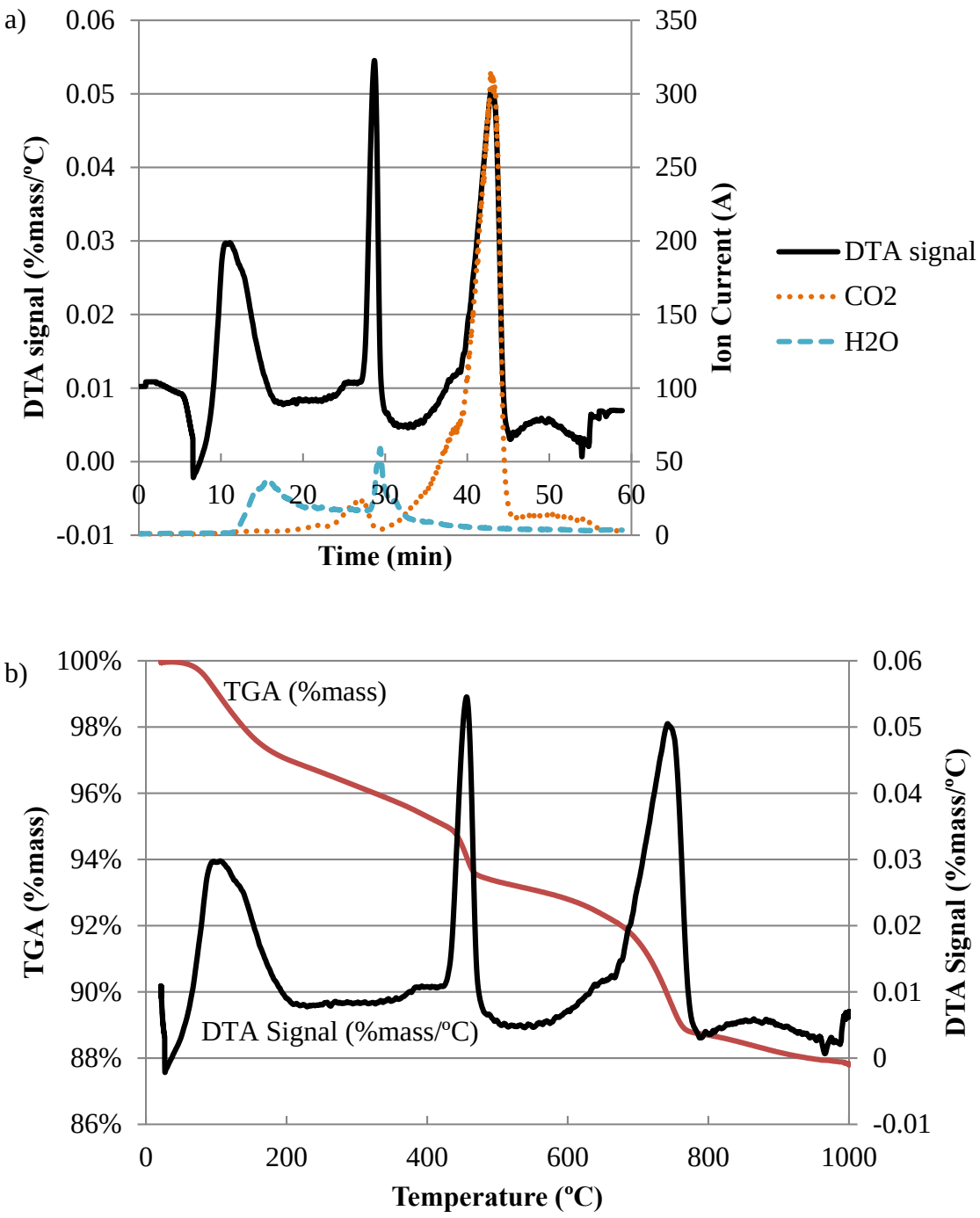

Figure 88. PureTi 09/17/15 at 15 mm Depth a) DTA-MS; b) TGA

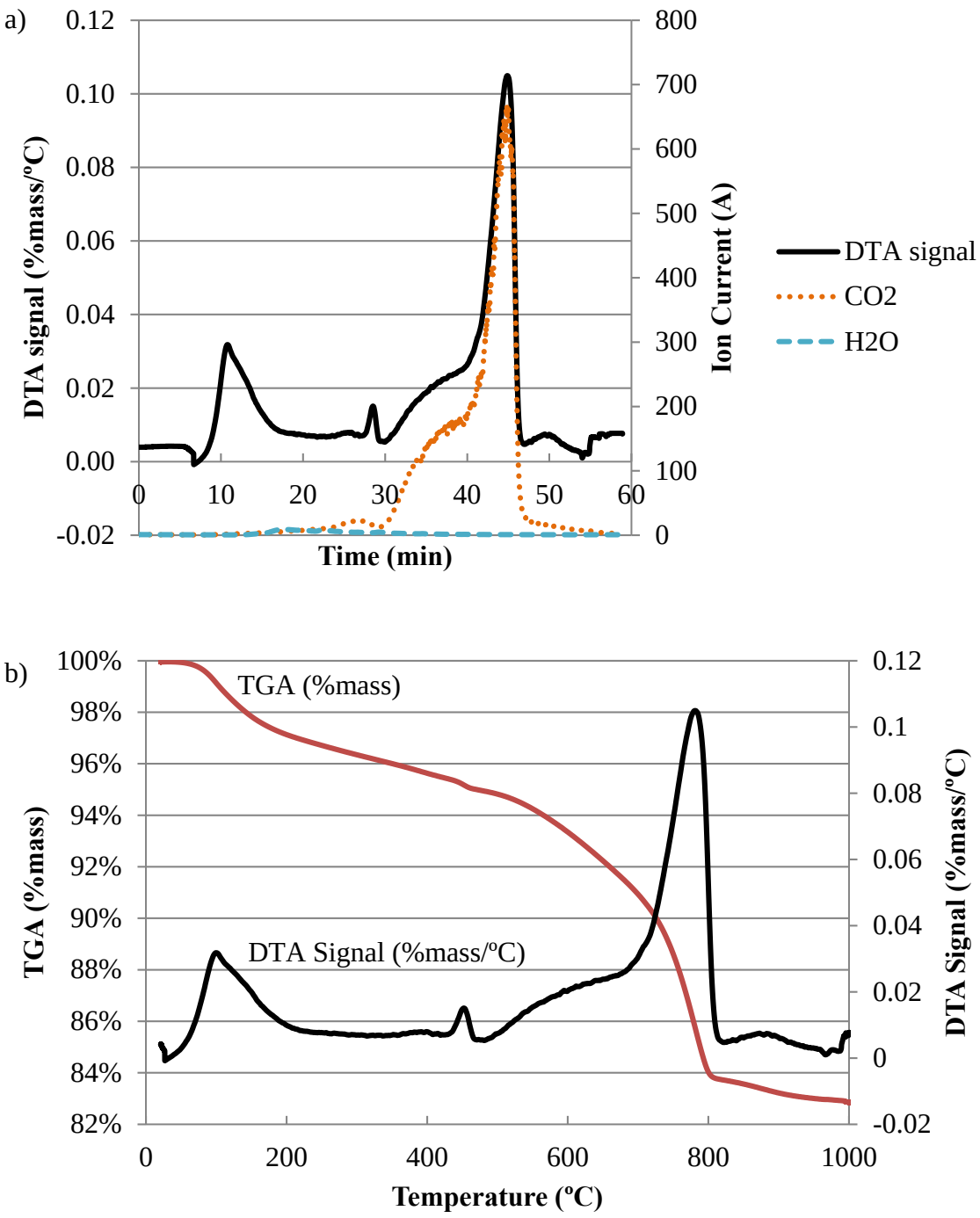

Figure 89. PureTi 10/28/15 at 5 mm Depth a) DTA-MS; b) TGA

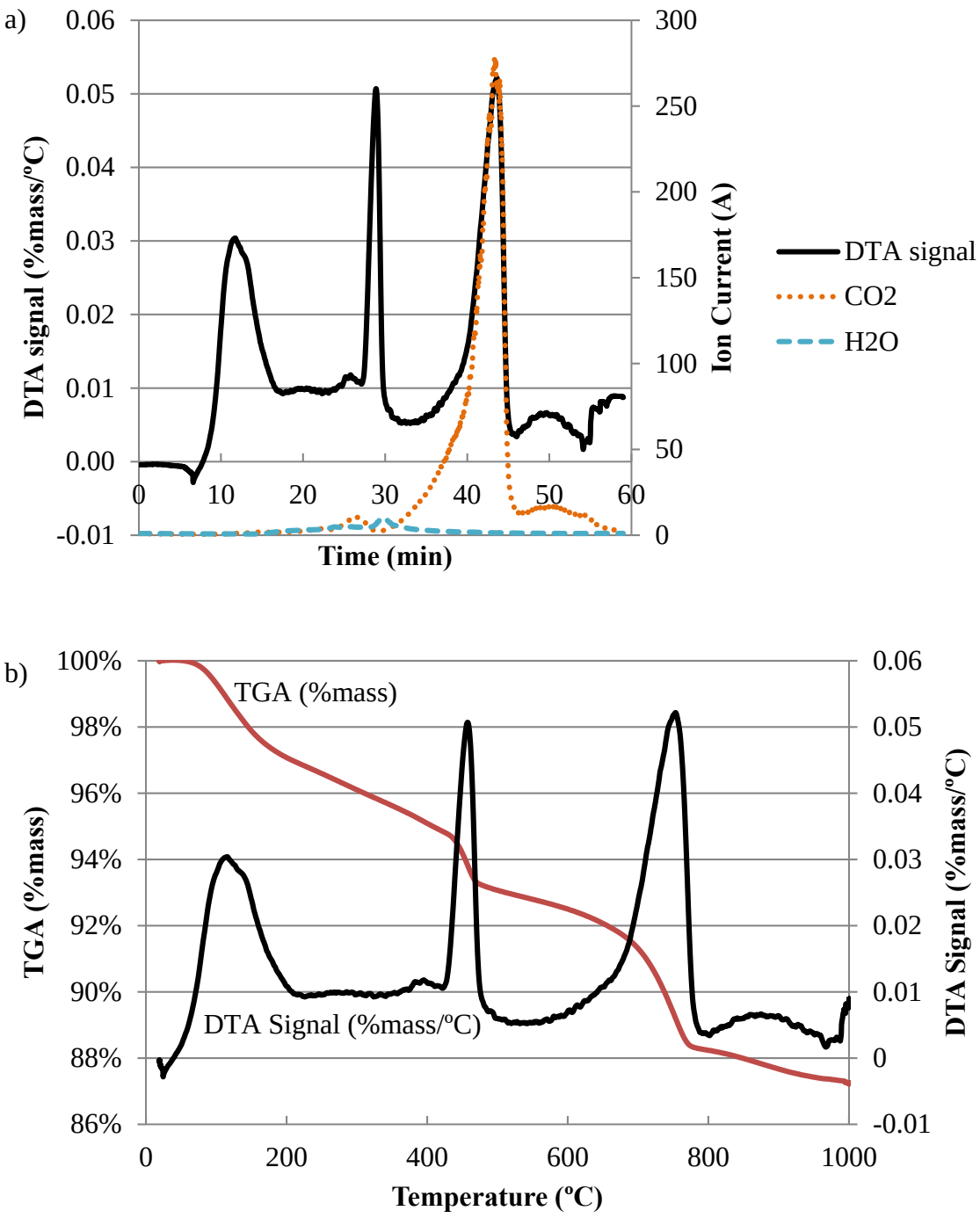

Figure 90. PureTi 10/28/15 at 10 mm Depth a) DTA-MS; b) TGA

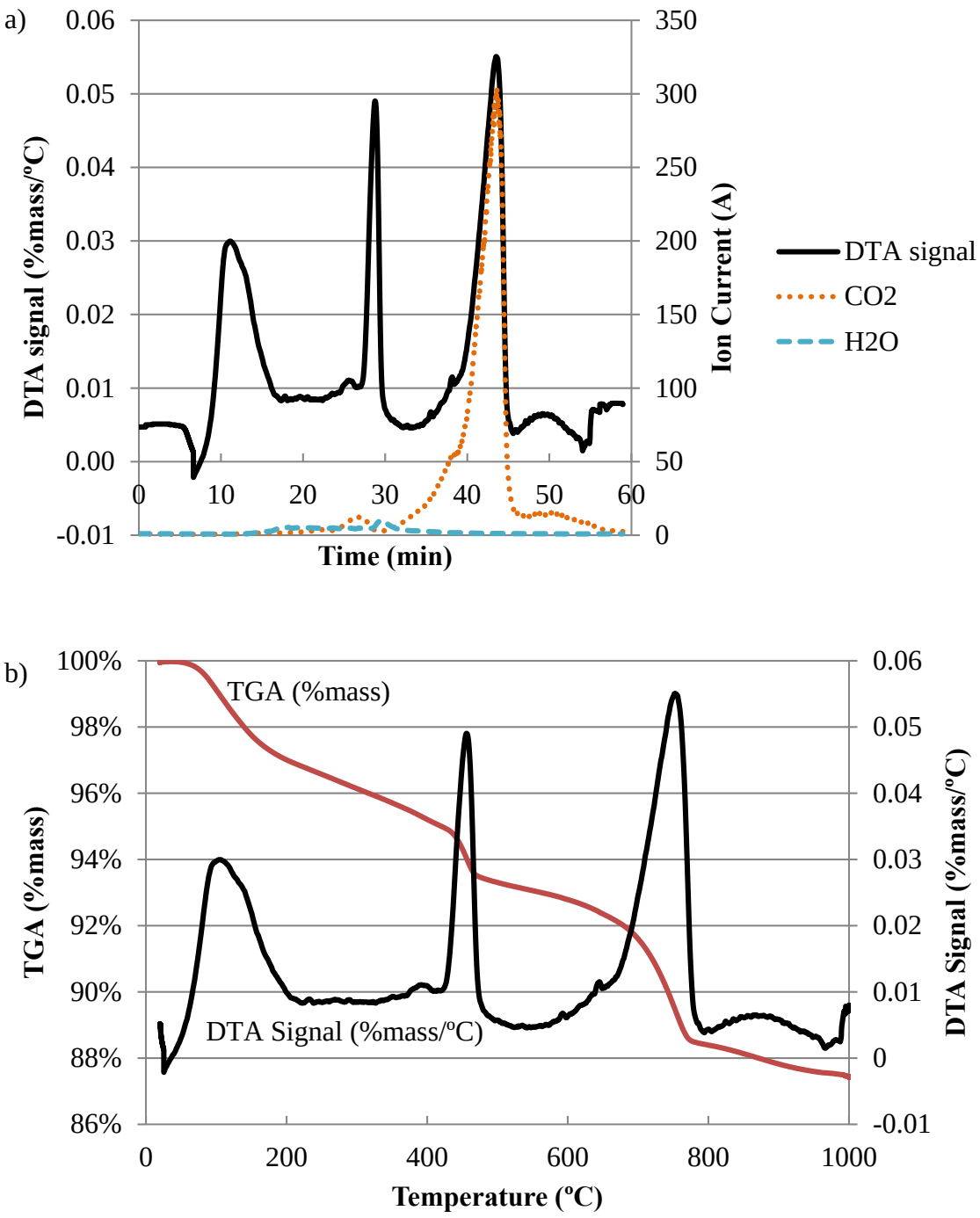

Figure 91. PureTi 10/28/15 at 15 mm Depth a) DTA-MS; b) TGA

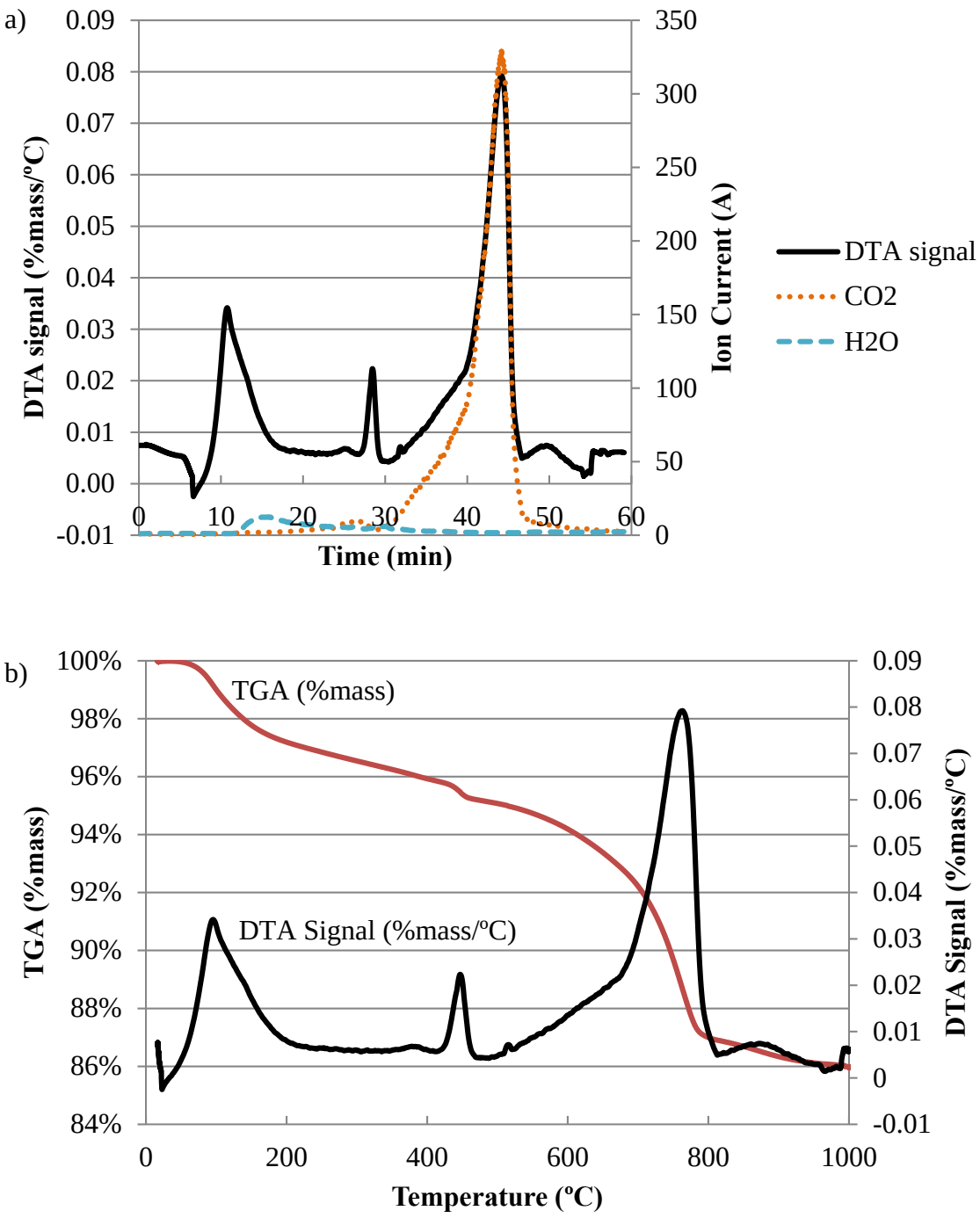

Figure 92. TiO_2 09/17/15 5 mm Depth a) DTA-MS; b) TGA

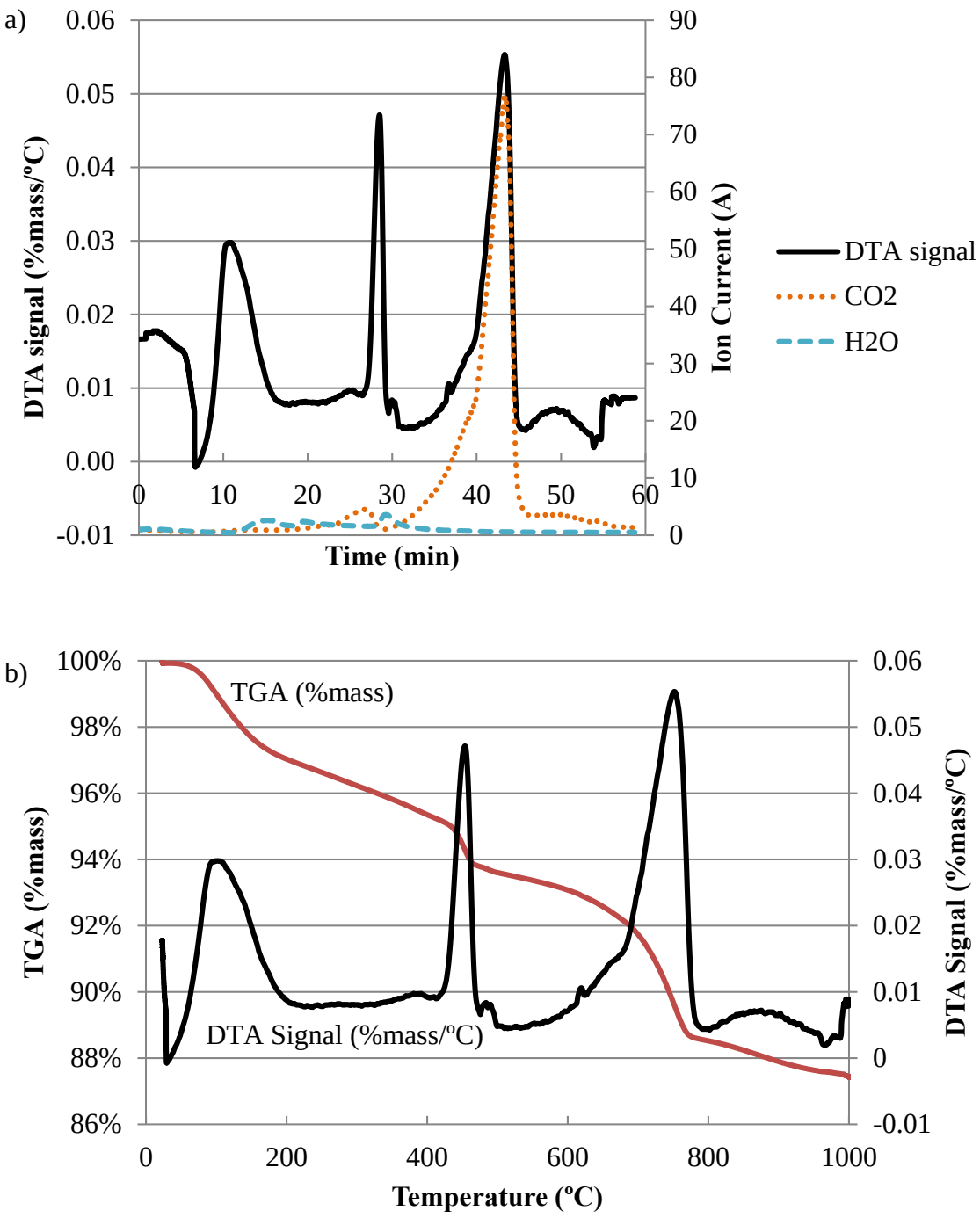

Figure 93. TiO_2 09/17/15 10 mm Depth a) DTA-MS; b) TGA

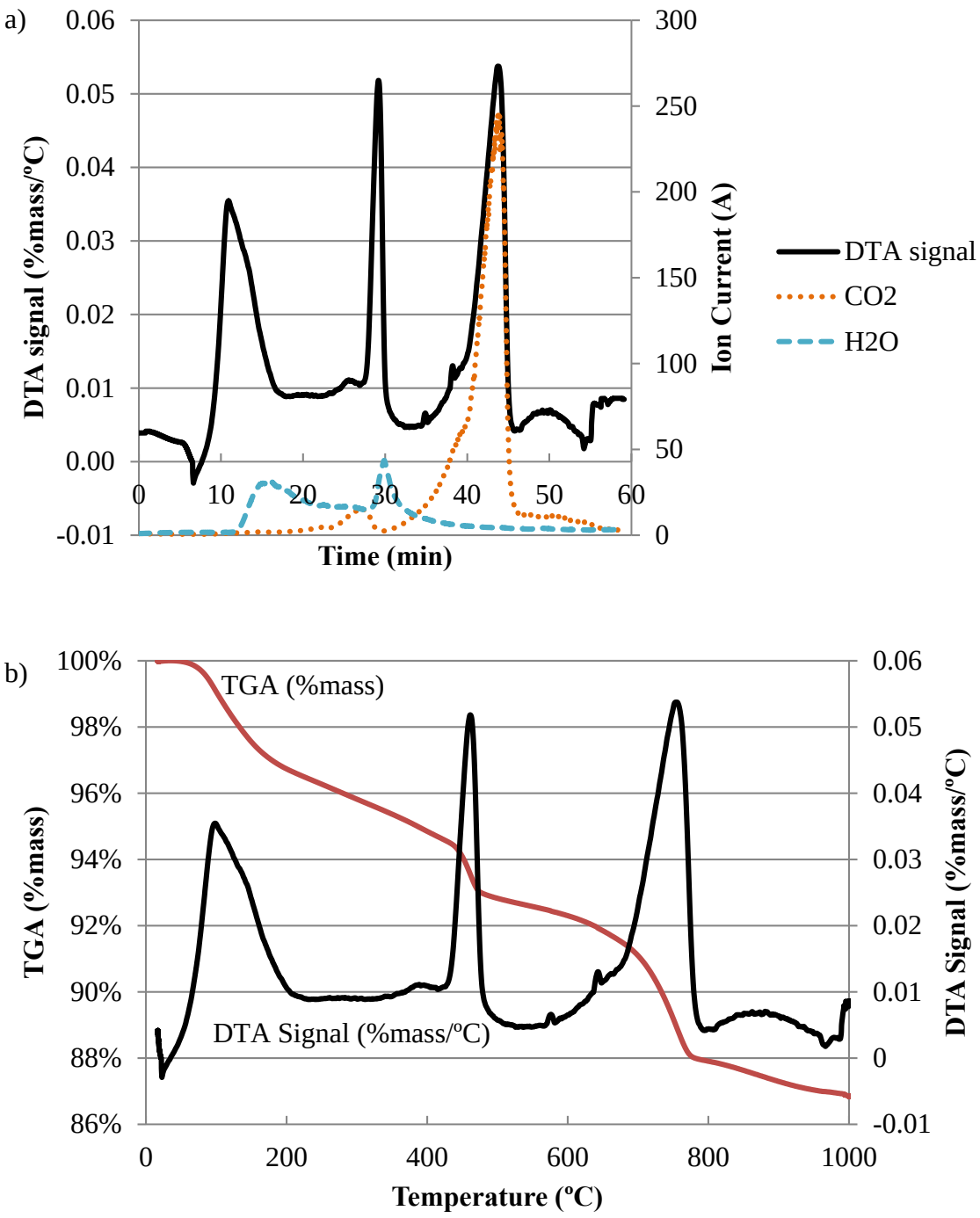

Figure 94. TiO_2 09/17/15 15 mm Depth a) DTA-MS; b) TGA

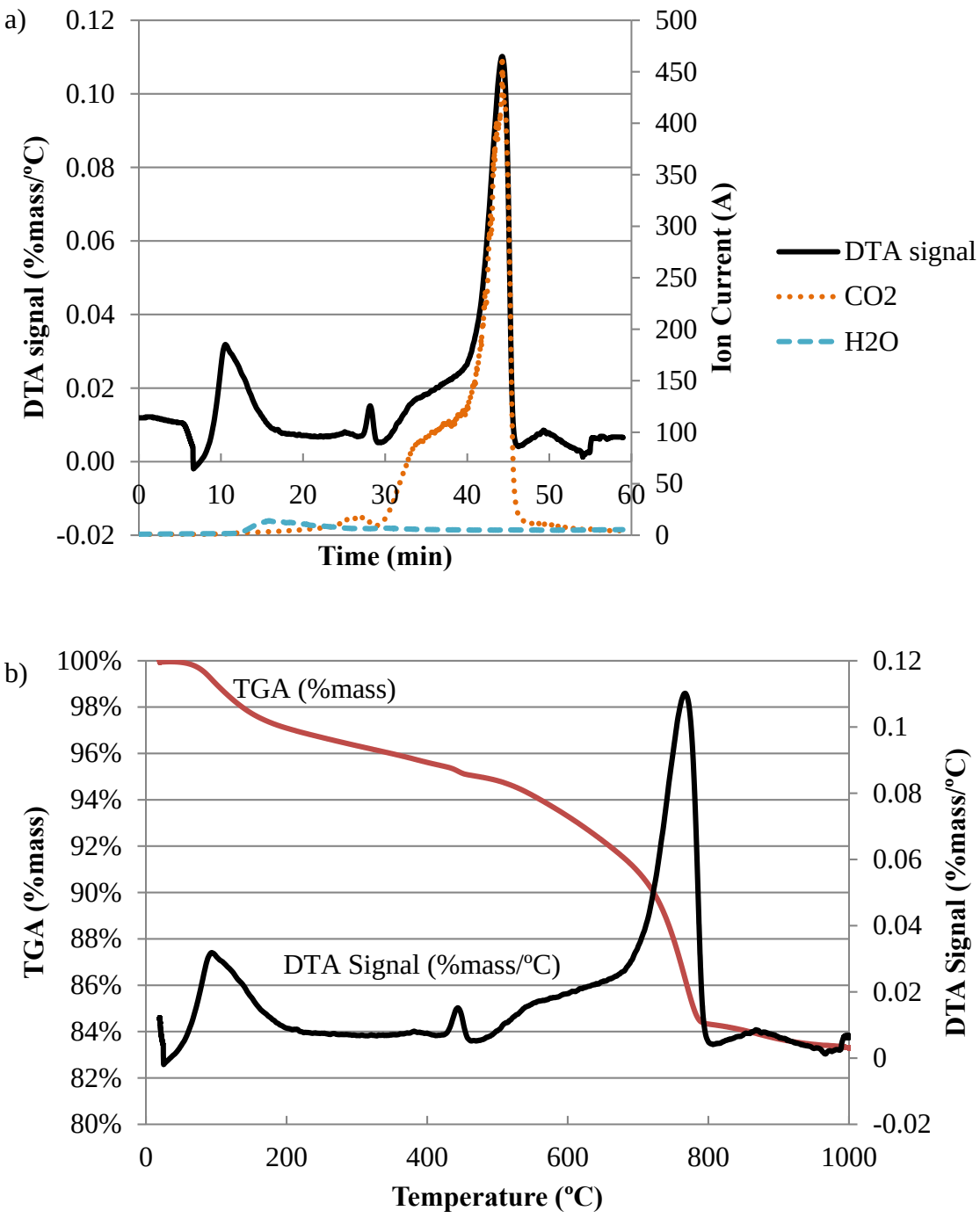

Figure 95. TiO_2 10/28/15 5 mm Depth a) DTA-MS; b) TGA

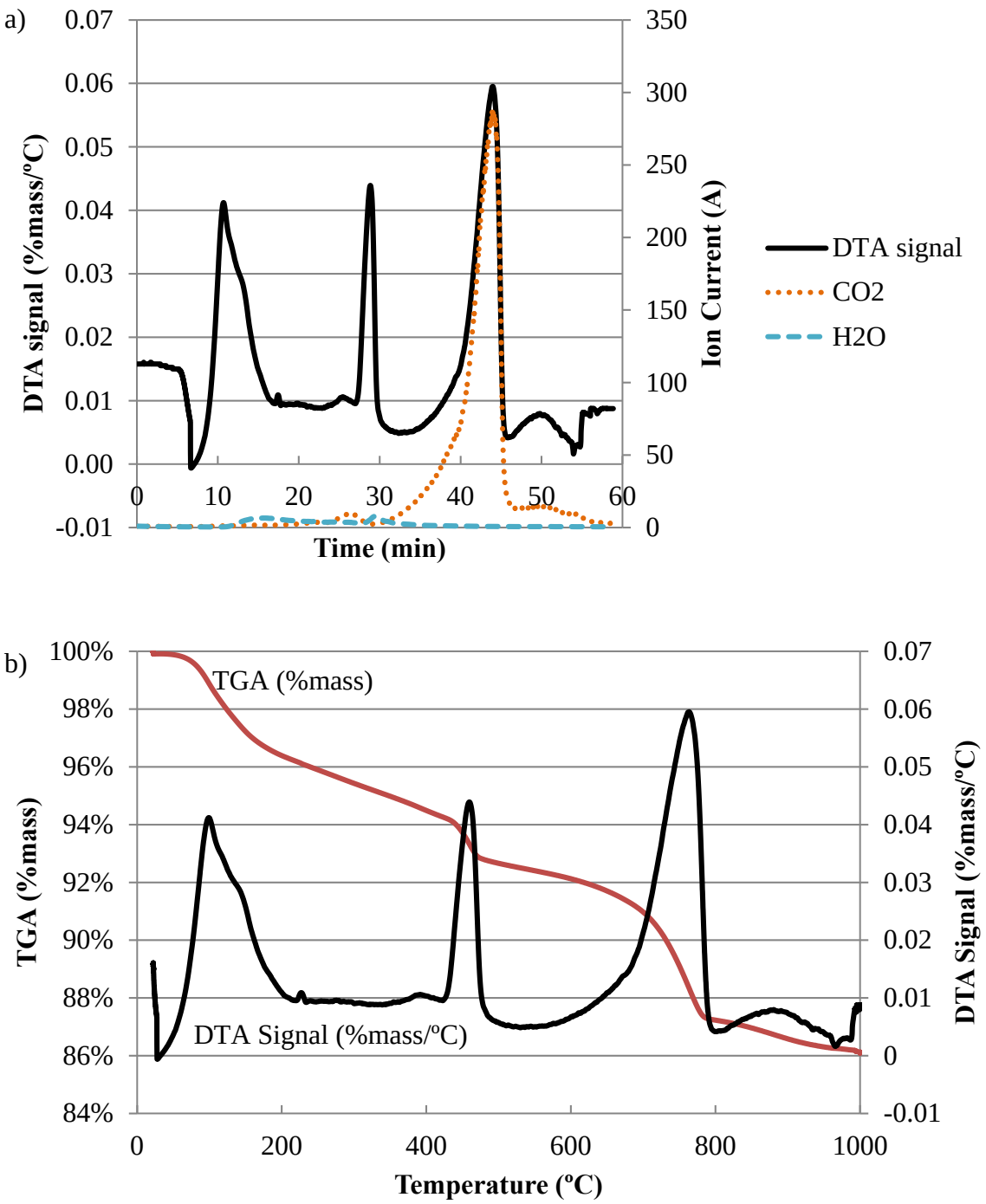

Figure 96. TiO_2 10/28/15 10 mm Depth a) DTA-MS; b) TGA

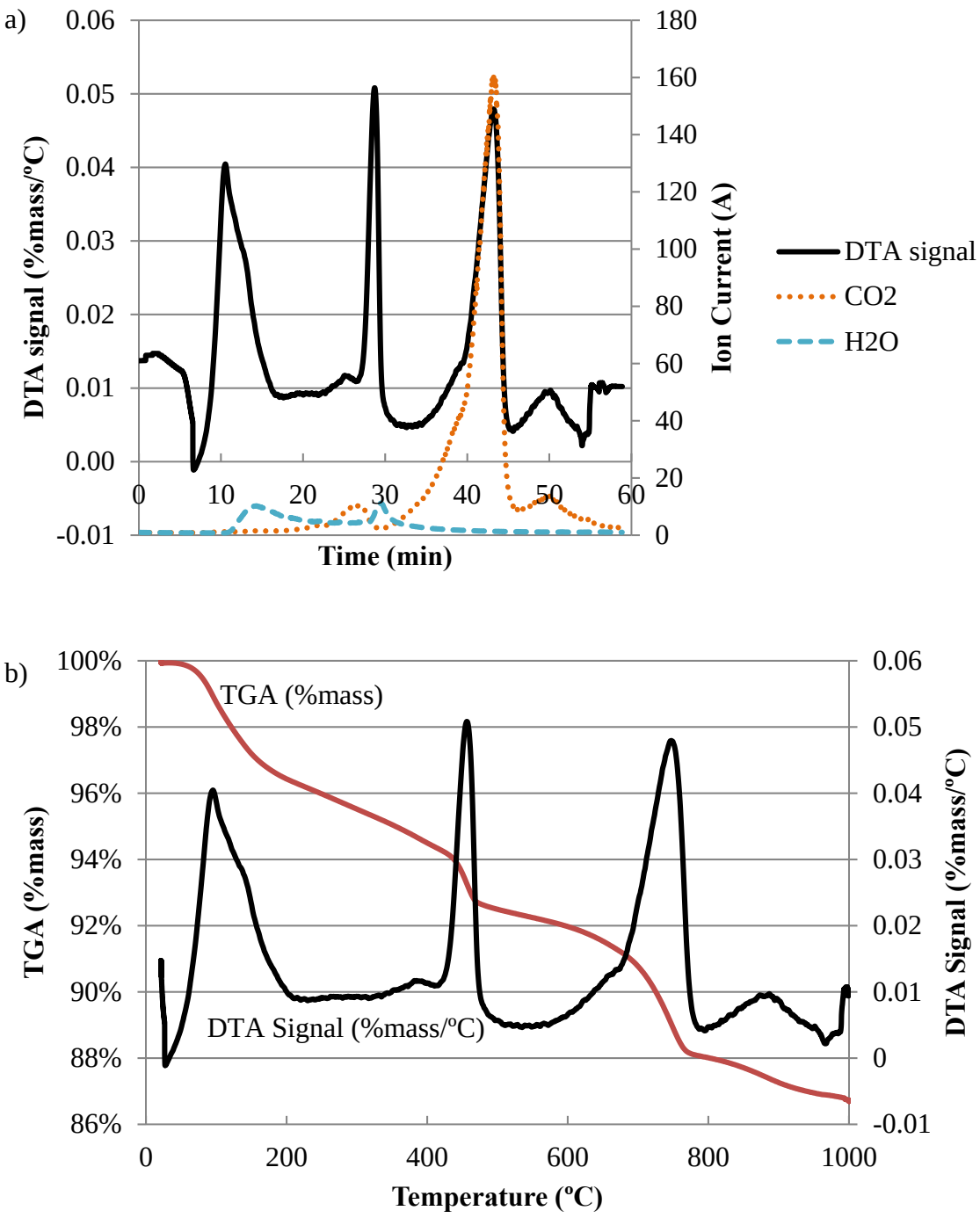

Figure 97. TiO_2 10/28/15 15 mm Depth a) DTA-MS; b) TGA

REFERENCES

A. Fujishima, K. H., and Kikuchi, S. (1969). "Photosensitized electrolytic oxidation on semiconducting n-type TiO_2 electrode " *Kogyo Kagaku Zasshi*, 72, 108-113.

ACI Committee 201 (2008). "201.1R-08 Guide for Conducting a Visual Inspection of Concrete in Service." American Concrete Institute.

ACI Committee 209 (1992). "209R-92: Prediction of Creep, Shrinkage, and Temperature Effects in Concrete Structures (Reapproved 2008)." American Concrete Institute.

Alsayed, S. H., and Amjad, M. A. (1994). "Effect of curing conditions on strength, porosity, absorptivity, ans shrinkage of concrete in hot and dry climate." *Cement and Concrete Research*, 24(7), 1390-1398.

Ashraf, W. (2016). "Carbonation of cement-based materials: Challenges and opportunities." *Construction and Building Materials*, 120, 558-570.

Ballari, M. M., and Brouwers, H. J. H. (2013). "Full scale demonstration of air-purifying pavement." *Journal of Hazardous Materials*, 254-255(1), 406-414.

Bažant, Z. P., and Baweja, S. (1995). "Justification and refinements of model B3 for concrete creep and shrinkage 1. statistics and sensitivity." *Materials and Structures*, 28(7), 415-430.

Bažant, Z. P., and Najjar, L. J. (1972). "Nonlinear water diffusion in nonsaturated concrete." *Matériaux et Constructions*, 5(1), 3-20.

Bogutyn, S., Arboleda, C., Bordelon, A., and Tikalsky, P. (2015). "Rejuvenation techniques for mortar containing photocatalytic TiO2 material." *Construction and Building Materials*, 96, 96-101.

Cebeci, O. Z., Al-Noury, S. I., and Mirza, W. H. (1989). "Strength and drying shrinkage of masonary mortars in various temperature-humidity environments." *Cement and Concrete Research*, 19(1), 53-62.

Chen, J., and Poon, C.-s. (2009). "Photocatalytic construction and building materials: From fundamentals to applications." *Building and Environment*, 44(9), 1899-1906

Chen, J., and Poon, C. S. (2009). "Photocatalytic cementitious materials: Influence of the microstructure of cement paste on photocatalytic pollution degradation." *Environmental Science and Technology*, 43(23), 8948-8952.

Cui, H., Tang, W., Liu, W., Dong, Z., and Xing, F. (2015). "Experimental study on effects of CO2 concentrations on concrete carbonation and diffusion mechanisms." *Construction and Building Materials*, 93, 522-527.

Diamanti, M. V., Lollini, F., Pedeferri, M. P., and Bertolini, L. (2013). "Mutual interactions between carbonation and titanium dioxide photoactivity in concrete." *Building and Environment*, 62, 174-181.

Domingo-Cabo, A., Lázaro, C., López-Gayarre, F., Serrano-López, M. A., Serna, P., and Castaño-Tabares, J. O. (2009). "Creep and shrinkage of recycled aggregate concrete." *Construction and Building Materials*, 23(7), 2545-2553.

Duan, P., Yan, C., Luo, W., and Zhou, W. (2016). "Effects of adding nano-TiO2 on compressive strength, drying shrinkage, carbonation and microstructure of fluidized bed fly ash based geopolymer paste." *Construction and Building Materials*, 106, 115-125.

Eguchi, K., and Teranishi, K. (2005). "Prediction equation of drying shrinkage of concrete based on composite model." *Cement and Concrete Research*, 35(3), 483-493.

Ekolu, S. O. (2016). "A review on effects of curing, sheltering, and CO2 concentration upon natural carbonation of concrete." *Construction and Building Materials*, 127, 306-320.

Fujishima, A., Rao, T. N., and Tryk, D. A. (2000). "Titanium dioxide photocatalysis." *Journal of Photochemistry and Photobiology C: Photochemistry Reviews*, 1(1), 1-21.

Goldstein, J. (2003). *Scanning electron microscopy and x-ray microanalysis*, Springer, New York.

Güneyisi, E., Gesoğlu, M., Mohamadameen, A., Alzeebaree, R., Algın, Z., and Mermerdaş, K. (2014). "Enhancement of shrinkage behavior of lightweight aggregate concretes by shrinkage reducing admixture and fiber reinforcement." *Construction and Building Materials*, 54, 91-98.

Hanson, S. (2014). "Evaluation of Concrete Containing Photocatalytic Titanium Dioxide." Doctorate, University of Utah, Salt Lake City, UT.

Karatasios, I., Katsiotis, M. S., Likodimos, V., Kontos, A. I., Papavassiliou, G., Falaras, P., and Kilikoglou, V. (2010). "Photo-induced carbonation of lime-TiO2 mortars."

Applied Catalysis B: Environmental, 95(1-2), 78-86.

Klenke, N. (2007). "Optimizing the use of fly ash in concrete." Skokie, Ill. : Portland Cement Association (PCA), c2007.

Klimesch, D. S., and Ray, A. (1997). "The use of DTA/TGA to study the effects of ground quartz with different surface areas in autoclaved cement: quartz pastes. Use of the semi-isothermal thermogravimetric technique." *Thermochimica Acta*, 306(1–2), 159-165.

Köliö, A., Niemelä, P. J., and Lahdensivu, J. (2016). "Evaluation of a carbonation model for existing concrete facades and balconies by consecutive field measurements." *Cement and Concrete Composites*, 65, 29-40.

Li, Z. (2011). "Advanced Concrete Technology." John Wiley & Sons, Inc.

Maggos, T., Plassais, A., Bartzis, J. G., Vasilakos, C., Moussiopoulos, N., and Bonafous, L. (2008). "Photocatalytic degradation of NOx in a pilot street canyon configuration using TiO2-mortar panels." *Environmental Monitoring and Assessment*, 136(1-3), 35-44.

McClenahan, H., and Rigling, A. (1929). "Drying behavior of shales and clays." *Journal of the Franklin Institute*, 207(1), 130-132.

Moon, J. H., and Weiss, J. (2006). "Estimating residual stress in the restrained ring test under circumferential drying." *Cement and Concrete Composites*, 28(5), 486-496.

O'Mahony, M. (1986). "*Sensory Evaluation of Food: Statistical Methods and Procedures*." CRC Press.

PCA (2002). "Types and Causes of Concrete Deterioration." Skokie, Ill. : Portland Cement Association (PCA).

Pickett, G. (1946). "Shrinkage stresses in concrete." *Journal of American Concrete Institute*, 17, 165-202.

Pihlajavaara, S. E. (1974). "A review of some of the main results of a research on the ageing phenomena of concrete: Effect of moisture conditions on strength, shrinkage and creep of mature concrete." *Cement and Concrete Research*, 4(5), 761-771.

Sakata, K. (1983). "A study on moisture diffusion in drying and drying shrinkage of concrete." *Cement and Concrete Research*, 13(2), 216-224.

Salvoldi, B. G., Beushausen, H., and Alexander, M. G. (2015). "Oxygen permeability of concrete and its relation to carbonation." *Construction and Building Materials*, 85,

30-37.

Shen, S., Burton, M., Jobson, B., and Haselbach, L. (2012). "Pervious concrete with titanium dioxide as a photocatalyst compound for a greener urban road environment." *Construction and Building Materials*, 35, 874-883.

Taylor, H. F. W. (1997). "Cement Chemistry." Thomas Telford Publishing, Heron Quay, London E144JD.

The Weather Company, L. (2015). "Historical Weather Data."*Wunderground.com*

Walker, H. N., Lane, D. S., and Stutzman, P. E. (2006). "Petrographic Methods of Examining Hardened Concrete: A Petrographic Manual (Revised 2004)." Federal Highway Administration.

Yoo, D.-Y., Banthia, N., and Yoon, Y.-S. (2015). "Effectiveness of shrinkage-reducing admixture in reducing autogenous shrinkage stress of ultra-high-performance fiber-reinforced concrete." *Cement and Concrete Composites*, 64, 27-36.